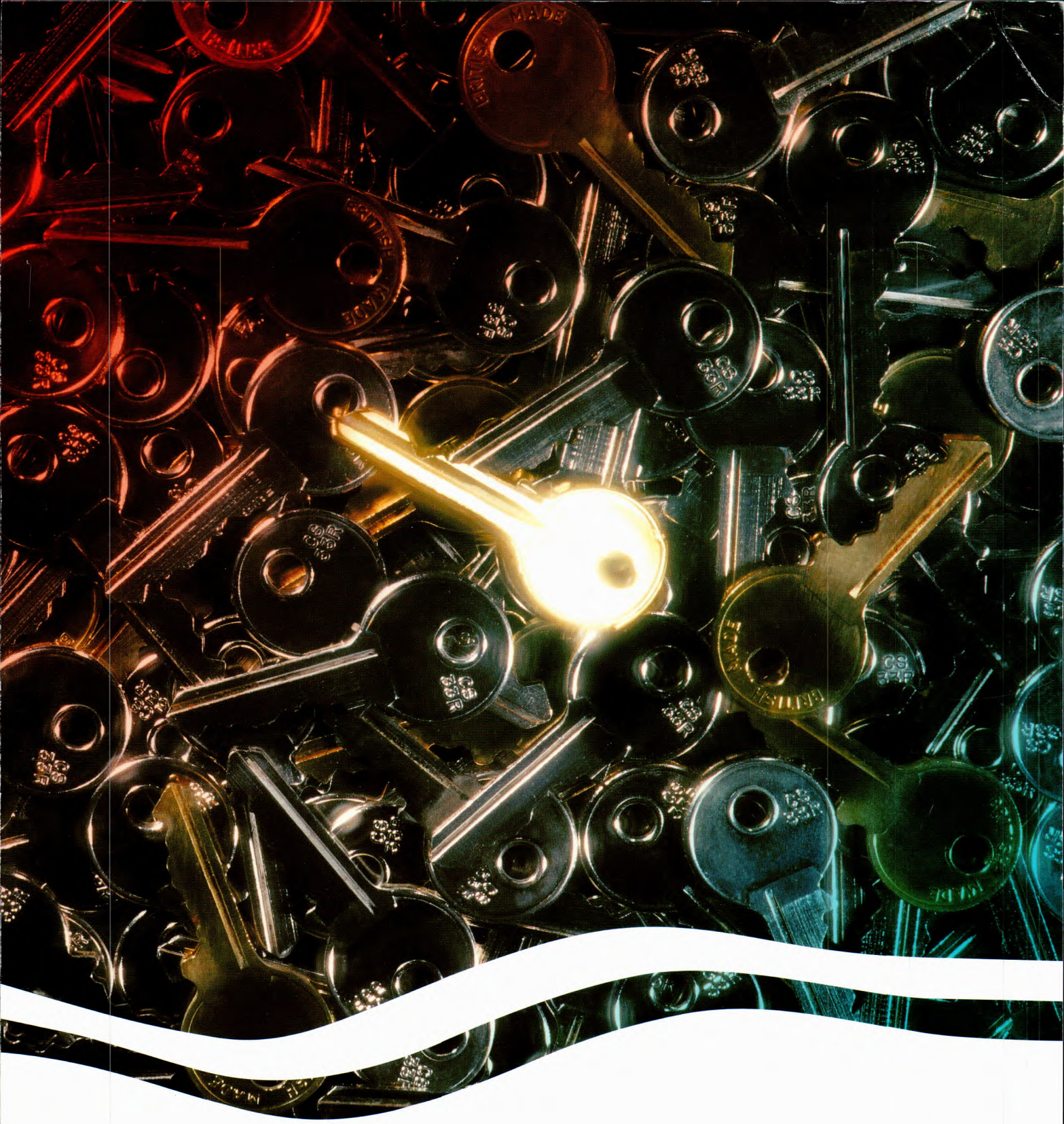

Scientific and Technical Review

2001/2

Met Office

An Executive Agency of the Ministry of Defence

Scientific and Technical Review 2001/2

Vision

Through unrivalled know-how, to enable individuals, society and enterprises everywhere to make the most of the weather and the natural environment

Goals

- To lead the world in advice on the weather and the natural environment
- To make the Met Office a source of pride to our staff, our owner and the public

Scientific and Technical Review 2001/2

Contents

Chief Scientist's introduction

As the Chief Executive's overview indicates, during the past year, Met Office staff have contributed to urgent work in response to national needs, both for the MoD and in response to foot-and-mouth disease. It was rewarding to see the dedication that the staff involved in the scientific and technical areas brought to these urgent tasks. At the same time as meeting these needs, this has been an outstanding year for wider achievement in science and technology. This has occurred in both the numerical weather prediction (NWP) and climate areas, as well as in the wider product and service areas.

The performance of the numerical weather forecasting models has improved by what is probably the largest single year increment to date, largely due to improved methods of incorporating data into the models, and the subsequent wider application of these methods to make use of satellite data. At the same time, our Hadley Centre for Climate Prediction and Research has continued work on climate prediction, achieving, yet again, confirmation of its world-leading performance with the publication of results with an advanced carbon cycle included within the model. The Intergovernmental Panel on Climate Change's Third Assessment Report contains references to Hadley Centre work in many of its chapters, showing further evidence of our wider contributions.

The numerical weather prediction and climate areas have done so well, but have both also been heavily involved in the development of a new basic model structure for their work. In the NWP model, such major developments have previously occurred roughly once a decade in response to new opportunities in numerical methods. In the past, their adoption has been associated with a dip in performance, due to the stress of the transition process in the change between models. On this occasion, the outcome has been exceptional with the pre-operational version of the new NWP model running alongside, and outperforming, the old operational model. Next year will see the new model's formal adoption as the operational model for both weather forecasting and climate work. This enormous dual achievement owes much to the flexibility of our research staff and their concerted effort.

With these major initiatives, I have focused on the core research function. Such excellent performance is not confined to these areas and this year's *Scientific and Technical Review* details the extensive progress being made with new observation methods, information technology and forecasting techniques and applications for our many customers.

Linking all these achievements over the past year was one common theme — 'unlocking our potential' — hence the cover of this year's *Review* showing keys. By 'unlocking potential', we mean not only finding ways to improve our own ability to provide high-quality products and services, but also helping customers unlock *their* potential by providing accurate information in the format most suitable for them.

Chief Executive's overview

The year 2001 will be a memorable one for us all — the Met Office, our owner the MoD and our many customers. The tragic events of 11 September 2001, and then the subsequent war on terrorism, saw the Met Office at its best, responding to the needs of the MoD and our armed services. This was based on up-to-date contingency plans and displayed our ability to deploy resources rapidly, both at our operations centre and in the field through our Mobile Met. Unit. At the same time, we maintained our activities in support of the fight against foot-and-mouth disease, and successfully forecast the many storms that hit the UK, which brought flooding as well as storm damage to business and domestic properties. Tragically, and in spite of the early and detailed warnings, the new year storms also led to a number of fatalities, raising the question of how to minimise the impact of such events, even when they are forecast well in advance.

In terms of overall business performance, we met five out of six key performance targets. In particular, we made an unprecedented improvement in the Numerical Weather Prediction Index — a measure of our forecasting accuracy — firmly establishing ourselves as the best in the world. We also made further improvements in cost-effectiveness, enabling us to invest some £15 million in future capability (a key element in our strategy) and to pass on some real cost-benefits to our customers. Although it was disappointing to miss our commercial contribution target again, we nonetheless made a contribution of £3.3 million from commercial sales to offset the cost to the taxpayer of the Public Met. Service. Finally, in terms of performance, we met over 80% of our Business Plan targets on time and within planned cost.

More widely, our work on climate change — carried out in our Hadley Centre for Climate Prediction and Research — has once again received international prominence and acclaim, particularly in support of the World Meteorological Organization's annual climate assessment and the Intergovernmental Panel on Climate Change Third Annual Report. We successfully launched our first joint venture — weatherXchange — which deals in weather derivatives, and we received high praise for our new health forecasting service, which is already saving many hundreds of thousands of pounds in the health service. We also won a number of major contracts for the provision of weather forecasting services to the private sector, including Shell and Granada.

Innovation plays a key role in our development both as Europe's leading national met. service and as a business. It is therefore pleasing to be able to report that we are well on the way to establishing a culture of innovation in the Met Office. Our new Innovation Centre is being well used by our staff,

often in conjunction with our customers. Our first Innovation Awards Ceremony — attended by customers and a representative of the Defence Met. Board — was a great success.

Any report of the past year would be incomplete without mention of our planned relocation to Exeter. I am pleased to be able to report that we signed the agreement with our private-sector partner Stratus in November 2001, and we are determined to meet our demanding schedule, which transfers our operations to Exeter by September 2003 and culminates with the last staff moves that December. Thanks to some good weather (well forecast by the Met Office!), site preparations were completed ahead of schedule and the building work is now well under way. There is, encouragingly, increasing excitement among our staff now that progress is visible and many of us are less than a year away from moving. For anyone wishing to keep up with progress, current pictures are available on our web site.

In reporting on our progress, I must acknowledge the vital role played by our people. Although it is something of a cliché to say that people are the most important asset of any business, it is nonetheless true of the Met Office. Our standing among the international science community, our performance in meeting our customers' needs and our success as a business are all ultimately down to the quality and commitment of our people — not just our scientific staff but also the many other technical, professional and support staff. I am therefore pleased to have this opportunity to pay tribute to them all, and to re-affirm our commitment to them, to their training and development and to their well-being, especially over the next 18 months as we move to Exeter. It is also an opportunity to assure our customers that we will do everything possible to ensure that our services to them are not interrupted or degraded during the move.

April 2002 saw the introduction of a new management structure: we moved away from being a 'functionally managed' organisation to a 'process-managed' business. This change will enable senior line managers to take real control of the operational business and to do so from a customer perspective. At the same time it will allow directors to focus on strategy, business development and performance management. This change ties in with the transition strategy for our move to Exeter and with our approach to ISO 9001 accreditation, both of which have their emphasis on 'process' rather than 'function'.

Last year I said in my overview that the weather business was changing fast. One year on and, if anything, it is changing faster than we expected. Not only has the economic, political and business climate changed, but we are also faced with new challenges, such as European Union data policy and competition policy. However, I am sure that our overall strategy of investment and growth is right, although growth will take longer to come through than originally planned. I am equally sure that our major themes relating to Europe, diversification into the wider natural environment, innovation and exploitation of internet technology are sound. We now need to redouble our efforts to build on our strengths, keeping a firm eye on our vision, goals and strategy, and delivering our plans on time and to cost. Above all, we must continually strive to do better in responding to our customers' needs, especially in offering better value for money. We can and will work with them to give real business benefit, unlocking their potential and, in so doing, ensuring we remain the supplier of choice for all our customers. 

Observations

Observations network planning

Surface observing

Marine networks

Remote sensing

Upper-air observing

Meteorological satellites

Analysing and assessing climate observations

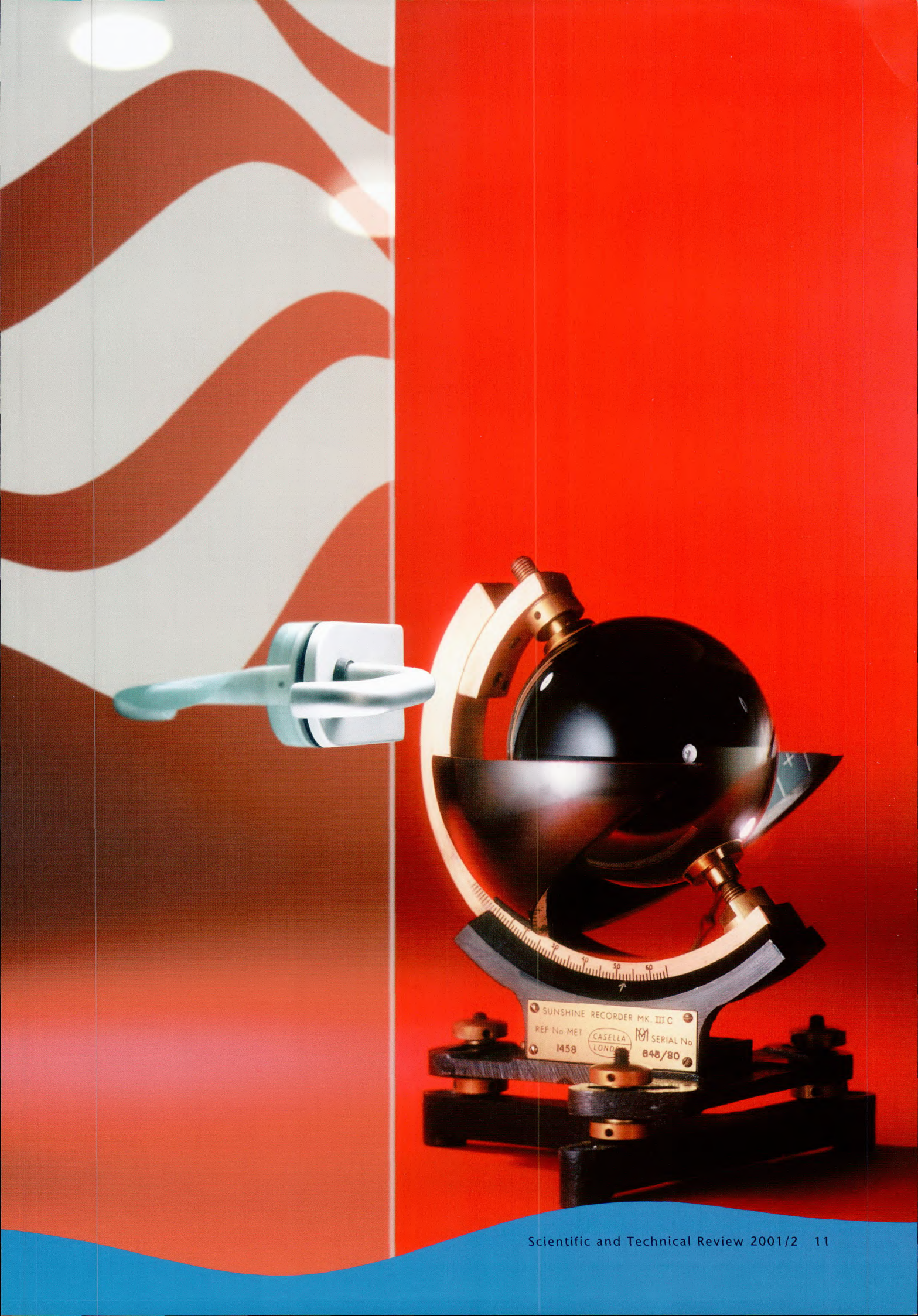
SUNSHINE RECORDER MK. III C
REF No MET
1458
CASELLA
LONDON
SERIAL No
848/80

Observations network planning

We started a review of the user requirements for surface-based observations, adopting the 'rolling requirements review' procedure developed by the World Meteorological Organization (WMO) (for satellite observations). This involves identifying the maximum and minimum requirements, comparing these with current capabilities and planning technical solutions using a cost–benefit approach. We also prepared a new climate data document using this approach.

We reviewed the role of the auxiliary synoptic station network, manned by co-operating observers. This followed on from surveys of the quality and usefulness of the observations they provide and the increased automation of the professional network. Network rationalisation and investment in automation and observer training were recommended, which should lead to more-frequent observations with improved content.

We continued our liaison with the Working Group for Planning and Implementation of World Weather Watch in WMO Region VI (Europe), meeting in Geneva in May 2001, where we reached agreement on revised networks of UK stations providing synoptic and climate data as part of the international exchange arrangements.

Surface observing

Roll-out of automation

Until now, reports from the key Met Office network of sites have relied on human observations. Automation of elements of the report had been seen as an aid to the observer, making the observing process more efficient. A trial project on automation of observing showed that fully automatic observations could replace human observations in the key network. Furthermore, automation offers the prospect of extra reports that would be straightforward for an automatic weather station (AWS) to obtain, but impossible for an observer to describe in anything other than a basic form.

Figure 1. New laser cloud-base recorder.

We began the roll-out of an expanded sensor suite to support the automation programme in March 2001. Initially, the extra sensors are an optical present weather sensor, a contact precipitation sensor, a sonic snow depth sensor, plus automatic sensors for sunshine and short-wave radiation. On completion of the development work, we plan to add further sensors, including a weighing rain gauge and a long-wave radiation sensor. During 2001/2, 15 key sites were fully automated, although at RAF flying stations, observers have been retained during flying hours. We installed the expanded sensor suite at five further sites to augment the network capability and reduce the reliance of forecaster systems on data from individual sites. We upgraded the software for our Semi-automatic Meteorological Observing System and distributed it to 90 sites in the observing network during the year.

Improved automatic present weather and cloud cover reporting

We significantly improved the capability of automatic present weather reporting with the operational introduction of the Present Weather Arbiter. This uses data from a number of sensors to determine the most appropriate present weather code to be reported by assessing the known strengths and weaknesses of the individual sensors.

A new laser cloud-base recorder (LCBR) that is more effective in precipitation is being introduced into the network (see Fig. 1). The project on automation of observing identified that reporting of cloud cover during precipitation events was particularly poor and so the new LCBR and a revision to the cloud cover algorithm have together significantly improved the performance in precipitation.

Ten-minute observations

The standard surface report, SYNOP, is produced hourly by either an observer or an AWS, and represents a snapshot of the meteorological conditions at the site. The AWS can report data more frequently and optimise the reporting of change in meteorological conditions. Observations will be sent by the AWS every ten minutes in two different forms — one that can be interpreted by front-line staff and one that provides numerical weather prediction (NWP) with an extended range of data. Information such as precipitation drop size distribution and cloud base profiles will be operationally available from up to 150 sites in the UK.

New thermometer screens

During the year, we finalised the design of a new plastic thermometer screen. The current wooden screens are expensive and have a short operational life, whereas the new plastic screens are made from recycled materials and will have a much longer lifespan. A trial of the new screens at four UK sites will begin in 2002 to demonstrate their operational acceptability for climate measurement purposes.

Figure 2. Met Office open-ocean data buoy.

Marine networks

We have continued our successful collaboration in the Republic of Ireland with the Marine Institute, the Department of Marine and Natural Resources and Met Éireann. Two Met Office data buoys were deployed, one to the west of Galway and the second to the east of Dublin Bay, and have been delivering high-quality data throughout the year (Fig. 2).

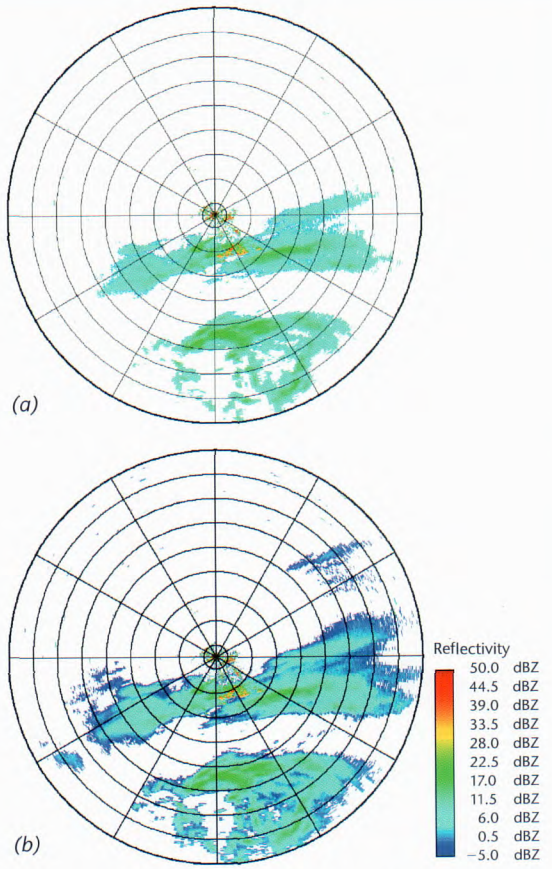

Figure 3. Sample data from the Chenies radar to the NW of London. (a) Signal processing system as at 1 Jan 2002; (b) new signal processing system. The maximum radar range plotted is 255 km.

The Marine Institute has ordered a third buoy for deployment off the south-west coast of Ireland. This buoy will be constructed by Marine Institute staff under the guidance of Met Office engineers, thus fostering the transfer of knowledge and skills that are a key element of the collaboration. The Marine Institute is funding the development of the electronics payload for next-generation data buoys. A prototype system is expected to be deployed for sea trials in 2002.

The Argo float deployment programme has progressed well. We have deployed 26 floats during the year and, so far, they are all providing profiles of sea temperature and salinity as expected.

Remote sensing

Enhanced lightning location facility

Electromagnetic radiation emitted from cloud-to-ground lightning discharges travels very long distances with relatively low attenuation at frequencies of around 10 kHz. The Met Office long-range lightning detection system observes at this frequency and times the arrival of the discharges at outstations located in Gibraltar, Cyprus, Finland and four sites within the British Isles. The times of arrival allow the original position of the lightning discharge to be located with an accuracy of between 2 and 5 km over most areas of Europe.

In the past, the rates of reporting were limited by the cost of communications and the limitations of the computer controlling the system. We have now replaced the computer and upgraded the communications so that the rate of reporting is an order of magnitude higher than in mid-2000. Further development work is needed on the system's software to raise the detection efficiencies to those required in summer (reporting rate for lightning of 10,000 flashes per hour in Europe). However, during winter, when running at an average reporting rate of 2,500 flashes per hour, the system is now clearly reporting all the main thunderstorms in Europe and the Middle East and all the storms across the Atlantic to the east coast of North America. In addition, all the main storms in South America and most storms in western and central Africa can be detected.

Improvements in weather radar capability

We have developed new radar signal processing algorithms that have enabled the minimum detectable radar signal to be reduced by up to 5 dB. As a result, the ability of the radar network to detect light rain can be significantly increased, particularly at long range (Fig. 3). We have also improved discrimination between signals from precipitation and those from non-meteorological targets (e.g. ground clutter), offering the opportunity to recover precipitation echoes in areas subject to ground clutter. In Fig. 4, the raw reflectivity data in (a) contains signals from ground clutter, and small areas of intense clutter are evident very close to the radar and in the south-east quadrant. The current signal processing algorithms remove the clutter, but at the expense of leaving large gaps in the data that must be 'filled in' later by interpolation (b). Using the new algorithms (c), fewer data have to be rejected and the requirement for interpolation is much smaller. This is particularly important for improving measurements of rainfall close to the surface.

These developments will benefit all users of weather radar data, particularly the Environment Agency, the Public Met. Service and TV broadcasters. The new processing algorithms are currently under test on a non-operational radar and will be ready for implementation on network radars later in 2002.

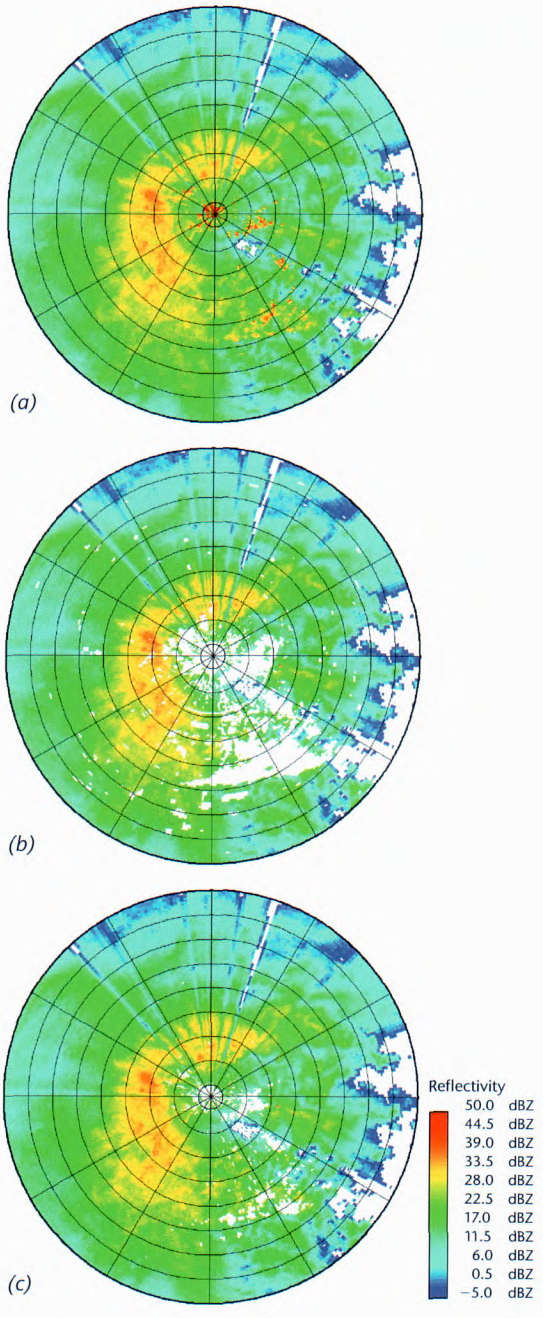

Figure 4. Sample data from the Chenies radar. (a) Raw reflectivity data and (b) signal processing system as at 1 Jan 2002; (c) new signal processing system. The maximum radar range plotted is 85 km.

Upper-air observing

Ground-based observing systems

While many upper-air observations are now provided by weather satellites, there is a continued requirement for high-quality measurements from weather balloons (radiosonde systems) and other ground-based systems.

We have introduced new radiosonde ground systems that allow operators at one site to monitor and edit the measurements at up to three other sites where the balloons are launched automatically. We have concentrated on

ensuring improved accuracy in wind and relative humidity measurements from the next generation of radiosonde designs. At the WMO Global Positioning System (GPS) Radiosonde Comparison in Brazil, Met Office staff launched more than 20 chilled mirror hygrometers to check the relative humidity measurements made by the commercial radiosonde designs.

Radars capable of measuring wind in clear air (wind profilers) have been brought to operational standard to improve the temporal sampling of the upper-air network over the UK. The backscattered power from these radars in clear air is often high when relative humidity changes very rapidly in the vertical. We are working towards integrating the information from these signals with brightness temperature measurements from microwave radiometers and total water vapour derived from GPS satellite signals received at the ground. Last August, we evaluated microwave radiometers during a field experiment held in the Netherlands. As part of the European Co-operation in Science and Technology 716 project this year, we achieved the provision of total water vapour from GPS signals in real time.

Figure 5. A British Airways aircraft fitted with AMDAR.

Aircraft Meteorological Data and Reporting (AMDAR)

The AMDAR system provides large numbers of wind and temperature measurements from commercial aircraft in support of general and numerical weather forecasting. The Met Office continues to manage the European Meteorological Network (EUMETNET) AMDAR project, and is responsible for operating and developing the European AMDAR network. This is undertaken in co-operation with Air France, British Airways, KLM, Lufthansa and SAS, who together operate 251 AMDAR aircraft (up by 76 since January 2001), see Fig. 5.

During 2001, the delivery of several ground-based systems has reduced duplication of effort between European national met. services and has enabled AMDAR aircraft to be operated more efficiently. A European AMDAR Data Acquisition System now receives and processes all AMDAR data from European airlines. Data optimisation systems allow AMDAR aircraft to be automatically activated on request, giving more-homogenous network coverage.

AMDAR data continue to be of high quality, comparable to more-traditional upper-air observing systems such as radiosondes. However, unlike radiosondes, European AMDAR aircraft do not provide humidity measurements. We continue to monitor the development of suitable sensors.

Meteorological satellites

Delays to the Meteosat Second Generation (MSG) and EUMETSAT Polar System (EPS) programmes have stabilised this year with first launch dates of

Summer 2002 and late 2005, respectively; however, MSG data will not be available operationally until the Summer of 2003.

Under its Amended Convention, EUMETSAT's first Optional Programme has been opened for subscription: the Jason-2 Ocean Altimetry programme, contributing to a joint US–European mission from 2005, is a step closer to providing operational data for oceanography.

EUMETSAT has addressed the question of requirements after MSG (2015–25), with two of the three expert groups, on Nowcasting and Very Short Range Forecasting, and Global NWP, being led by Met Office scientists.

Preparing for the World Radio Conference in 2003, we are working with the Radiocommunications Agency, EUMETNET, the WMO and the International Telecommunication Union (ITU) in the debates on frequency allocations, in which some proposals could interfere with, or constrain, our use of meteorological frequencies — for example, for radar and passive remote sensing. A database is being developed to track the Met Office's use of the radio-frequency spectrum.

Analysing and assessing climate observations

The upgraded system for analysing and mapping climate data (described in the *Scientific and Technical Review 2000/1*) has proved to be a valuable and flexible tool. Examples of its use include:

- production of monthly climate statistics on grids and for counties and regions;
- production of grids for the 1961–90 and 1971–2000 long-term averages (Fig. 6);
- identification of suspect data for quality control purposes;
- estimation of missing values and generation of climate estimates for any arbitrary location.

To complement the existing mapping capability, we have developed a new climate database that holds a comprehensive range of information, including monthly climate statistics, long-term averages and details of noteworthy weather events. The data include averages, highest and lowest values, dates when certain values were last exceeded, records of the longest and most recent spells of unusual weather and areal values.

We are encouraging use of the database through the development of a user-friendly, web-based interface, while the combination of a more sophisticated mapping facility with a comprehensive climate database has resulted in more-timely and more-detailed assessments of recent weather events.

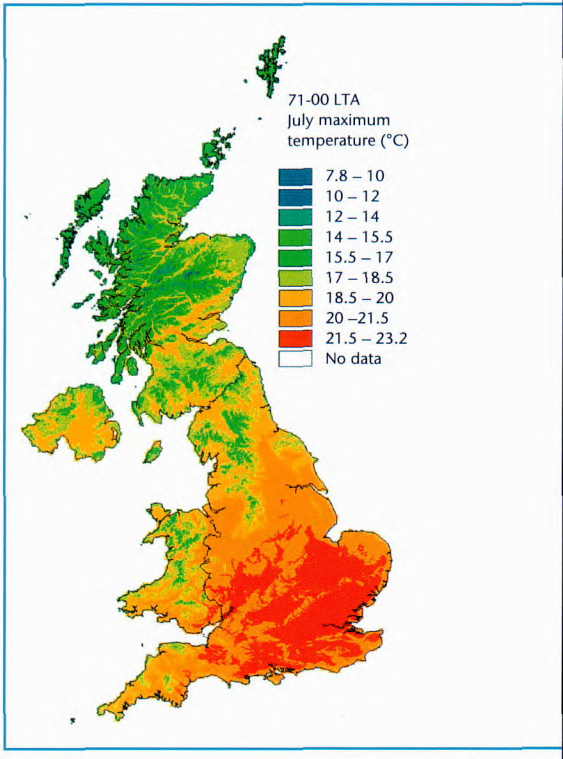

Figure 6. Average daily maximum temperature over the UK, July 1971–2000.

Information Technology

Distribution of data and products
Underlying computer capability


TIF320 FS
GND
IBM27F4094
MN53015SRU

Distribution of data and products

In support of its services to customers, the Met Office is making ever-increasing use of the internet as a means of supplying information. Although a variety of formats is required — text, graphics, images — many customers have a standard list of desired products that we supply on a regular basis. The original system for doing this, the Data and Products Distribution System (DPDS), was very successful, but we are installing a replacement system to run all services supplying information to customers, with far greater processing power and data storage space, and capable of being expanded to meet any further market demand.

By clustering several web-server computers, the system will have an overall greater capacity and will be more resilient to system failure. For protection against hard disk failure, they share a pooled area of disk space, known as a 'redundant array of inexpensive disks'. The capacity of the internet link has also been upgraded and it can now operate at a speed of 8 Mbits s^{-1}.

Horace

Horace is the Met Office's in-house visualisation system for monitoring real-time weather and exercising quality control on forecast products. During the past year, we have developed and delivered a version of Horace to the Australian Bureau of Meteorology (BoM) (Fig. 7). This was a landmark event as it has enabled the BoM to move away from pencil-and-paper methods — they can now produce and disseminate their forecast charts directly from Horace in the form of faxes.

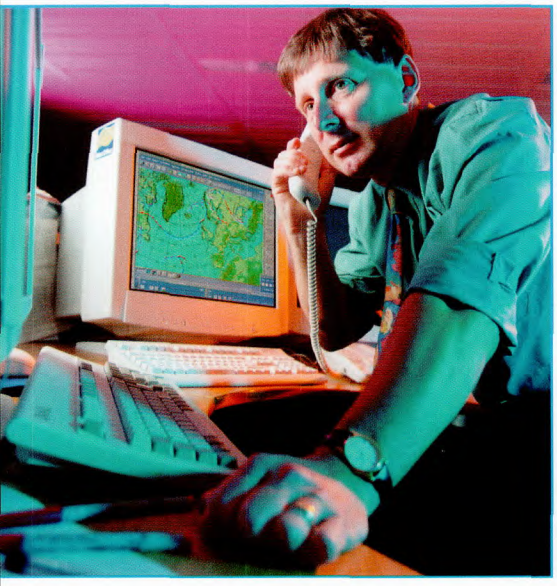

Figure 7. We delivered a version of Horace to the Australian Bureau of Meteorology.

Horace is now a mature system, fully meeting the demands of its many varied users. Some development is still taking place, with particular emphasis on product creation for the web. By using an automated macro command language, products may be set up by the user in a genuine 'What you see is what you get' (WYSIWYG) environment and saved in a number of graphic formats straight to a specified location. Products may be personalised for a specific recipient by adding a logo to the graphic. Other developments have included the presentation of Aircraft Meteorological Data and Reporting (AMDAR) profiles (see *Observations*), a pop-up display of bathythermograph data, improved maintenance of the customer database and improved production of the aviation charts, particularly the significant weather chart.

Nimbus

Nimbus is a Met Office system that supports forecasters at front-line stations through visualisation of data and by running forecasting applications to create extra products. The system has been very successful in enabling the delivery of services to a range of customers. A major upgrade brought some important enhancements, including a much improved contouring algorithm, cross sections and context-sensitive help. The military version of Nimbus, the NATO Automated Meteorological Information System (NAMIS), also benefited from these enhancements and continues to be the NATO system of choice. Operation Veritas once again proved the worth of the Nimbus family of systems and we were able to respond to some high priority requests, thus ensuring full support for the military in Afghanistan.

Figure 8. A field met. office in Afghanistan: Nimbus can be used in isolated locations.

Delivering data to systems such as Nimbus is becoming more important, especially as they are increasingly being used in remote deployments (Fig. 8). The NAMIS system receives data via a satellite broadcast system, but this does not work for areas outside the satellite footprint. However, delivery via the DPDS allows the user to set up a list of requested data that may be sent directly by file transfer protocol. Nimbus and NAMIS have been enhanced to use this facility and may now be deployed anywhere in the world.

Geographical Information Systems

Geographical Information Systems (GISs) are becoming increasingly important components in the Met Office's visualisation systems as the technology completes the link between the display of meteorological data and the underlying terrain. The interaction is quantitative in that it can combine GIS data such as catchment areas, power lines, roads, topography, etc., with real-time meteorological data.

Agencies with environmental responsibilities have taken an interest in this work and a desktop GIS has been developed for the Environment Agency (North-West) for heavy rainfall warnings. The move from a desktop application to a web-browser utilising the internet has proved to be very important. Although we are still in the early stages of exploiting GISs, further customer applications are being developed for severe weather impact, weather and health, air quality and hydrological forecasting.

Underlying computer capability

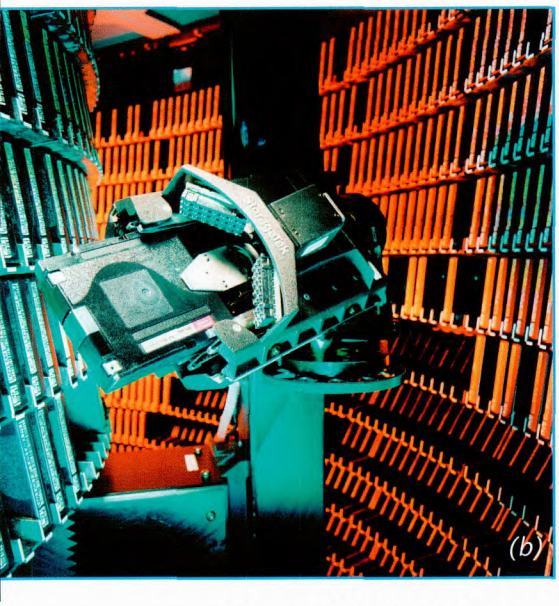

Figure 9. Views of MASS. (a) Outside and (b) the robot arm inside MASS.

Data management and storage

The Met Office has an unusually demanding requirement to store and retrieve a vast and ever-increasing amount of data — such as observational data from automatic sources, raw satellite and radar products, climatological archives, high-resolution numerical model data and output from the Climate Prediction Programme. Both hardware and a data management system — our managed archive storage system (MASS) — have been introduced to facilitate management of these data.

For the development of MASS, we received a Process Innovation Award, from Kinetic Information, at the eSolutions World Conference in August 2001 (Figs 9 and 10). We developed MASS using an automated tape library supplied by FileTek to create one of the world's most sophisticated, leading-edge data storage systems. At the start of 2002, it went into full production as the Met Office's strategic data repository, providing internal customers with a standard access method to all our data resources. MASS significantly improves responsiveness and staff productivity compared with the previous storage facilities. Business users and researchers now have access to powerful interactive facilities enabling access to any stored data.

Since late 2001, MASS has been based on eight high-density StorageTek 9940 drives, in addition to the existing 16 high-performance StorageTek 9840 drives. The use of higher-density media means we can make greater use of space in the existing StorageTek PowderHorn Automated Tape Library. MASS will cater for our projected data archiving requirement for at least the next five years — an anticipated data growth of almost up to a petabyte (i.e. 10^{15} bytes).

Supercomputer facility

We use two Cray T3E supercomputers to run our operational numerical weather prediction models, climate research models and some other environmental model work (see later chapters). We need increased capacity and capability to improve the performance of our models, especially in weather forecasting for a few hours ahead and in the prediction of extreme and significant weather events. Finer detail in the modelling is also required for climate studies. Increasing volumes of observational data, especially satellite data, will help to achieve this but they will require more computing power. Improved model resolution is also necessary but this requires increased computer capacity.

We are replacing the current supercomputers when we relocate to Exeter, Devon. We will choose a supplier for the new computer later in 2002 so it will be ready for installation in Exeter.

General Purpose Computing Service

The General Purpose Computing Service (GPCS) is run on a mainframe platform based on IBM's proprietary operating system (OS/390). It forms the Met Office's main system for data processing both for operational production and for other work. It provides the necessary added value to the raw model data generated by the supercomputer before products can be released to customers. Use of the mainframes has continued to grow by about 12% per annum. External benchmark tests conducted during the year demonstrated that this system continues to give excellent value for money.

We carried out a project to assess the advantages of transferring the GPCS to a Unix-based platform. As a result of the positive outcome of this assessment, GPCS will migrate to Unix, but we will delay the transfer until after our relocation to Exeter. Some groundwork for the conversion has already been completed.

Developments in data communications

The world meteorological community depends on a reliable and speedy exchange of observational data on both a national and international scale. These data are essential for the rapid generation of accurate meteorological forecasts. The same data communications systems are required for the distribution and exchange of forecast products to internal, external, national and international customers.

The Weather Information Network was the communication network infrastructure that delivered weather data to and from front-line stations. It was designed before internet protocol (IP) standards became widespread, and was based on highly specialised X25 protocol software. We completed our project to move to using IP methods in December, giving access to a wider skills pool and to cheaper technology, and allowing us to retire many old communications lines. The new network, the Met Office Remote Sites Network (MORSN), provides a more reliable and speedier exchange of data.

The current main message switch, which meets our international commitments for the exchange of worldwide data as well as internal requirements, is being replaced by new hardware running Unix operating system software and externally provided message-switching software. The

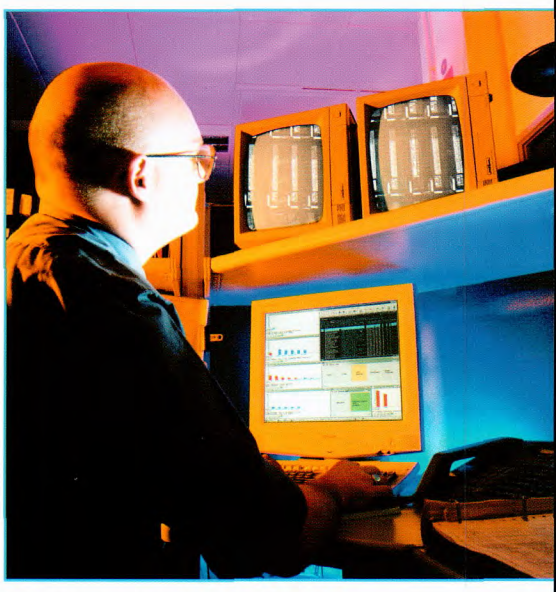

Figure 10. Monitoring MASS.

new system, Future options for Tropics (FROST), has been designed to provide a fast and reliable service now and, in addition, to ensure that future expansion requirements can be met.

Desktop

The desktop computing environment is an essential tool for many of our business processes and for scientific research. As many components of our current desktop service are nearing the end of their useful life, our relocation to Exeter provides an opportunity for an innovative approach to the replacement of these systems.

The Desktop Replacement Project is intended to take advantage of a number of technological advances in order to enhance our productivity by increasing standardisation and reducing complexity. It is also expected to increase opportunities for effective collaboration, by improving and further standardising electronic communication facilities, and enable flexible working patterns, by improving the facilities for remote and mobile workers. The new desktop is scheduled to coincide with our relocation to Exeter in 2003.

Managing IT Operations

Running the Met Office's operational IT requires the support and management of a wide variety of systems, including the mainframe system, the supercomputers, MASS, the various telecommunication systems and many production systems. To enable IT Operations Centre staff to manage these on a continuous 24-hour, 7-day basis, we use Tivoli automated systems management to monitor and recover systems. This provides a more consistent interface and enables staff to concentrate on aspects of managing the system where their expertise will provide maximum benefit.

During 2001, we introduced a new integrated incident and change management system. Incident Management is now fully operational and the majority of support teams are now using this to manage the incidents raised against their systems. A new change control interface is being developed and will be introduced in 2002, enabling the monitoring of change requests, from the initial request through to its implementation in operational systems. The integration of incident and change management will improve the quality of service to customers, both internal and external.

Forecasting

Nowcasting

Automated site-specific forecasting

Evaluation

Aviation

Defence

Health forecast services

Marine forecast services

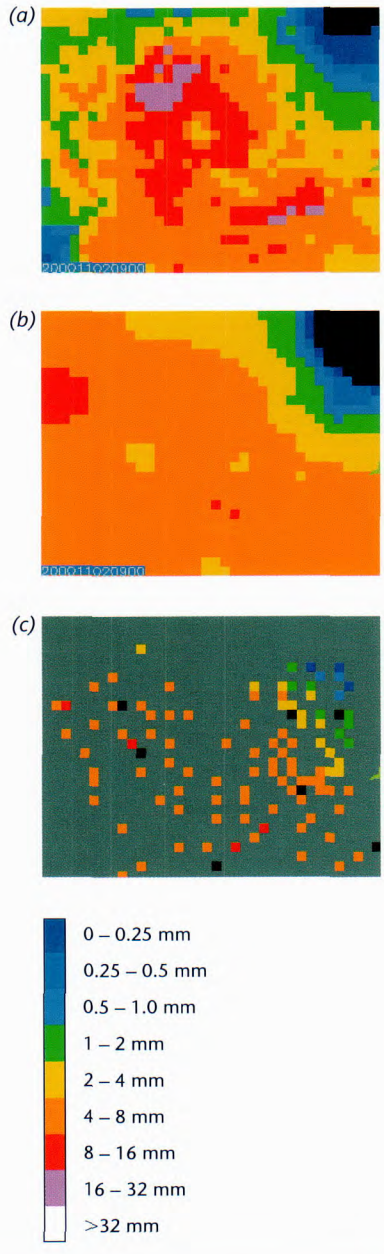

Figure 11. One hour rainfall accumulations from 2 November 2000. (a) Chenies radar accumulation; (b) radar/gauge combination using KED; (c) independent verification gauges (not used in KED). Residual bright-band effects, noticeable in the radar accumulation, are removed in the radar/gauge combination.

During 2001/2 we have widened our development activity and continued to work on the key automated facilities for site-specific forecasting and nowcasting. Our wide range of work characterises the applied research carried out for defence and civil aviation. Verification is taking a higher profile as the demand increases for justification of the cost of forecast production and development.

Nowcasting

Rainfall accumulation analyses

As part of the Met Office/Environment Agency Rainfall Network Collaboration Project, we have carried out a study to establish the best method for combining quality-controlled radar data and rain-gauge data to provide optimum estimates of rainfall accumulation for hydrological use. The study was undertaken to ensure that best use is made of around 400 Environment Agency gauges that will become available in real time. We tested several methods and found that a geostatistical technique known as kriging with external drift (KED) performed best (Fig. 11). This technique improved on radar-only accumulations down to a one-hour accumulation period, using the projected gauge density. KED is not a real-time radar adjustment technique and will be applied in near real time to radar data that have already been quality controlled. The new analysis has been implemented and will be made available operationally when the additional rain gauges come online.

Nimrod's surface hydrology and soil state model

We have implemented a soil state diagnosis model as part of the Nimrod nowcasting system. We input Nimrod's analyses of precipitation, snow probability, cloud cover, near-surface temperature, humidity and wind into the model, which then calculates run-off, evaporation and soil moisture hourly on Nimrod's 5 km grid (Fig. 12). The calculations are performed by the Met Office Surface Exchange Scheme (MOSES), modified to include the Probability Distributed Moisture (PDM) model developed at the Centre for Ecology and Hydrology (CEH), Wallingford. The PDM enables MOSES to represent soil heterogeneity and thereby calculate more realistic run-off. The soil moisture field from Nimrod will be used to initialise the corresponding field in the mesoscale numerical weather prediction (NWP) model if trials are successful. A comparison with the Met Office Rainfall and Evaporation Calculation System (MORECS) is under way to support customers' migration to the new products.

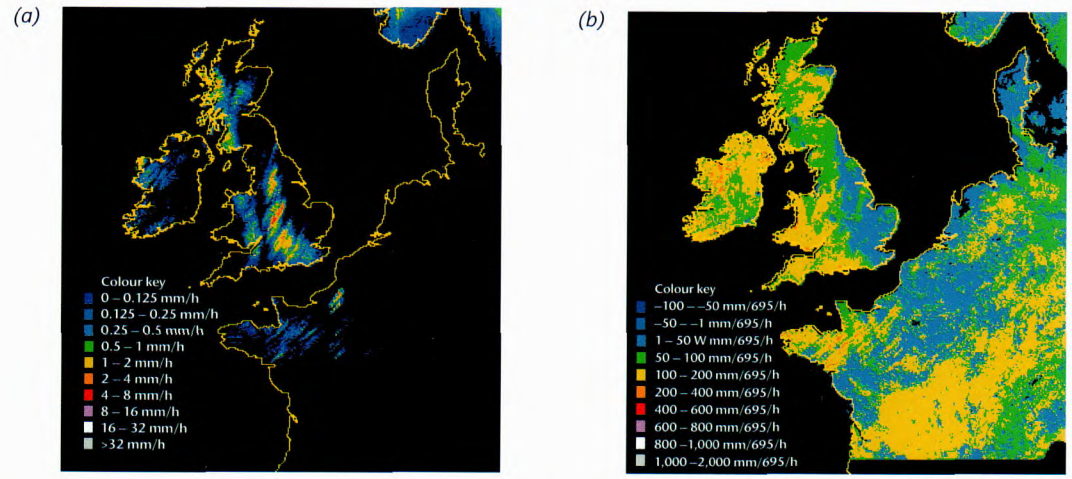

Figure 12. (a) Accumulated surface run-off (mm h^{-1}) and (b) mean surface evaporation (mm/695/h is equivalent to W m^{-2} of latent heat), both calculated by Nimrod's hydrology model from 1300–1400 on 15 October 2001.

Severe convective weather

Following a series of case studies last year, we have developed statistical equations to predict the likelihood of severe weather occurring in conjunction with convective storms in the UK, including equations for the occurrence of large hail (larger than 2 cm), tornadoes, and frequent lightning (Fig. 13). A detailed performance study shows that these provide useful results for hail and lightning prediction, although they are not yet as accurate for tornado prediction. Forecasters can now access the results through a web interface.

GANDOLF nowcasting scheme

The 2 km-resolution GANDOLF precipitation nowcast scheme combines the functionality of the Nimrod extrapolation scheme, developed for short-range prediction of widespread, stratiform precipitation, with several object-oriented, conceptual, life-cycle models designed for the nowcasting of severe convective precipitation (Fig. 14). After extensive trials, we introduced products from GANDOLF operationally in August.

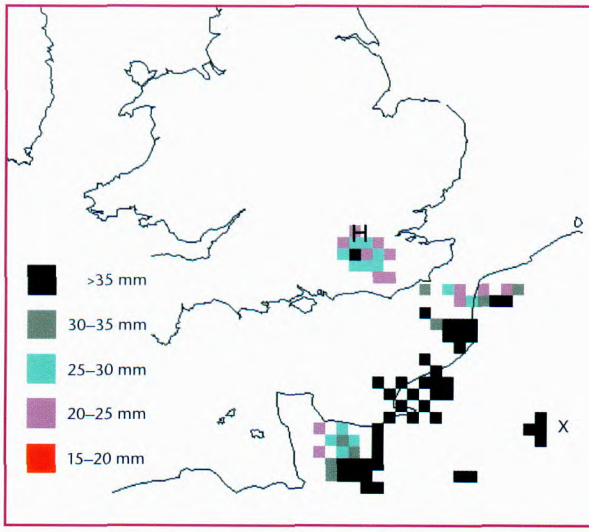

Figure 13. Two-hour forecast of expected large hail size if hail occurs. The bottom left hand corner of the letter 'H' indicates the location of 'golf ball' size hail (approximately 40 mm in diameter) observed at Kingston in Surrey at 1645 UTC on 5 September 1999.

Cloud diagnosis

Using Meteosat images, we have developed a new cloud detection scheme for Nimrod. The visible component remains unchanged from the previous scheme; the new infrared component uses mesoscale model forecast data and a radiative transfer model to compute threshold values for each grid

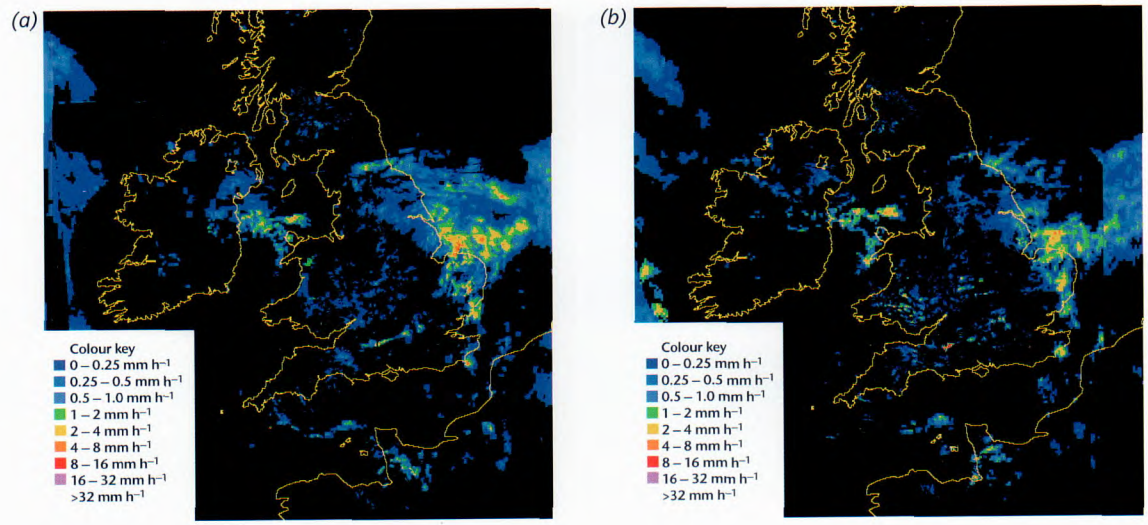

Figure 14. (a) GANDOLF 60-minute rain rate forecast and (b) verifying rain rate analysis (2 km resolution) valid at 1100 UTC, 6 August 2001.

point. We compare them with the Meteosat infrared values to determine whether a pixel is mainly cloudy or mainly clear. The outputs from the visible and infrared components are combined to produce a cloud cover map that is significantly more accurate than the previous scheme, particularly over the sea and at night (Fig. 15). We introduced the new scheme operationally in November.

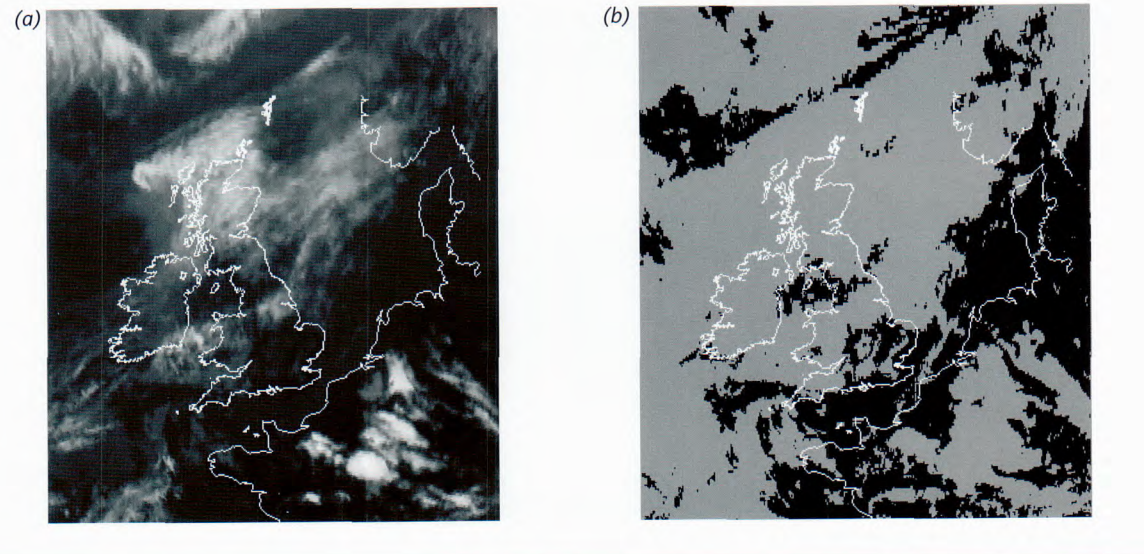

Figure 15. (a) Meteosat infrared image and (b) new Nimrod cloud cover map on 26 July 2001 at 1700 UTC. The cloud cover map was derived from Meteosat infrared and visible images (grey = cloud, black = no cloud).

Automated site-specific forecasting

Site-specific forecast model

We have further developed the Site-specific Forecast Model (SSFM). After improving the efficiency of data extraction and forecasts on the T3E, forecasts for 3,000 sites were produced using the global Unified Model (UM) as forcing (Fig. 16). Only limited assessment of the results has been possible to date, but several sites have been identified where anomalies in the model output statistics (MOS) forecasts have been corrected by moving to the SSFM.

Figure 16. World map showing the locations of forecast sites as red dots.

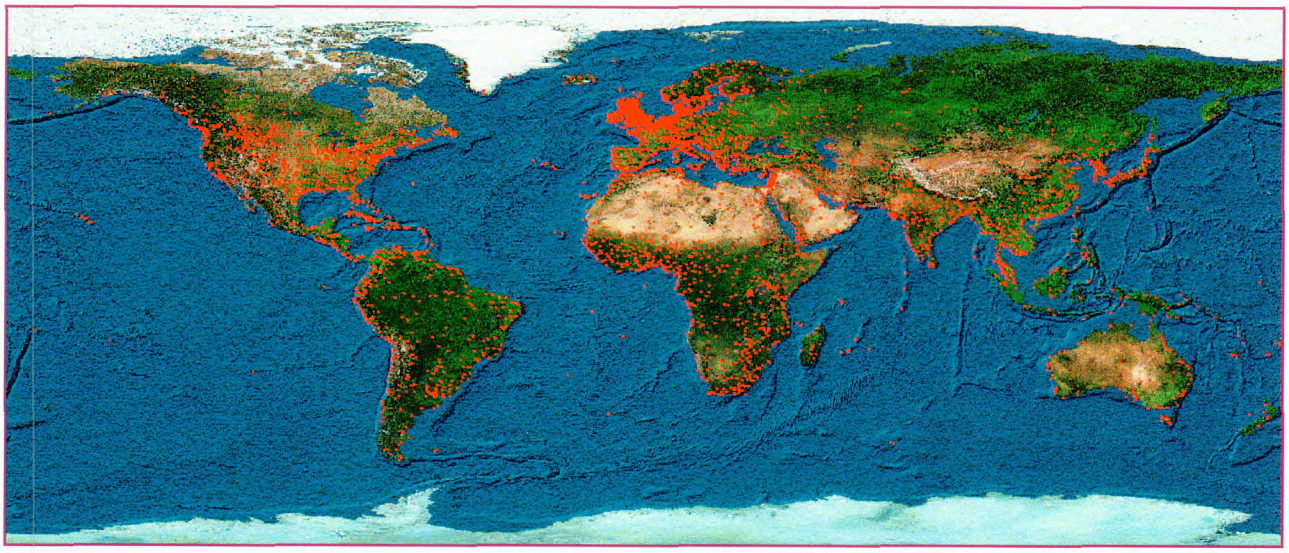

Road-surface temperature model

We have made further enhancements to the Met Office Road-surface Temperature (MORST) model, mainly to include the effects of nearby buildings and traffic. In trials, the principal benefit was a significantly reduced cold bias in urban areas. We implemented the enhanced model for operational use in Winter 2001/2 (Fig. 17).

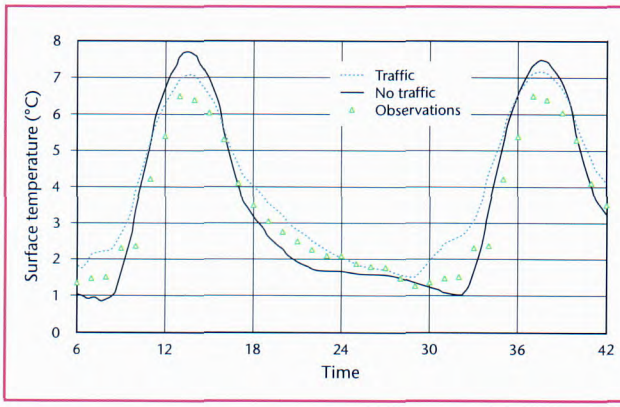

Figure 17. Average forecast of road surface temperature for a site on the A40 near Carmarthen in January 2001, with and without the effects of traffic, compared with average observations from the site.

Automated text

Automated text forecast production has long been seen as a means of improving efficiency. The structure of many text forecasts is adapted to manual production and has proved difficult to replicate automatically. However, there are many services that need a text component without the requirement for grammatically correct composition. This is especially true for simplified forecasts such as those

Predicción para MADRID 320016
válida desde 00:00 el 21/02/2002
hasta 12:00 el 22/02/2002

Madrugada

Cielo: despejado

Temperatura: temperaturas sin cambio a 4 grados C

Viento: oeste girando al noroeste 3

Tiempo: seco

Visibilidad: buena

Figure 18. Extract from an automated Spanish language forecast for Madrid.

delivered through mobile phones. In response to this, we developed a generic text generation facility using the language Prolog. It currently provides forecasts for a single time, or period of time, at a single location. The benefits are its speed of production and flexibility — thousands of forecast locations are available. We are currently testing a web-based demonstrator, offering four languages: English, French, German and Spanish (Fig. 18); Dutch, Italian, Portuguese and Greek will be added shortly. We are also using a version of the code to provide forecasts to Orange.

Medium-range ensemble forecasts

Forecasting the weather with a numerical model involves significant uncertainty due to the sensitivity of the forecast to small errors in the initial state. This becomes particularly acute when forecasting further ahead, beyond about three days. To help assess this uncertainty, we use output from the Ensemble Prediction System (EPS) run by the European Centre for Medium-range Weather Forecasts (ECMWF). Ensemble prediction is designed to estimate uncertainty by running multiple forecasts, 51 in the case of the EPS, each from slightly different initial conditions, within typical analysis errors. We can use the output to assess the most likely outcome and range of uncertainty, and to generate probability forecasts. To allow automated production of ensemble forecasts for specific locations, we have implemented a statistical method to derive local forecasts of temperature, wind speed and rainfall amounts from the EPS output. We have found that ensemble distributions do not fully account for the uncertainty in a forecast, so we calibrate them using statistics from past forecasts (Fig. 19).

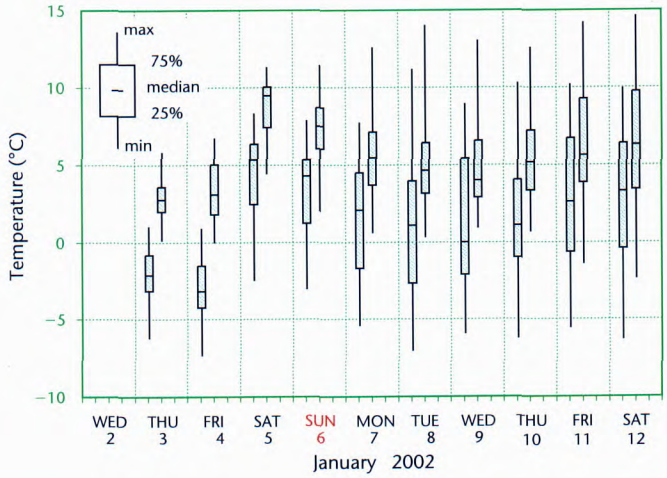

Figure 19. Ten-day calibrated ensemble forecast of maximum and minimum temperatures (° C) for Heathrow from 1200 UTC, 2 January 2002. Each symbol shows the spread of uncertainty (2% and 98% confidence limits) from bottom to top, the inter quartile range (25% to 75%) in the central box and the median at the horizontal line. There is high confidence in a transition from cold to milder conditions after the first two days, with increasing uncertainty later.

We have carried out comparisons between calibrated ensemble temperature predictions and manual forecasts. Previously, comparisons with raw ensemble output showed that manual forecasts added little to the accuracy of the mean value, but were significantly better at defining the range of uncertainty. In Figure 20, the green bars show that the calibrated ensemble predictions now have comparable accuracy in defining the 95% uncertainty range. They replaced the raw ensemble products operationally during the year. Blue and red columns make the same comparison for the lower and upper 2.5% outliers, respectively. The two versions of the day 2 forecast refer to different times of issue of the manual product — the automated product is identical.

Monthly and seasonal ensemble forecasts

We developed an interface to extract site-specific forecast data from the Met Office nine-member monthly and seasonal forecast ensembles for storage in the site-specific forecast database. Gridded monthly anomalies are interpolated in time and space before storage in FSSSI. On extraction, they are combined with daily site-specific climate values, also stored in the database, to give a monthly mean site-specific forecast centred on each day (Fig. 21). The system became operational, in support of weather derivatives services, in February.

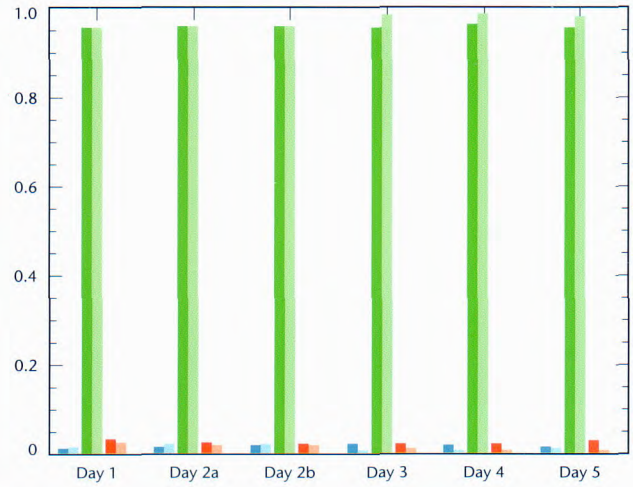

Figure 20. Comparison of manual (dark colours) and automated (light colours) probability predictions of minimum temperature for 10 UK locations in Autumn 2001. For a perfect forecast, the green column would have a value of 0.95.

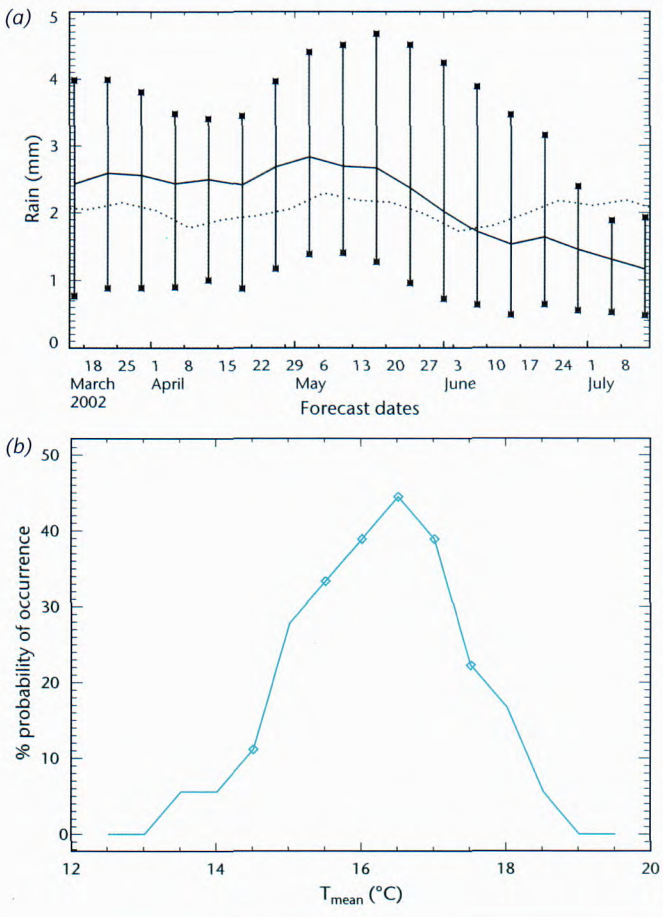

Figure 21. Output from the seasonal ensemble for Paris Orly airport. (a) Time series of monthly mean daily rainfall. The full line shows the mean; the bars show the ensemble range. The dotted line is the climatological average. (b) Monthly mean probability distribution of mean daily temperature on day 84 of the forecast.

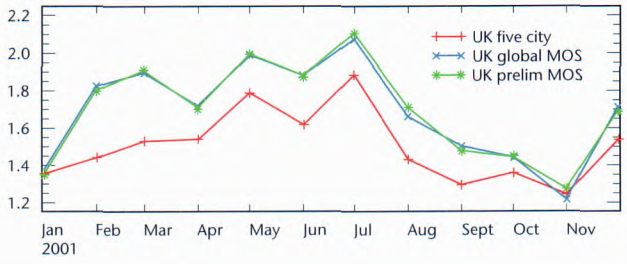

Figure 22. Five cities forecast verification: average r.m.s. error (°C) of 24-hour maximum temperature forecasts for five cities.

Evaluation

Five cities forecast verification

We provide a key measure of forecast accuracy using the five cities verification, part of the Service Quality Index. The forecasts are published on the Met Office web site and comprise temperature, wind and weather predictions for up to three days ahead for Manchester, Edinburgh, Cardiff, Belfast and London. To assess the value of manual input, a verification scheme has been introduced operationally to compare the forecasters' performance with MOS forecasts. Results in 2001 for the 24-hour maximum temperature forecast (Fig. 22) show an average reduction in r.m.s. error of about 0.2 °C, confirming the value of manual modification.

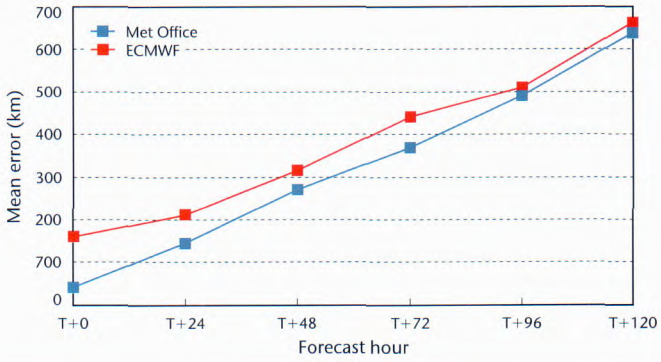

Figure 23. Comparison of the mean absolute deviation of Met Office and ECMWF forecasts of tropical cyclone track from actual track against forecast lead time for all cyclones identified in 2001.

Tropical cyclone verification

The performance of our tropical cyclone forecasts continues to be world-leading due to ongoing improvement and use of a tropical cyclone 'bogusing' scheme based on official advisories. In 2001, the results for mean position error continued to show the benefits of this approach (Fig. 23).

Warnings verification

We developed a new verification system for coastal wind warnings to enable monitoring of these important safety products. Owing to the lack of observations in coastal waters, the verification code was developed with several estimates of the true state. Table 1 shows the results, expressed as hit rate, false alarm rate and threat score, for one coastal area during 2001. Observations alone under-represent the maximum wind speed, and hence result in the highest hit rate and false alarm rate. The other two estimates of truth allow for the variation of wind at sea in different ways, but both incorporate NWP model information. It is encouraging that the hit rates of these two techniques are so close. We shall carry out further trials before implementing an operational scheme.

Estimate of truth	Hit rate (%)	False alarm rate (%)	Threat score (%)
Observations	85.8	27.8	64.5
Nimrod	76.0	17.0	65.8
On-screen analysis	78.7	22.2	64.3

Table 1. Verification of 176 coastal wind warnings issued in 2001 for the coastal area from Solway Firth to Colwyn Bay, using three estimates of truth: coastal observations alone; the Nimrod automatic wind analysis; and an interactively generated 'on-screen analysis'.

Altimeter pressure settings (QNH)

Production of pressure ('QNH') nowcasts for aviation altimeter settings has been semi-automated for many years. The forecaster interactively modifies the NWP first guess using the Horace 'on-screen analysis' tool. The QNH forecast message is generated automatically from this analysis and then subjected to a final manual check before issue. On the basis of operational verification results, forecasters have been encouraged to reduce the frequency of these final amendments. Results for 2001 show that the first step introduces substantial gains in accuracy (Fig. 24). The frequency of modification at the second step has been reduced to 2.5% and produces a further slight gain in accuracy.

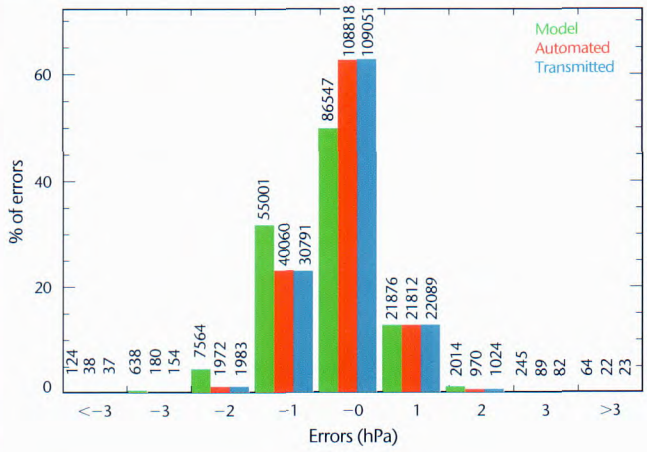

Figure 24. Forecast QNH verification: 12-month distribution of errors for 2001 from forecast QNH comparing model, automated (using an interactively enhanced wind analysis) and final transmitted forecasts. Errors are in 1 hPa bands.

Feature verification

The histogram in Fig. 25 contains a full record of cyclone frequency for lead times (in hours) during 2000 in Met Office model analyses (bar cluster labelled '0', representing what actually happened) and forecasts (other clusters). Bar colour indicates intensity, with the most extreme, damaging cyclones in yellow, green and red. Intensity categories are defined by the severity of the surface winds around each cyclone; strengths increase from left to right within each cluster. Reassuringly, a comparison of bar heights shows that there is no clear systematic tendency for the Met Office's model to over- or under-predict extreme cyclones. However, the frequency of more modest cyclones (pink and dark blue) is under-predicted by about 25% at lead times of two days or more. These results are based on new, automated techniques for identifying and categorising cyclones that have been developed over the past few years.

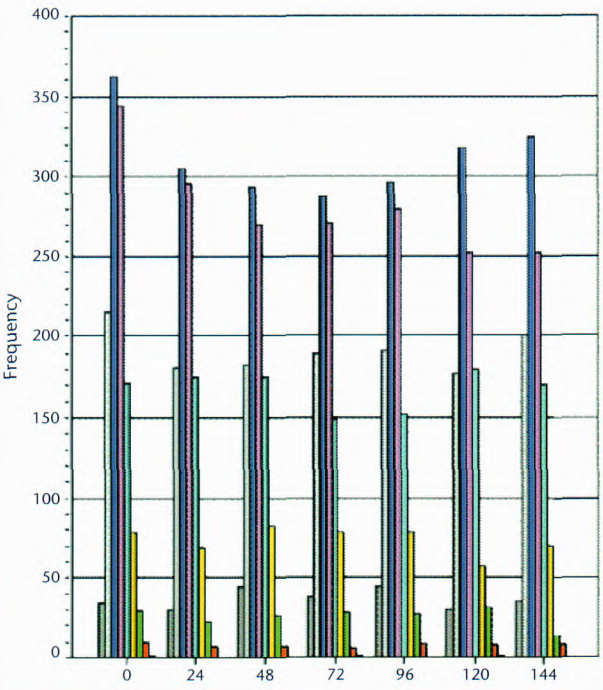

Figure 25. Forecast 'cyclone spectra' for 2000 for an extended North Atlantic sector.

Aviation

Optimum route calculation

We have developed a web-based demonstrator using our optimum route diagnosis interface. The web interface allows the user to specify characteristics of the required flight, including departure and arrival

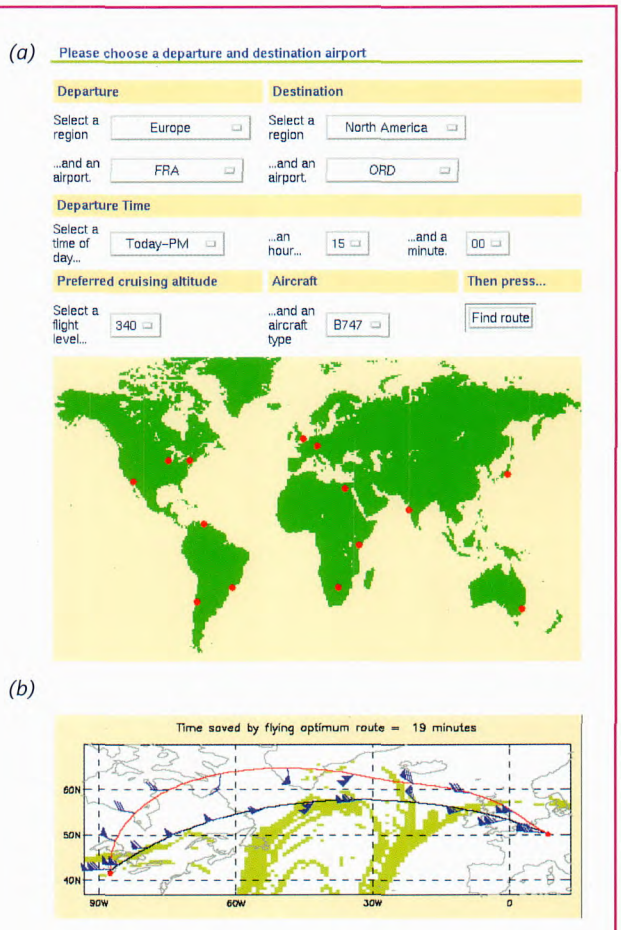

Figure 26. (a) User specification web page for the optimum route demonstrator. (b) Optimum route in red, with the equivalent great circle route in black and forecast spot winds along each track. Green shading indicates areas of possible turbulence.

locations and aircraft type, and then returns a map showing the optimum and great circle routes (Fig. 26). The user can gain additional information from this presentation — winds along the track are displayed by rolling the mouse pointer along it, while clicking the mouse on the track brings up information for the whole route, together with forecasts for nearby aerodromes.

Volcanic ash detection

Volcanic ash poses a serious threat to aircraft safety, so accurate and timely information about the location of volcanic ash is essential to the aviation industry. Met Office forecasters act as the London Volcanic Ash Advisory Centre, issuing advisories to aviation customers about the presence of volcanic ash in their designated area. We are developing two products to support them.

The first product displays differences between radiances measured at two infrared wavelengths by the Advanced Very High Resolution Radiometer (AVHRR) satellite instrument. Volcanic ash in the atmosphere typically produces negative values, while clear atmosphere, water and ice clouds typically produce positive values. This product is now provided operationally every three hours. Figure 27 shows a volcanic ash cloud from Mount Etna's eruption on 23 July 2001 at 1243 UTC.

The second approach provides a quicker response using the more-restricted data available half-hourly from Meteosat. It searches infrared images for clouds near a volcano that have a shape which may indicate volcanic ash, given the local wind and temperature conditions. With the system parameters calibrated to detect seven test eruptions, it successfully detected the Etna eruption but missed an eruption of Montserrat. The false alarm rate is currently too high for operational use, but our future work should reduce this by accounting for the temporal and spectral characteristics of volcanic ash.

Uplinking forecasts to aircraft

Using the Met. Research Flight C-130, we have demonstrated the capability to uplink nowcasts of clear air turbulence (CAT) to an aircraft in flight. During flight, the C-130 regularly communicated its position to the ground.

This information was used by a system running at Bracknell to create a CAT forecast for the area surrounding the aircraft based on mesoscale forecast data. The forecast can have a lead time of up to nine hours, so it was nudged towards the latest commercial aircraft observations using an optimal interpolation scheme called WAFTAGE. We then applied the Roach–Keller CAT indicator to predict the severity of turbulence and produced T+0 and T+1 forecasts for three pressure levels above and below the height of the aircraft. The severity of turbulence was then coded as an integer between 0 and 3 to minimise the length of the message sent to the aircraft (Fig. 28).

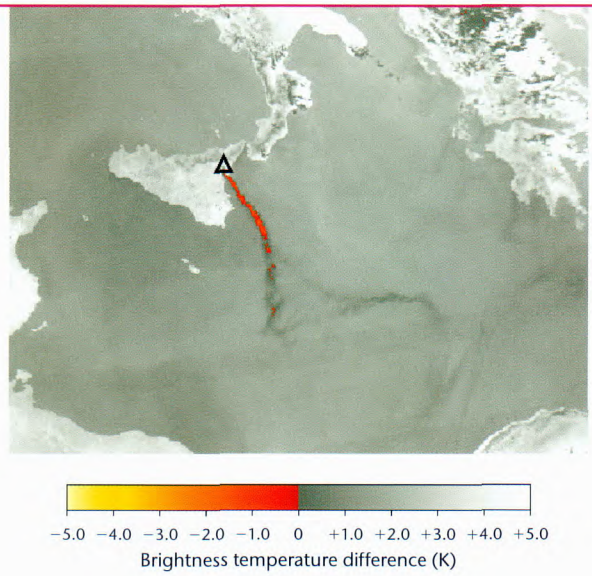

Figure 27. Volcanic ash cloud from the eruption of Mount Etna, Italy, displaying the difference between AVHRR measurements at two wavelengths. The location of volcanic ash is shown by the negative values (red to yellow colours). The black triangle marks Etna.

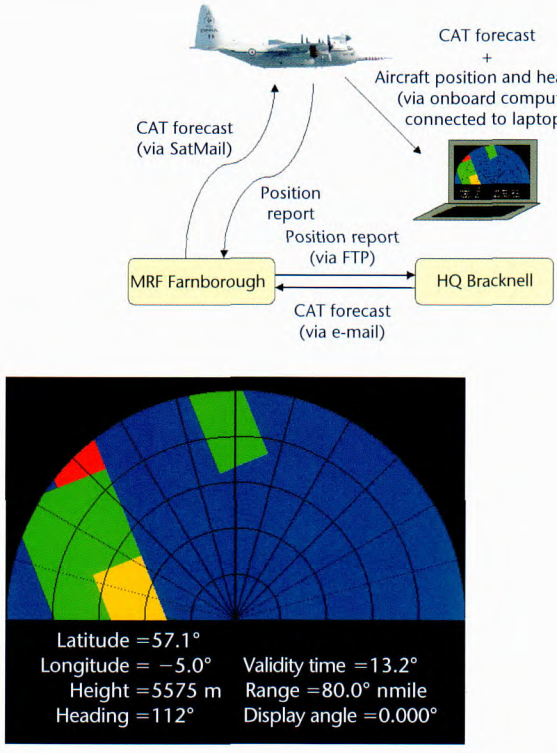

Figure 28. (a) Information flow for the automatic downlinking of position, and subsequent uplinking of a clear air turbulence nowcast to an aircraft in flight. (b) Sample cockpit laptop display, showing turbulence areas relative to the aircraft heading.

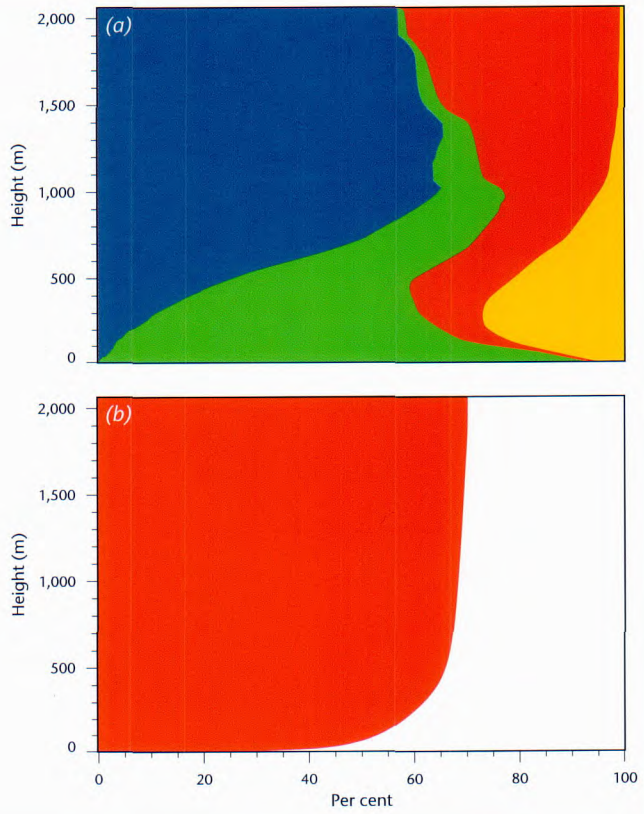

Figure 29. Vertical profiles of WVBC for London Heathrow runway 09L-27R. (a) Profiles for site-independent WVBC. Blue: null class ($Ri \geq 1$ and $N < 0.014\ s^{-1}$); green: turbulence class ($Ri \leq 0.25$); red: stable stratification class ($Ri \geq 1$ and $N > 0.014\ s^{-1}$); yellow: wind shear class ($S < 0$ and $0.25 < Ri < 1$). (b) Profile of the crosswind WVBC with a 6 kn threshold. The horizontal extent of each colour gives the percentage of time that a given class occurs.

Climatological study of wake vortex behaviour

Wake vortices form at aircraft wingtips during flight and pose a hazard to following aircraft. At busy airports, the frequency of aircraft movements is restricted by aircraft separation rules imposed to address safety concerns associated with wake vortex encounters. The current separation rules have been highly effective in reducing wake vortex encounters, but there are situations where they appear to be too conservative.

Atmospheric conditions play a key role in the evolution and behaviour of wake vortices. In collaboration with Deutsches Zentrum für Luft- und Raumfahrt, DLR-PA (Germany) and Météo-France, we are developing several discrete Wake Vortex Behaviour Classes (WVBC) as part of the European Commission project S-Wake. In these classes, vortices are expected to exhibit differing evolution characteristics and behaviour. Four of the classes — turbulence, stable stratification, wind shear and null — are site independent and mutually exclusive. They are determined by the bulk Richardson Number (Ri), Brunt Väisälä Frequency (N) and wind shear (S). The fifth class — the crosswind class — is site-dependent. It indicates whether the crosswind across the runway exceeds a threshold. This often reduces the risk of a wake vortex encounter because the vortices are swept off the runway. However, if a parallel runway is present, the level of risk may increase due to one or both vortices being blown onto the adjacent runway. As part of the S-Wake project, we established climatologies for these WVBC at a variety of airports worldwide, using the Met Office Site-specific Forecast Model (Fig. 29). We compiled the climatologies over a seven-year period, from 1979 to 1985, and found that at many airports, WVBC favouring rapid dissipation of wake vortices are prevalent more than 30% of the time.

Defence

Met Office Night Illumination Model (MONIM)

Tactical decision aids (TDAs) are used to support training and operational activities at RAF stations throughout the UK and abroad. As part of an upgrade programme, we implemented a new physically based night

illumination TDA (MONIM) operationally during the year. Use of the TDA is through a simple PC-based graphical interface with results plotted for a range of cloud conditions (Fig. 30).

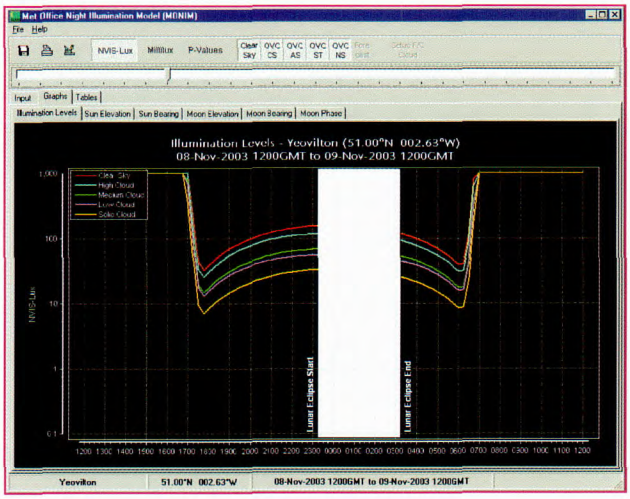

Figure 30. Screen display of MONIM-predicted illumination for Yeovilton for the night of 8/9 November 2003 in units of NVIS-Lux. Because of the full moon, even beneath solid cloud the illumination levels are acceptable for night flying except perhaps during a lunar eclipse. No attempt is made to predict light levels during an eclipse as this depends upon factors such as the dust levels in the Earth's atmosphere.

Airflow near coasts

As part of a research programme to develop improved models of airflow in the littoral zone, experiments have been carried out with the New Dynamics version of the UM, using the Strait of Dover as an example. The model has been run on nested grids of 12 km (as operational), 4 km and 2 km horizontal resolution. At 12 km, the Strait of Dover is poorly resolved, but the higher-resolution forecast produces a well-formed, low-level Channel jet (Fig. 31). Numerical experiments with physical parameters in the model show that both the land–sea surface roughness contrast and the orography are important for jet formation.

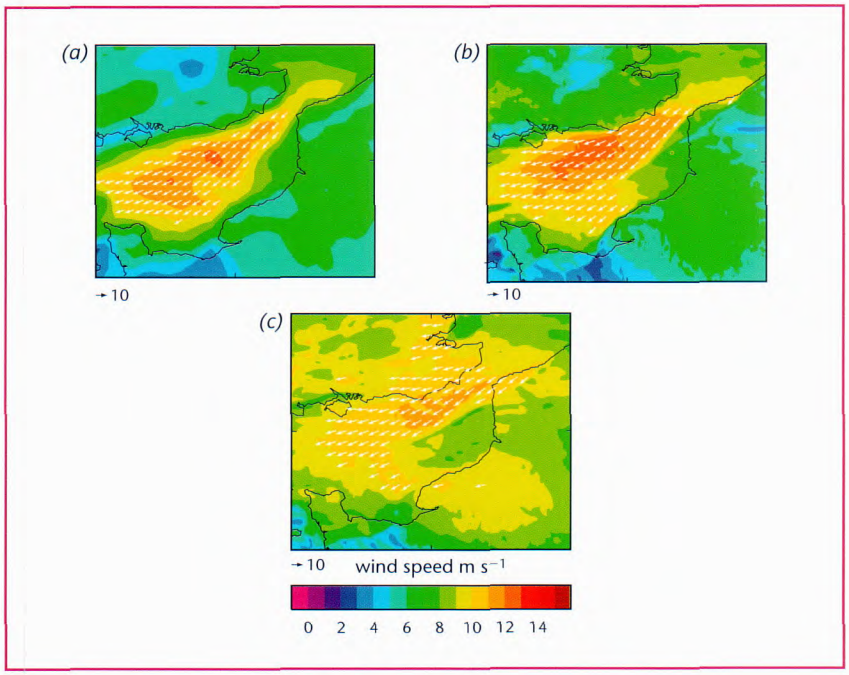

Figure 31. Detail from the 10 m wind forecast for 23 July 2000 using the New Dynamics mesoscale model at (a) 12 km and (b) 2 km horizontal resolution. At higher resolution, the forecast low-level jet is stronger and closer to the coast. (c) Weakened jet when surface orography is removed and surface roughness over land reduced.

Health forecast services

There is increasing evidence that changes in the weather, especially of temperature, can influence the workload of the National Health Service (NHS). We carried out a winter trial in 2000/1 to assess the viability of using real-time NHS data, infectious disease data and weather forecasts to predict

workload for a selection of NHS services. The trial was a success, with especially favourable comment from the Royal Berkshire Hospital, which avoided costs of £400,000 by taking the forecast into account when managing workload.

Subsequently, a pilot service was offered for Winter 2001/2 to collect, store and disseminate NHS data from 30 hospitals, 30 GP Co-ops and the 22 NHS Direct regions in England (Fig. 32). The front end of the system is a password-protected area of the Met Office web site where admissions and infectious disease data are entered. All data arrive as e-mail attachments, which are stripped out, processed and the data automatically stored in a database.

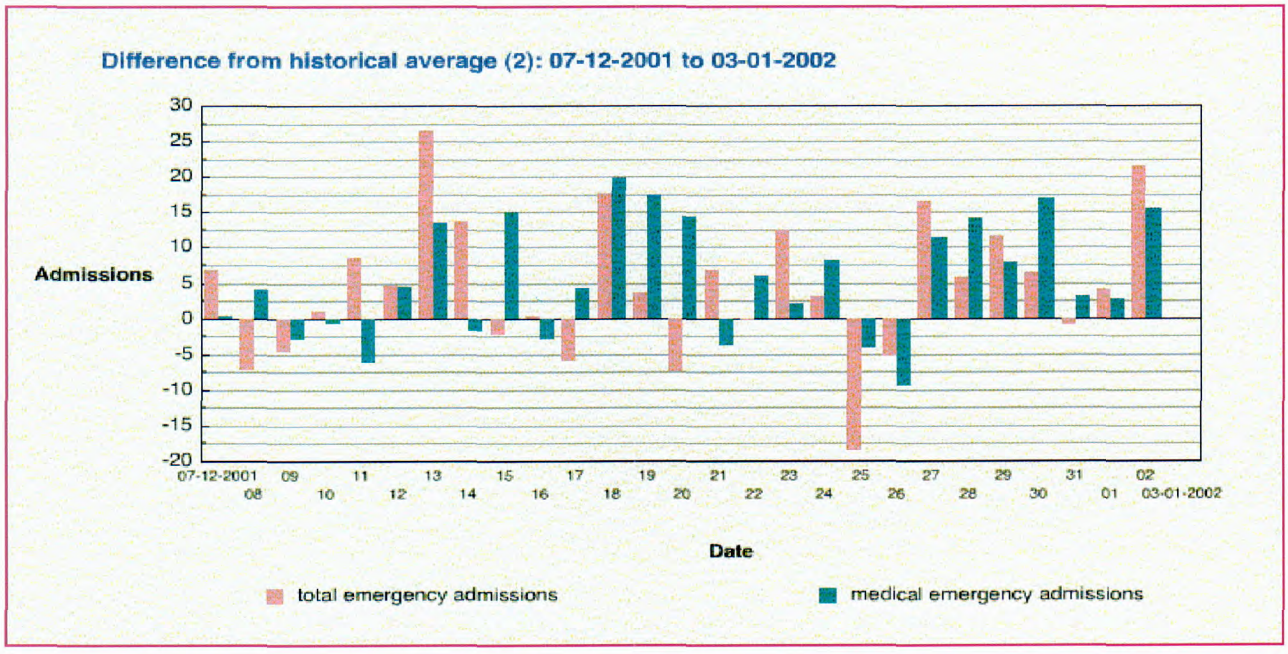

Figure 32. Extract from 'Forecasting the nation's health' *web site, showing deviations of actual from the historical average of hospital medical emergency admissions (in blue) and total emergency admissions (in pink) for the period 7 December 2001 to 3 January 2002.*

The current workload situation is displayed to users, together with regional weather forecasts and workload forecasts. Workload is currently forecast manually, but an automated model is being developed by the University of Southampton. This will forecast at postcode level, using historical and socio-economic data together with weather forecasts.

Marine forecast services

For some years, we have generated standard forecast products for the North Sea industry using an interactive production system at Met Office Aberdeen. During the year, we began migration of operational services to an improved, fully automated Marine Production System (MPS) following thorough testing (Fig. 33). The move followed analysis of extensive verification of offshore wind and waves, which showed that, on average, there was little benefit to these forecasts from manual input. The benefits of the new system lie in its flexibility, timeliness, update frequency and efficiency.

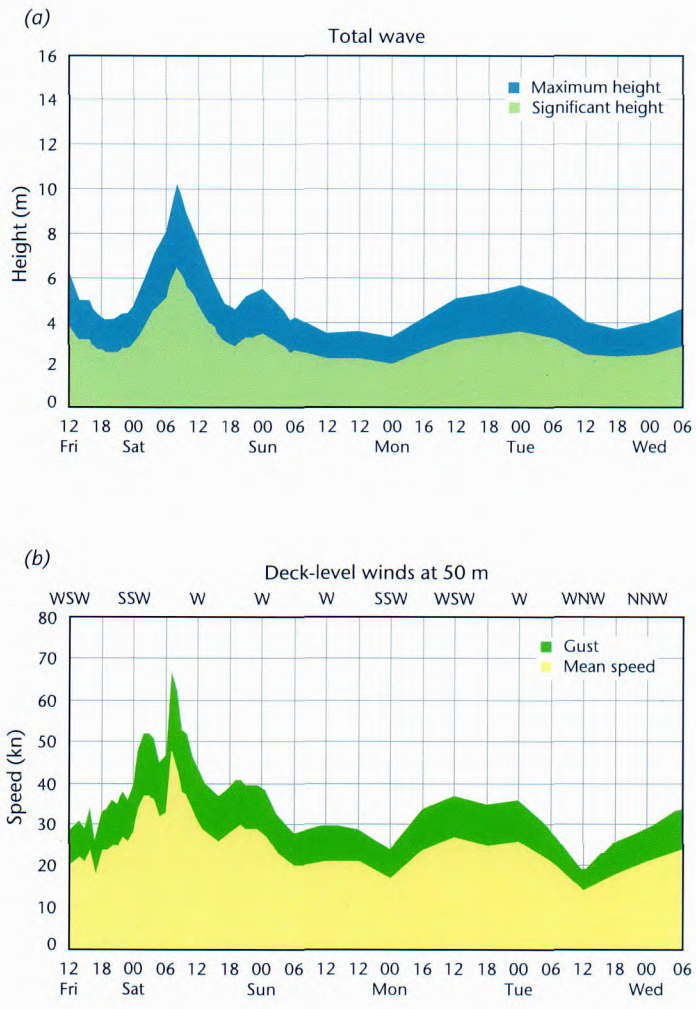

Figure 33. Samples of five-day automated MPS forecast products now being used for services to the North Sea industry. Both show site-specific forecasts, with an hourly interval at first, which increases as lead time increases. (a) Significant and maximum wave heights, (b) mean and gust wind speeds at 50 m (deck level), with wind direction marked at the top.

Numerical Weather Prediction

Development of the operational forecast models

Representation of physical processes

Applications of satellite data

Numerical weather prediction (NWP) forms the basis of most of the weather forecasting services provided by the Met Office. The numerical models that we use to produce these forecasts are developed within our Unified Model (UM) system, which provides the computational and scientific framework required for both NWP and climate prediction. We run these models at regular intervals throughout the day, to tight deadlines, in order to provide up-to-date forecast information. A global configuration of the UM using a 60 km grid provides forecasts out to five days ahead; a higher-resolution UK regional configuration using a 12 km grid provides more-detailed forecasts for the UK for up to two days ahead.

We undertake research into all aspects of the NWP system, with the aim of improving the accuracy of the operational forecasts. In the following, we have singled out three areas of research in particular.

The first is the ongoing development of a completely new formulation of the UM, known as the 'New Dynamics'. This work has involved not only a reformulation of the dynamical equations, but also a number of improvements to the way in which various physical processes are treated. This new formulation is scheduled for operational introduction in Summer 2002.

The second area of research concerns improving the prediction of cloud cover and cloud condensate in the UM.

The third area covers research into the use of satellite data. Successful developments in the processing and assimilation of these data continue to bring about improvements in the accuracy of forecasts produced by the operational NWP system.

Development of the operational forecast models

New Dynamics

The Unified Model uses finite-difference techniques to solve the equations describing the motion and thermodynamics of the atmosphere. A New Dynamics for the models has been developed that uses alternative numerical methods for solving these equations in a more robust and accurate manner. One of the differences is to have fewer approximations in the equations solved and, in particular, to take account of vertical accelerations making the UM fully non-hydrostatic. This new dynamical formulation provides the scientific foundation for very high resolution modelling, which is a key element of the long-term strategy for improving weather forecasts for the UK.

Atmospheric processes, which operate on scales smaller than those resolved by the current model resolutions, must be 'parametrized' to account for their effect on the large-scale flow. We have developed a number of improved parametrizations that form part of the New Dynamics implementation in the global forecast configuration, as follows.

- An improved radiation scheme, incorporating a more consistent treatment of the interaction of clouds with both long-wave and short-wave radiation. (*)
- An improved mixed-phase microphysics scheme, including a prognostic ice water content variable. (*)
- An improved boundary layer turbulent mixing scheme, including non-local mixing in unstable conditions and an entrainment parametrization.
- An additional eight vertical levels in the boundary layer for the global model. (*)
- Improvements to convection, including a shallow convection scheme and new parametrization of convective momentum transports. (**)
- Revised definition of cloud coverage, accounting for anvil cirrus clouds and cloud fractional variations in the vertical (Fig. 34). (**)
- Improved representation of orography:
  - use of new, global 1 km elevation source data to generate the orography fields, replacing the 20 km resolution US Navy data; (**)
  - smoothed orography fields to remove numerically undesirable gridscale and near gridscale forcing; (**)
  - use of a new sub-gridscale orography scheme that is both simpler and more robust than the existing scheme. (***)

(*) Many of these parametrization developments are already in use in the UK regional configuration of the Unified Model.

(**) Some developments are unique to the global forecast configuration.

(***) Others are also seeing their first implementation in the UK regional configuration.

Figure 34. An anvil cloud.

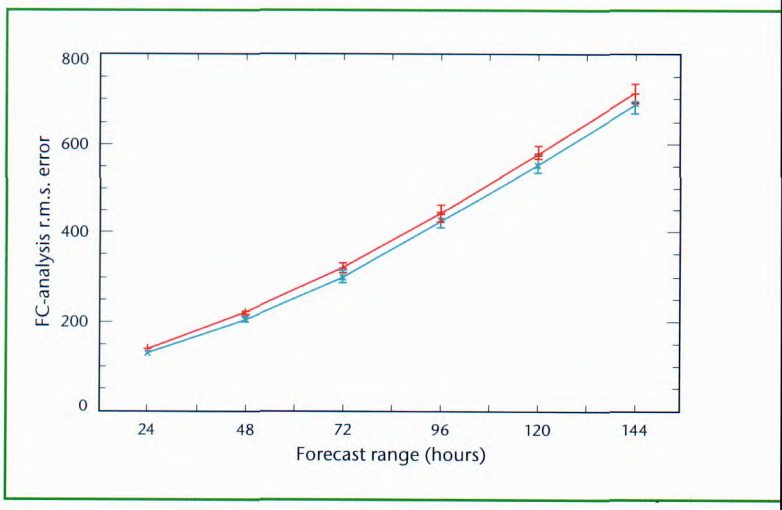

Figure 35. R.m.s. error growth against forecast range for mean sea-level pressure over the northern hemisphere. Verification is against analyses. Operational model (red) and New Dynamics formulation (blue) are shown. Error bars are shown at the 90% confidence level.

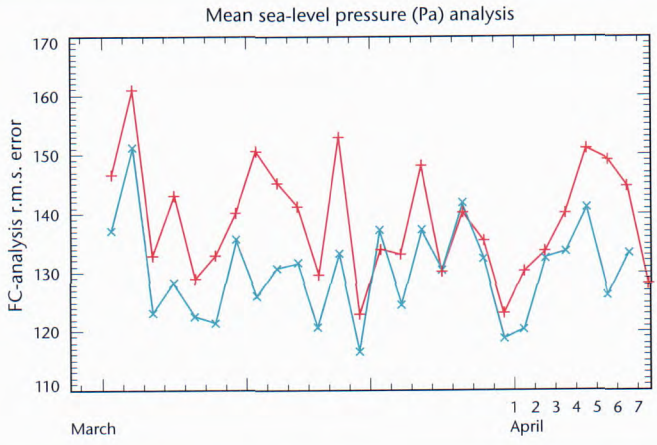

Figure 36. Time-series of T+24 r.m.s. errors for the 26 forecasts. Operational model (red) and New Dynamics formulation (blue) are shown for consecutive dates in March and April 2001.

These changes unify the treatment of physical processes between the different Unified Model configurations. Amongst other benefits, this will lead to a more consistent form of the global model boundary conditions used to drive the UK regional model.

An extensive series of trials carried out during 2000–1 has shown the new model to be an improvement over the current operational version.

Improved global model performance

These changes give an overall improvement in forecast verification. For example, during a trial over the period March–April 2001, 23 out of 26 forecasts showed smaller errors at day one than with the operational model. Figures 35 and 36 show the root-mean-square (r.m.s.) error of the forecasts.

The trials have also provided evidence of improved forecasts of extreme events. Deep extratropical cyclonic storms have been better predicted, such as the 'Danish Storm' of 1999 (Fig. 37), and forecasting of tropical cyclones has also consistently improved. From the figure, we can see that the New Dynamics forecast is 9 hPa deeper and closer to the verifying analyses. Statistics calculated over a large number of tropical cyclones show that the New Dynamics can better maintain the intensity of cyclones throughout the forecast period (Fig. 38) compared to the old model, which tends to systematically reduce the intensity of tropical cyclones. One example is Typhoon Podul, which was better predicted both in terms of its position and its intensity (Fig. 39). We can attribute these improvements to the accuracy of the New Dynamics and the ability to run the model with less numerical diffusion. The new integration scheme is also more numerically stable, which means the New Dynamics method is less prone to the occasional 'numerical noise' seen in the operational model.

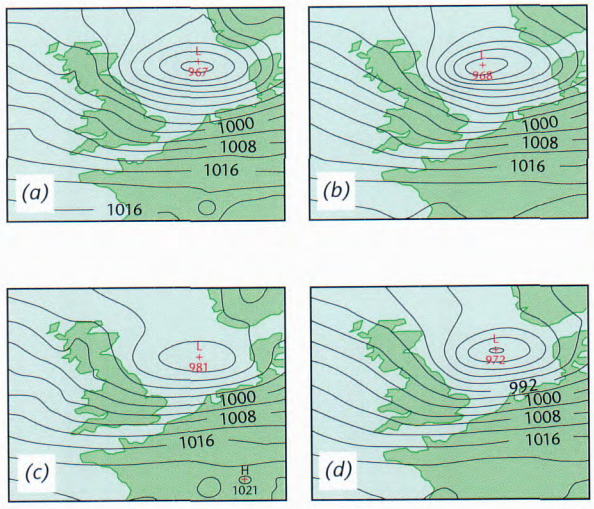

Figure 37. The Danish Storm of 12 UTC on 3 December 1999. (a) Operational model and (b) New Dynamics analyses of the event. T+24 forecast of the Danish Storm by (c) operational model and (d) New Dynamics.

Finally, there has been a decrease in some long-standing systematic model biases. The cold bias in the UM has been reduced, with particular improvements in the stratosphere and in near-surface temperatures (Fig. 40). We can attribute this to both improved numerics within the New Dynamics and the improved radiation scheme.

Improved UK model performance

The UK regional model will, for the first time, use parametrizations of sub-gridscale orography and cumulus momentum transports. Trials of this new formulation have shown a positive impact on the prediction of several important weather parameters. There is a beneficial reduction in systematic biases in forecasts of near-surface wind speeds (at 10 m), temperatures and relative humidity (both at 1.5 m) (Fig. 41). In addition to the reduced biases, the overall accuracy of visibility forecasts (Fig. 42) and temperature has been improved.

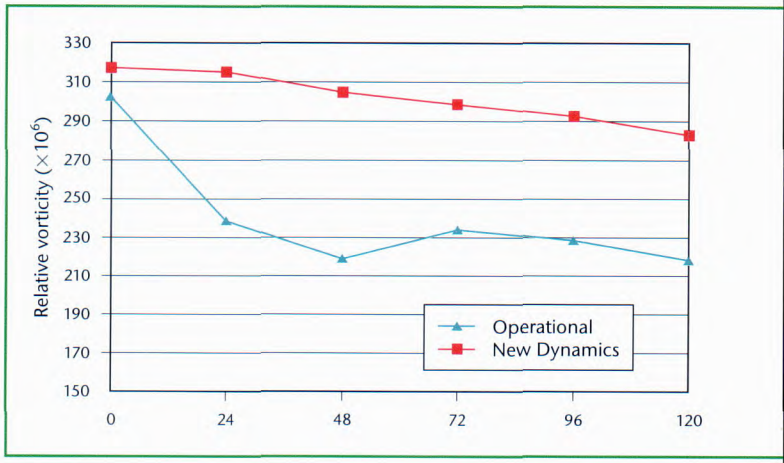

Figure 38. Tropical cyclone forecast intensity (relative vorticity) against forecast range (hours).

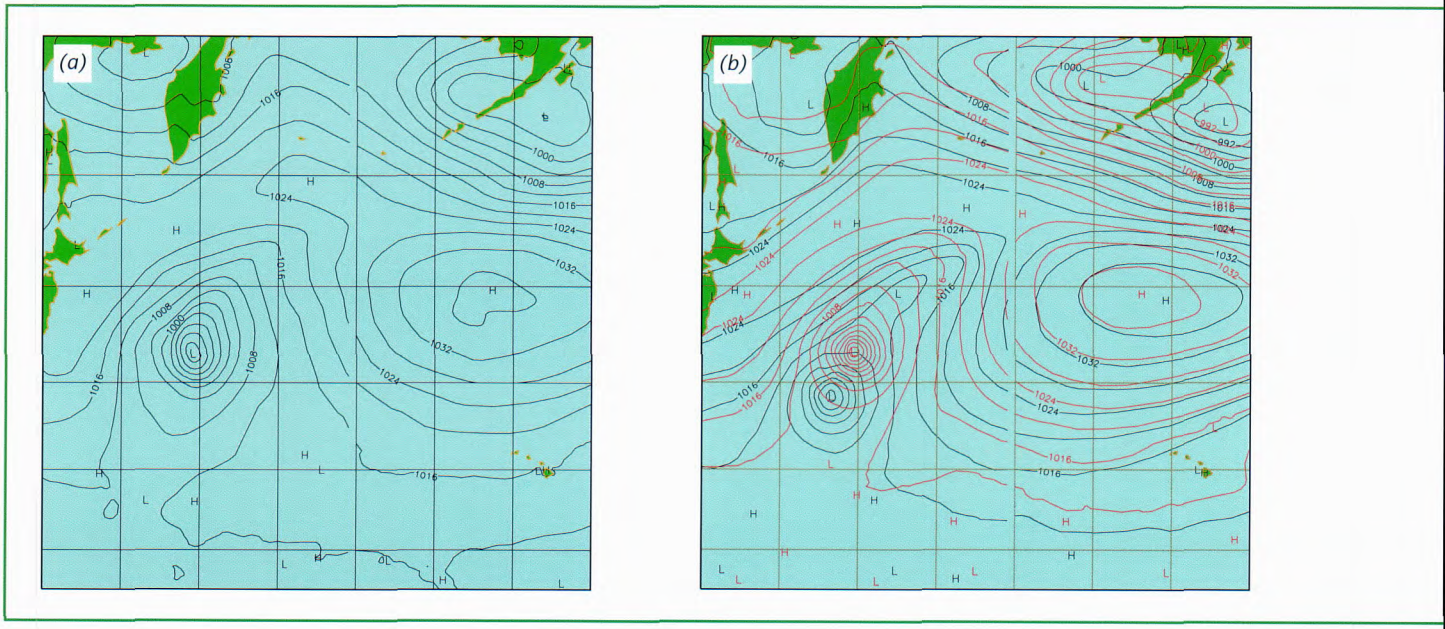

Figure 39. Forecasts of Typhoon Podul from 27 October 2001 in the north-west Pacific Ocean. (a) Operational analysis and (b) T+96 forecasts. The New Dynamics forecast is overlaid in red and is better for both position and intensity.

High-resolution modelling

The New Dynamics method provides, for the first time, the capability to run the UM at very high horizontal resolutions of around 1 km or less, opening up the possibility of significantly improving predictions of severe weather over the UK. This was not possible with the old numerical integration scheme because it used the hydrostatic approximation.

Operational use of very high horizontal resolutions is still a long way off since it will require an increase in computing power of at least two orders of magnitude. However, it is now possible to carry out tests in research mode.

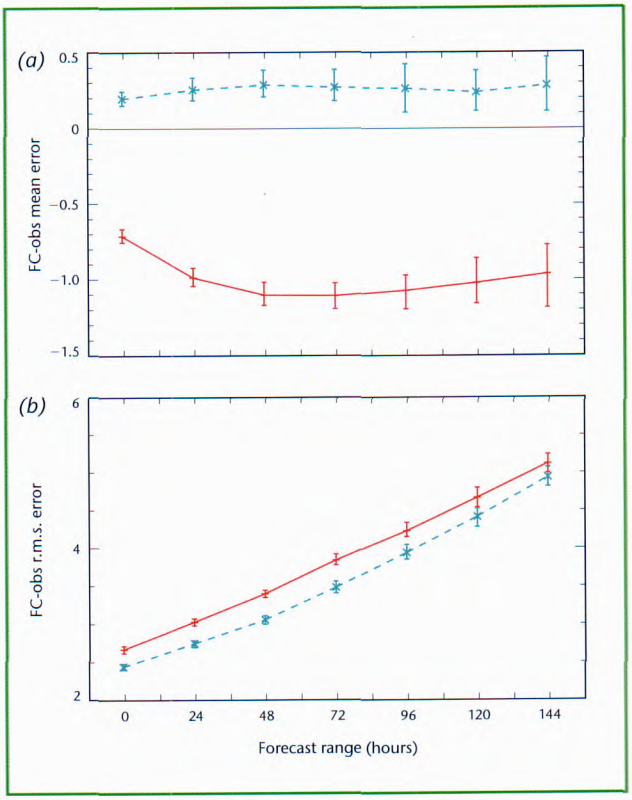

Figure 40. 1.5 m temperature verification averaged over 37 forecasts covering the period 19 December 2001 to 24 January 2002. Operational model (red) and New Dynamics formulation (blue) are shown. (a) Model bias, which is much smaller with the New Dynamics; (b) r.m.s. error, showing reduced error with the New Dynamics. Error bars are shown at the 90% confidence level.

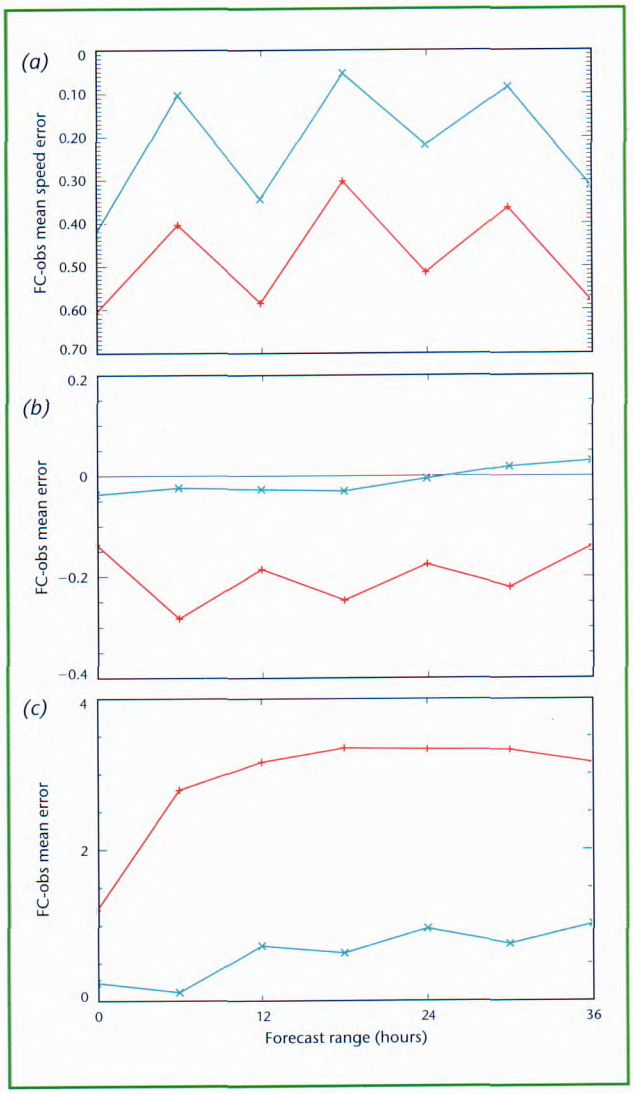

Figure 41 (right). Biases in near-surface weather parameters from the mesoscale model over the whole UK against forecast range. (a) 10 m wind speeds; (b) 1.5 m temperatures; (c) 1.5 m relative humidities. Operational model (red) and New Dynamics formulation (blue) are shown. The New Dynamics has smaller biases for each of these parameters.

Recent forecast tests on the Kent/Sussex floods of 10–12 October 2000, have been very encouraging, showing that precipitation is more intense at higher resolutions (Fig. 43) and verifies better against the radar observations (Fig. 44). Clearly, the 2 km forecast gives the highest precipitation rates.

Representation of physical processes

Analysis of observations of clouds from aircraft and satellites, and verification of NWP output have demonstrated the need to improve the representation of clouds within the UM. We are therefore developing a new scheme to predict cloud and condensate, involving equations for the temporal evolution of cloud fraction and condensate. The scheme takes explicit account of the impact of individual physical processes on clouds and

treats ice and water clouds separately. We are now testing a prototype scheme that will be developed into a version suitable for use in both NWP and climate modelling.

Satellites provide a wealth of observations of the atmosphere that are very useful for validating numerical models. Usually, atmospheric properties are retrieved from the observed radiances and the retrievals are compared with modelled quantities. A valuable complementary approach is to simulate the radiances from model parameters and make a direct comparison with the observed radiances. We have developed this capability within the UM, applying it to several channels in the infrared region of the spectrum. Figure 45 shows a comparison between simulated and observed water vapour images, revealing the distribution of water vapour and condensate in the middle and upper troposphere. High brightness temperatures represent drier regions where radiation originates at low levels in the atmosphere; high clouds are characterised by low brightness temperatures. Overall, the model reproduces the observations very well, although systematic differences related to clouds are apparent in the tropics. These comparisons will be made on a routine basis when the Meteosat Second Generation satellite is launched in 2002.

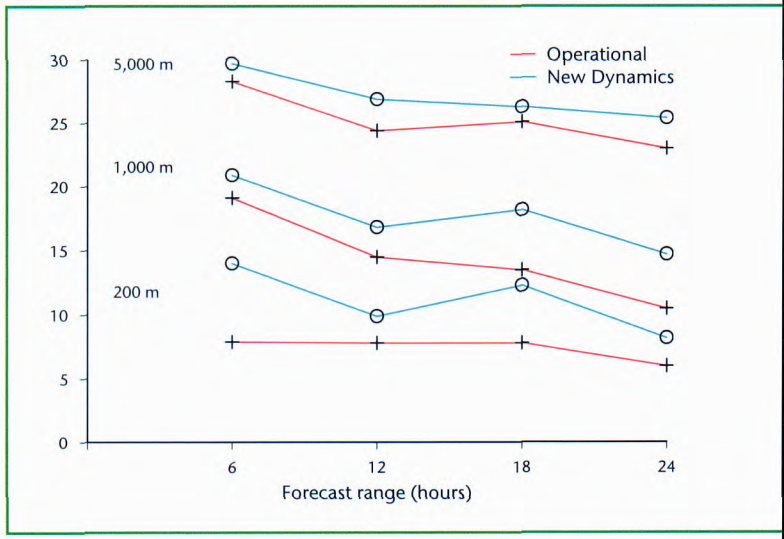

Figure 42. Equitable Threat Score for visibility against forecast range and visibility threshold (5,000 m, 1,000 m and 200 m). The higher score for the New Dynamics means improved forecasts at all visibility thresholds.

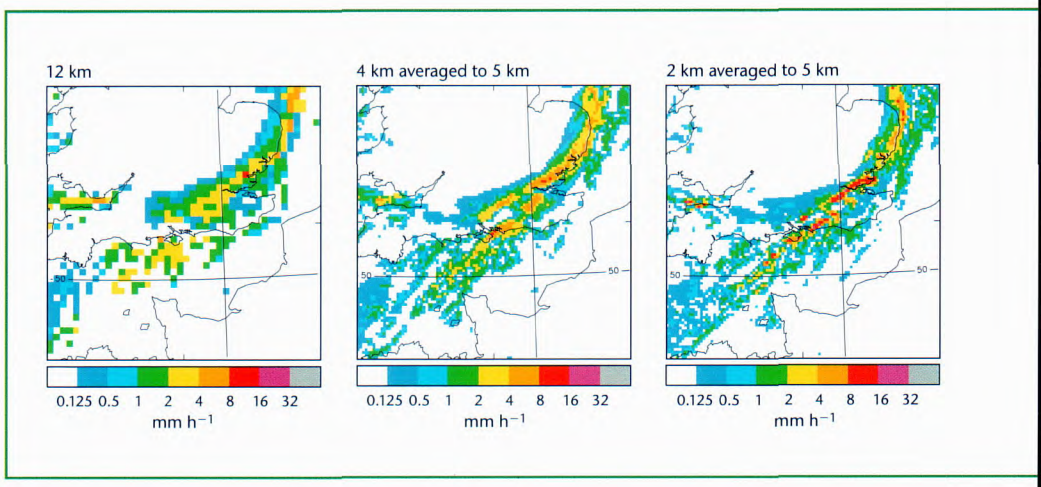

Figure 43. Six-hour forecasts of instantaneous precipitation rates for the New Dynamics version of the UK model run at 12 km (current operational resolution), 4 km and 2 km.

Applications of satellite data

Recent developments

We have continued with development of the Advanced TIROS (Television Infrared Observation Satellite) Operational Vertical Sounder (ATOVS) data processing, with three significant operational upgrades in February, April and October 2001.

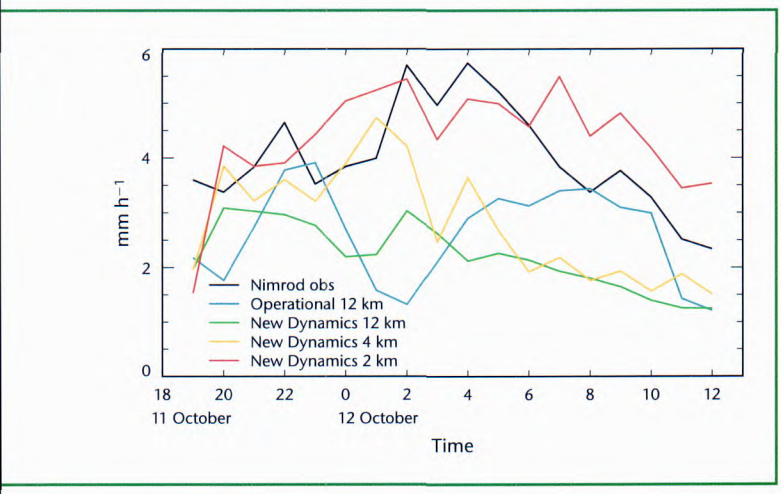

Figure 44. Hourly maximum precipitation accumulations for the Kent/Sussex heavy precipitation event integrated over the south of the UK.

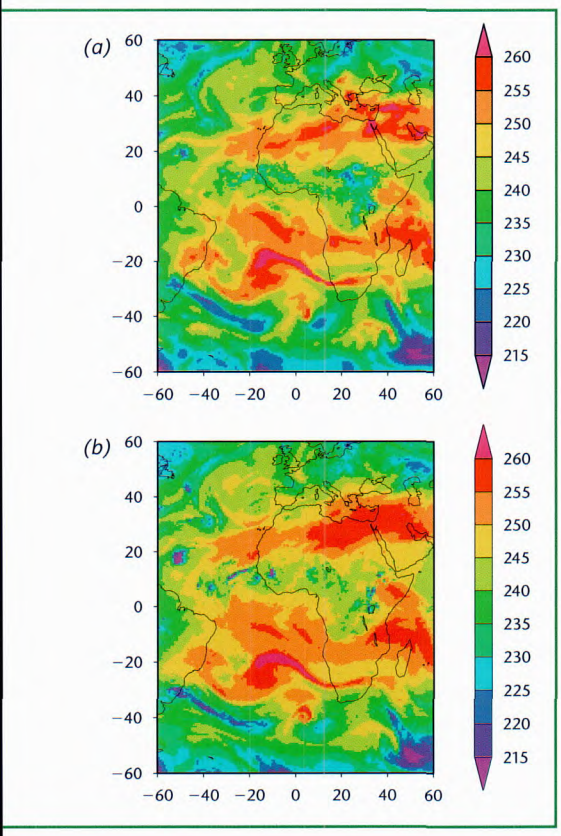

Figure 45. Brightness temperatures (K) in the Meteosat water vapour channel (a) simulated from the global forecasting configuration of the UM for 12 UTC on 4 September 2001 and (b) the corresponding Meteosat image.

The most important of these upgrades was the introduction of moisture information from the AMSU-B instrument. When NOAA-15 was launched in 1998, we exploited the temperature information quickly, but the moisture information could not initially be exploited, owing to problems on board the satellite and deficiencies in scientific understanding. In particular, improvements in cloud detection and radiative transfer model accuracy were required. We undertook work in these areas, resulting in a new scheme to distinguish thick cirrus, which is semi-transparent at the wavelengths observed by AMSU-B, from transparent, thin cirrus. The impact of AMSU-B data on moisture forecasts was significant, with substantial falls in r.m.s. error at short range, especially in the tropics. For example, the difference between 24-hour forecasts of 500 hPa relative humidity and collocated radiosonde observations fell by 10% (Fig. 46).

Other important changes include the introduction of NOAA-16 ATOVS observations, improved use of ATOVS data over sea ice and in cloudy areas, and the use of data from two Special Sensor Microwave Imager instruments.

Studies of geostationary satellite wind vectors indicated that too much weight was being assigned to them in the assimilation process. Although the assumed errors were consistent with their differences from the background field, this did not fully take account of spatially correlated errors, the effects of which were exacerbated by the increased use of winds at high horizontal density. We conducted forecast impact trials using increased estimates of observation errors, and results showed that doubling the wind errors produced an increase in forecast accuracy for many atmospheric parameters. This change was implemented operationally in October 2001.

Data from new satellite instruments

The Advanced Infrared Sounder (AIRS) was successfully launched on NASA's Aqua spacecraft on 4 May 2002. It is the first 'hyperspectral' sounder with data in thousands of spectral channels, giving information on profiles of temperature and humidity of considerably enhanced vertical resolution compared with the current generation of operational satellite sounders. AIRS is a research forerunner of instruments with similar performance on

operational satellites later in the decade. Through collaboration with NASA and NOAA/NESDIS, the Met Office will obtain AIRS observations in near real time. We will conduct forecast impact trials and, if they are successful, we plan to assimilate AIRS data operationally. In a quasi-operational manner, we have been receiving AIRS data simulated by NESDIS (using global forecast fields from the National Centers for Environmental Prediction). These data have been ingested and pre-processed (including cloud detection, quality control and a one-dimensional variational retrieval) to test the flow of data through our system in preparation for the real AIRS observations expected during 2002. Figure 47 shows an example of the output from this processing, illustrating the differences between 'observed' NESDIS-simulated brightness temperatures and cloud-free brightness temperatures calculated from our global NWP model background field.

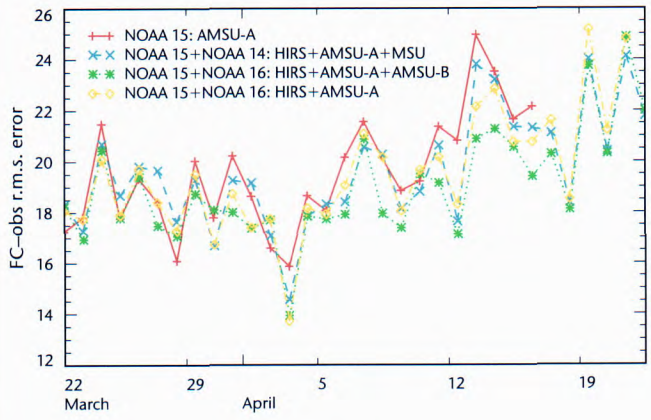

Figure 46. R.m.s. difference for 500 hPa relative humidity between 24-hour forecasts and collocated radiosondes in the tropics for experiments using different combinations of data in March/April 2001.

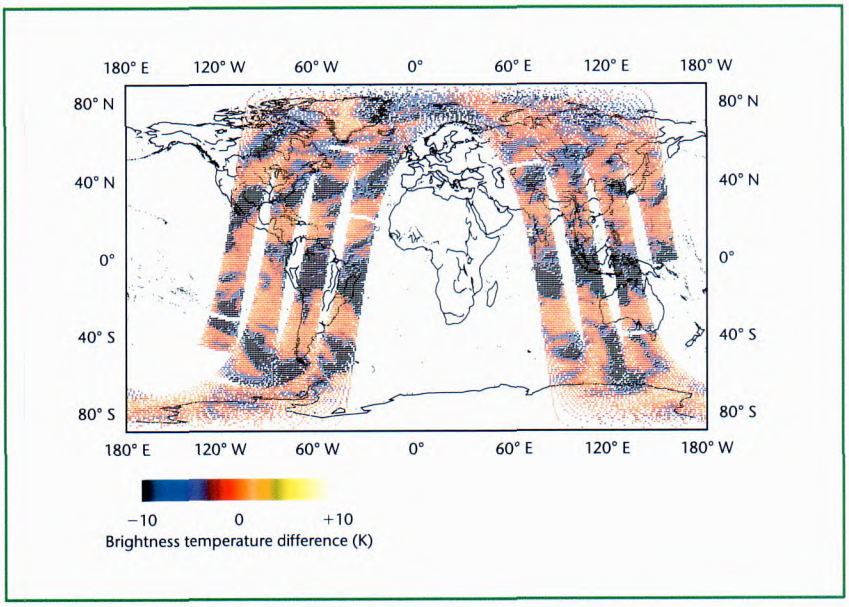

Figure 47. Differences between 'observed' NESDIS-simulated brightness temperatures (including the effects of cloud) and cloud-free brightness temperatures calculated from our global NWP model background field.

Atmospheric Processes Research

Measurement of Arctic surface emissivity

Ice nucleation observations in lenticular wave clouds

Atmospheric humidity distribution: observations and model studies

Mesoscale Alpine Programme

Figure 48. Photograph from the Met Office C-130 over Hopen Island during a campaign to measure the surface emissivity of Arctic ice.

Atmospheric Processes Research is about conducting well constrained observational or modelling experiments, with the aim of ensuring that the physical processes occurring in the atmosphere will be represented in weather and climate models in the most appropriate and consistent way. Detailed high-resolution models are often first validated against available detailed observations. The model can then be used as proxy for real observations to investigate the sensitivity of a process to conditions, or the way it is represented in the larger scale model. To illustrate this approach, we are presenting four examples of our work. In two of the cases, more basic information is required, as well as a better understanding of the physics; in the other two cases, there is a need to improve the parametrization of the process for numerical weather prediction (NWP).

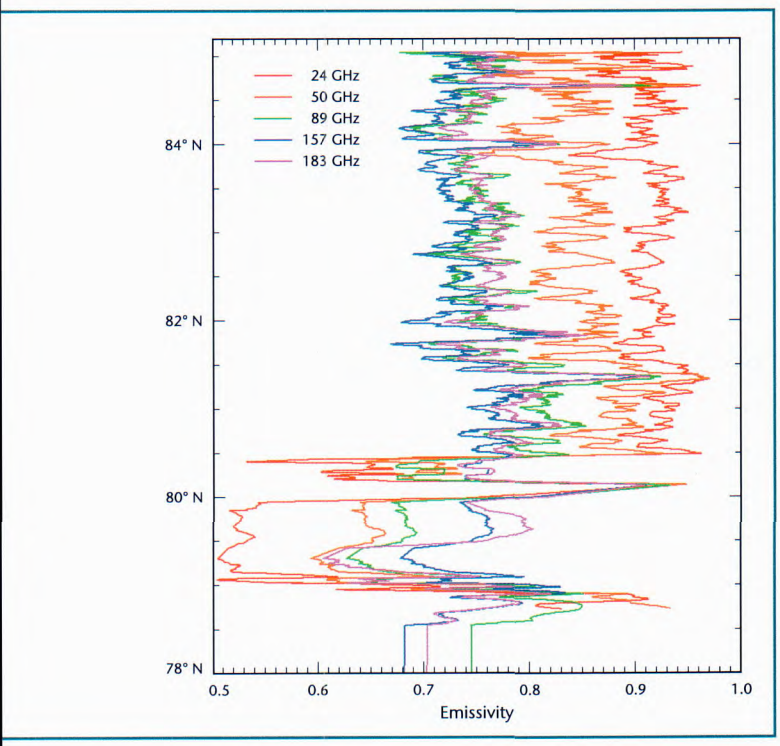

Figure 49. Latitudinal variation of emissivity derived from data from aircraft radiometer operated at 600 m altitude on 20 March 2001.

The scientific effort that goes into modelling is matched by an equal effort in analysing data collected either by the met. research flight (MRF) C-130 aircraft or by the range of surface-based instruments operated at Cardington, Bedfordshire. In March 2001, the C-130 was retired. In collaboration with other organisations, we are currently fitting out a new aircraft with instrumentation; it is expected to start operation at the start of 2003.

Measurement of Arctic surface emissivity

The Arctic is an important area for synoptic development and is also very sensitive to climate change. Instruments on polar-orbiting satellites have great potential for retrieving atmospheric and surface information in these areas; in particular, the current Advanced Microwave Sounding Unit (AMSU) and the future Infrared Atmospheric Sounding Interferometer. However, to fully exploit data from these instruments, we need to know the surface emissivity, which is highly variable over ice and snow.

The last experiment of the C-130 was aimed at improving our knowledge in this area. A series of flights was conducted in March 2001 from Tromsø, Norway, to measure surface emissivity using instruments on the aircraft similar to those on current and future satellites (Fig. 48). We also used these

flights to study radiative fluxes over a range of surfaces, including first-year, multi-year and glacier ice, as well as snow-covered land and forest. Figure 49 shows the emissivities measured at five microwave frequencies.

One of the outcomes of the experiment was to develop an algorithm to retrieve the total water vapour (TWV), a column quantity, from AMSU data as part of a collaboration with the University of Bremen and based on a technique developed for Antarctica. This algorithm uses three channels centred on a water vapour absorption line at 183 GHz, with surface emissivity assumed as constant. Figure 50 shows TWV retrieved from AMSU data (from the same aircraft track as for Fig. 49) using this algorithm. It was validated using data from our aircraft radiometers and dropsondes released during high-level flight. To extend the algorithm to higher humidities, data from other channels must be included. This requires knowledge of how emissivity varies with frequency, which will be gained from the detailed measurements made from the aircraft at low altitude. In Fig. 50, the white areas represent open water, for which the retrieval algorithm cannot retrieve the high TWV values.

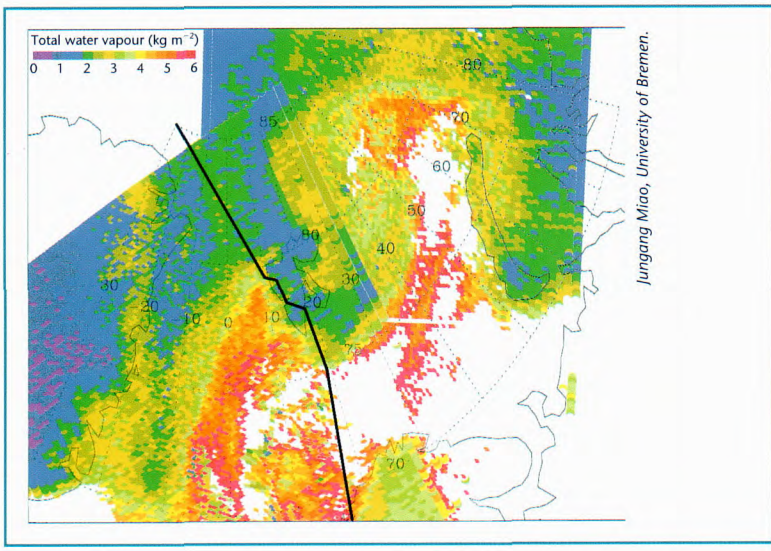

Figure 50. TWV retrieved over the Arctic from AMSU data. The black line represents the northward track of the aircraft on 20 March 2001, crossing first over open water, new ice, glaciers on Svalbard, then measuring first-year and multi-year ice to the north of Greenland. (Flight time funded under EC contract no. HPRI-CT-1999-00095.)

Ice nucleation observations in lenticular wave clouds

The radiative properties of ice clouds depend on their microphysical properties, such as ice water content, size spectra and crystal habit. These same properties also determine the precipitation rate. The primary ice nucleation determines the ice production rate and size spectra, so an understanding of ice nucleation is necessary if ice clouds are to be modelled correctly. The study of ice nucleation in cirrus is hampered by the difficulty in measuring the environmental conditions at the time of nucleation and an uncertainty in the age of the ice crystals sampled. Orographic lenticular wave clouds, however, provide a simpler dynamical and microphysical environment.

During a campaign over the Swedish mountains in 1999, we measured various isolated wave clouds. One wave cloud was especially interesting, having significant liquid water (reaching 0.15 g kg^{-1}) at its leading edge, with the dominant phase changing from liquid to ice during the downdraught, where the ice concentrations reached 10 cm^{-3}. The air temperature varied from −18 °C at the cloud base to −32 °C at the top. At these temperatures, homogeneous freezing of the supercooled water droplets is negligible, so ice nucleation must take place heterogeneously. Heterogeneous ice nucleation

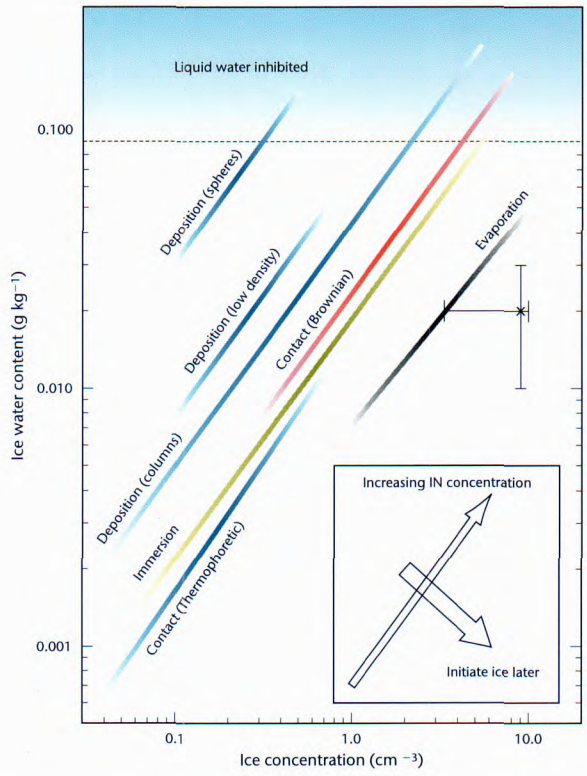

*Figure 51. Model values of the peak ice number and IWC found in the downdraught region for a number of different nucleation modes. The three different deposition models represent the likely extreme assumptions. The observed value is shown by the * symbol with 95% confidence limits.*

requires ice-forming nuclei (IN), which are a special subset of atmospheric aerosols. Several heterogeneous nucleation modes are understood and parametrized, each occuring at a different time. For example, deposition nucleation occurs above some critical ice supersaturation point when water vapour is absorbed directly onto the surface of the IN and transformed into ice; this initiates ice crystals in the updraught before water supersaturation is reached and liquid cloud formed.

We used a detailed microphysical model to simulate the observed wave cloud to determine the characteristics of the ice nucleation and establish which, if any, of the heterogeneous nucleation modes are consistent with the observations. One example is shown in Fig. 51. The cloud simulation consists of repeatedly running a parcel model, with each parcel starting at a different height and following a different trajectory. Upwind temperature and humidity profiles define the parcel's initial temperature and water vapour mixing ratio, and measured horizontal and vertical winds define the trajectories. For each nucleation mode, increasing the number of active IN moves the results towards both higher ice number and high ice water content (IWC), as well as affecting the relative time onset of nucleation between the different modes (see inset). When nucleation occurs early during the passage of air through the wave, this suppresses further nucleation as the growing ice crystals deplete the ambient water vapour, inhibiting any increase in supersaturation. These two effects mean that the IN modes of deposition, immersion freezing and contact freezing are unable to reproduce the observed combination of ice number concentration and IWC. To reproduce these values, nucleation must occur rapidly within a narrow time window when liquid droplets are evaporating in the wave downdraught. We have postulated an evaporation mode to fit the observations, but, in order to understand the physical mechanism, laboratory experiments are required.

Atmospheric humidity distribution: observations and model studies

Spatial variations of the atmospheric moisture field occurring on scales too small to be resolved by NWP or climate models have a big impact on the dynamic and radiative structure of the atmosphere because moist processes have a non-linear

relationship with the Earth's radiative balance. It is a significant challenge for cloud parametrizations to represent these processes and further research is needed to improve their accuracy. Hence, we have conducted modelling and observational studies to test assumptions in the current Unified Model (UM) cloud scheme and assist work to develop a new scheme.

Mathematically, the treatment of moisture variations typically involves the probability density function (PDF), which effectively quantifies the relative amounts of air with particular humidity values. Observations made with a tethered balloon have been used to quantify the errors incurred in predicted cloud fraction when the real humidity PDF is not represented correctly. Figure 52 shows four types of PDF fitted to an observed one. Figure 53 shows the errors in predicted cloud fraction for each of the fitted distributions. The triangular PDF assumed in the current cloud scheme produces reasonable results, but only if its width is scaled properly. PDFs that can represent asymmetries in the data produce better results.

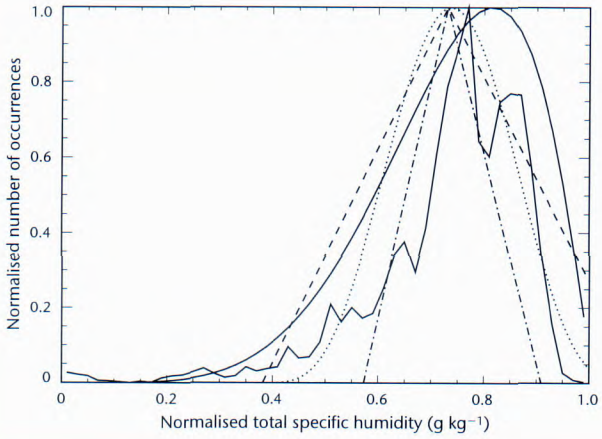

Figure 52. An observed PDF (solid jagged line) in specific humidity, together with four modelled PDFs. Solid line: beta distribution (b); dotted line: symmetric beta (β_s); dashed line: fully scaled triangular (T_a); dot-dashed line: simplified triangular (T_i).

Further study of the observations has revealed that properties of PDFs can alter significantly for a given air mass over relatively short periods. Thus, accurate cloud forecasting also requires models to predict the evolution of the PDF. High-resolution numerical simulations are being conducted using the Met Office's cloud resolving model to investigate the dynamical properties and evolution of the moisture field in a systematic way. For initial simplicity, these simulations examine the response of a 2 km-deep atmospheric layer (Fig. 54) to homogeneous radiative cooling of a few degrees per day. They also assume that any clouds formed are non-precipitating.

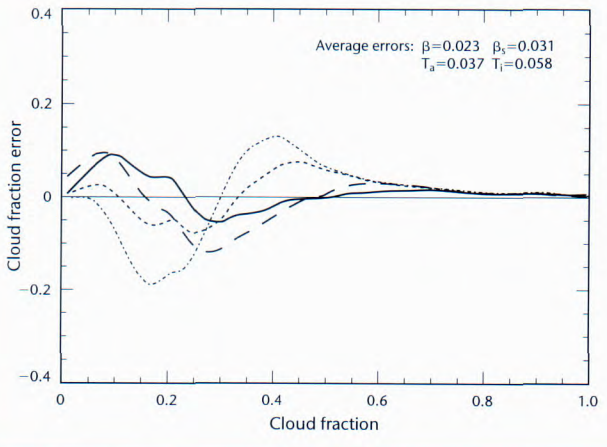

Figure 53. Corresponding errors in predicted cloud fraction for the four fitted functions (Fig. 52) against cloud fraction. The beta distribution PDF ((b), solid smooth line) that can represent asymmetries in the distribution has the smallest error.

Even for this idealised situation, Fig. 55 shows that there is a considerable change in the moisture PDF, its width (and hence the magnitude of moisture fluctuations) decreasing from the initial triangular distribution (black curve) to the tall, bell-shaped light blue curve (via red, green and dark blue) in response to the cooling. This is in contrast to most cloud parametrizations, but is supported by some aircraft observations. In the figure, the temporal increase in the cloudy fraction (i.e. air parcels that are saturated) is shown by the near-vertical dashed lines that have cloudy air to their right. Physically,

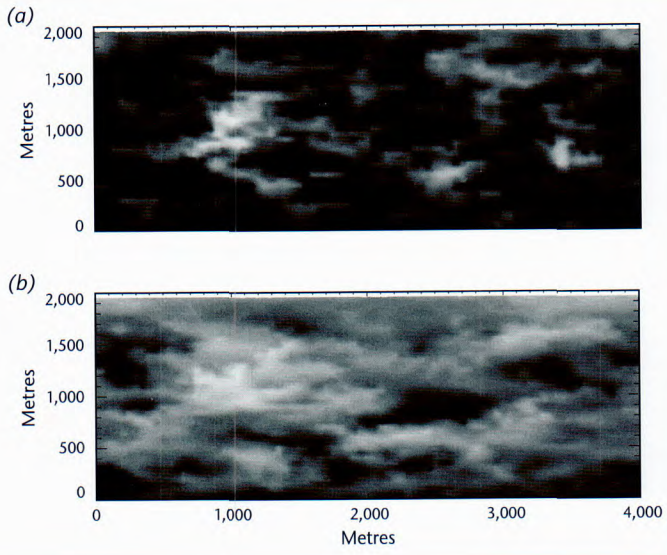

Figure 54. Cloud resolving model simulations showing the increase of cloud cover in the studied layer between (a) an early stage and (b) a later stage of the cooling process. Vertical cross sections of the liquid water content are shown. The black regions are cloud free. The height displayed on the vertical axis is relative to the 700 hPa level.

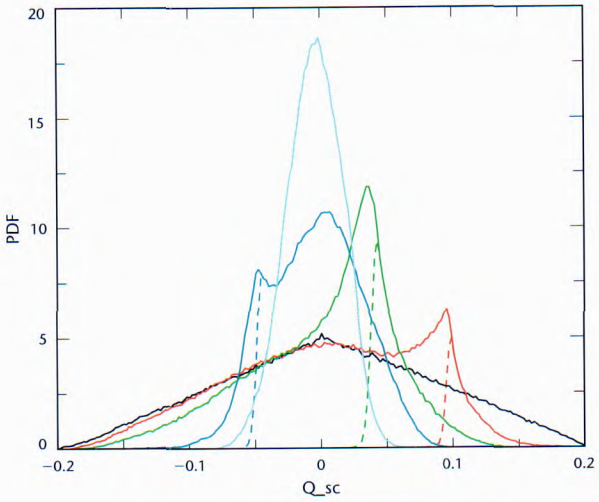

Figure 55. PDF of an appropriately scaled moisture variable, Q_sc, for different times during the cooling process.

this behaviour is explained by a slow circulation driven by the inhomogeneous release of latent heat in the fluctuating moisture field. An insight into the mechanisms allowed identification of a number of non-dimensional parameters that describe the cloud's response to the cooling process. Predictions based on these parameter values agreed well with the numerical simulations. In particular, we saw that low thermal stability enhances the narrowing of the moisture PDF, while strong vertical moisture gradients result in its broadening.

Mesoscale Alpine Programme

The Alps have a major influence on European weather (Fig. 56). For example, orographically enhanced precipitation can produce flash floods with devastating results. Mountain-forced gravity waves affect the large-scale momentum budget of the atmosphere, and may produce downslope wind storms and clear air turbulence, which endanger aircraft. However, much of our current understanding of mountain waves comes from simplified studies of flow over highly idealised orography. Although useful for understanding the basic science of flow over orography, the simplifying assumptions used are often not valid. We participated in the international Mesoscale Alpine Programme (MAP) to gather data to help improve our understanding of orographically influenced flow-fields. The MRF C-130 took part in four gravity wave flights in November 1999, along with US and other European research aircraft and comprehensive ground-based instrumentation. The scientific aim was to better understand the dynamics of gravity waves induced by complex orography, which will in turn bring improvements in gravity wave drag parametrizations for NWP.

On 2 November, strong south-westerly flow and a positive wind shear from a jet stream provided conditions favourable for trapped lee-wave formation. A quasi-steady lee-wave field was observed over Mont Blanc between 0900 and 1300 UTC, with shorter waves trapped lower down and longer waves reaching higher levels. The non-hydrostatic formulation of the new dynamical core of the UM means that the model can represent vertical flow

accelerations and therefore run at very high horizontal resolution where non-hydrostatic effects such as wave trapping become important. We have produced simulations of the 2 November event over exact orography using grid nesting. A run with 1 km horizontal resolution was successfully completed for the north-west of the Alps, for which the vertical velocity field shown in Fig. 57 demonstrates the complexity of the wave-field (upwards is positive). The diagonal line is the track used by the research aircraft sampling at different levels and using dropsondes. In the area covered by the model, there are a number of mountain peaks that produce gravity waves, which may produce complex interference patterns. The evidence so far suggests that the model simulates the wave-field well. Figure 58 shows a simulated cross-section of the vertical velocity field along the flight track. This agrees well with aircraft observations, with quasi-steady trapped lee-waves present below 10 km and an apparent increase in horizontal wavelength with altitude; the wave amplitudes are also reasonably consistent. This simulation therefore shows potential for helping us to unravel the complex processes occurring in this highly three-dimensional wave-field.

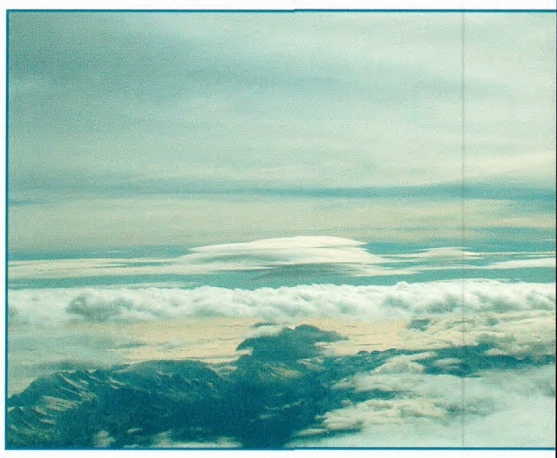

Figure 56. Mont Blanc (centre), photographed from the C-130 on 2 November, capped at high level by lenticular cloud.

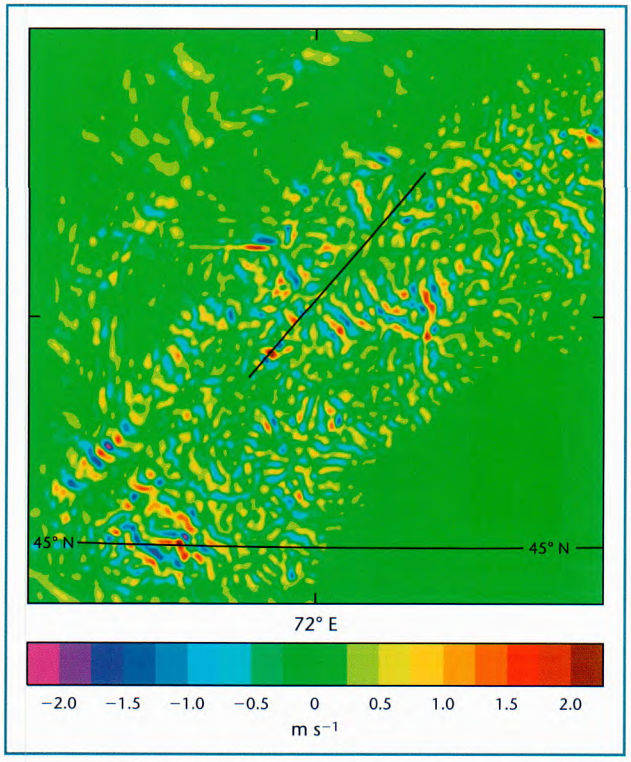

Figure 57. A simulation of the wind's vertical velocity field at an altitude of 5,780 m. The domain is 284 km².

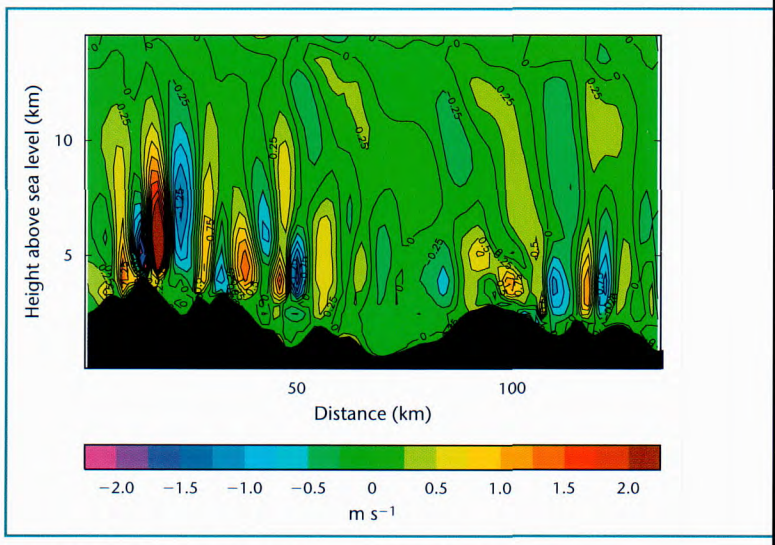

Figure 58. A vertical section along the aircraft track for the same simulation as in Fig. 9. Mont Blanc is the black peak to the left of the plot. The C-130 was flying at 7.6 km altitude and observed maximum vertical wind velocities of +/− 2 m s^{-1} and a wavelength of around 15 km. At a lower altitude, 5.5 km, the US Electra aircraft observed shorter wavelengths, as simulated, but the observed magnitude was much smaller than in our model, probably due to inadequate representation of the finer scale orography in the simulation.

Climate Research

Climate variability

Climate change predictions

Stratospheric processes research

Atmospheric chemistry modelling

Observation of sea-surface temperature

Model development and parametrizations

Intergovernmental Panel on Climate Change


980
990
1000
970
1010
29
CHANGE
960
1020
RAIN
30
28
FAIR
960
1030
Foster Gellear
INCHES
MILLIBARS
31
1040
1050

Climate variability

Global and UK climate trends

Available data indicate that 2001 was the second warmest year globally in the past 142 years, with temperatures 0.42 °C above the 1961–90 normal. Nine of the 10 warmest years have occurred since 1990, including 1999 and 2000; only 1998 was warmer than 2001. The year 2001 saw the warmest October on record in terms of the Central England Temperature, with an average of 13.3 °C, 2.7 °C above the 1961–90 average. However, in central England, the year as a whole was only an unexceptional 0.48 °C warmer than the 1961–90 average. The copious rains of 2000 continued into early 2001, making the 24 months from April 1999 to March 2001 the wettest two-year period in the England and Wales precipitation series that began in 1766.

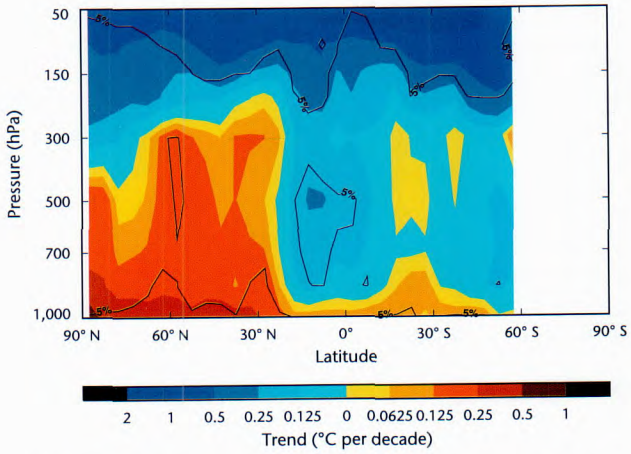

Figure 59. Trends in annual zonal-mean temperature anomalies for 1979–2000, based on radiosonde data. When known instrument changes occurred, the stratospheric data were adjusted to be consistent with the MSU Channel 4 record. Trends significant at the 5% level are marked by a thick black contour line. Linear trends were calculated using a restricted maximum likelihood technique.

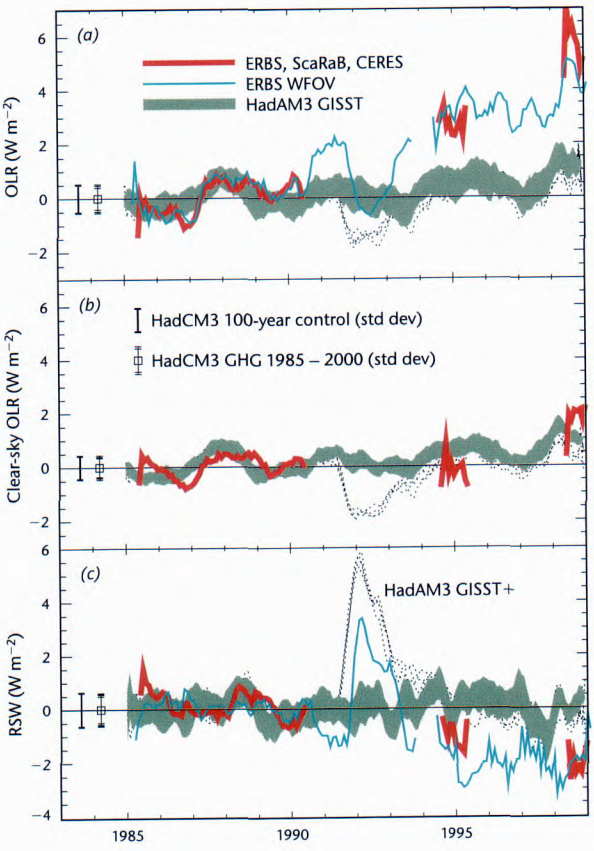

Figure 60 (right). Low-latitude seasonal anomalies of (a) OLR, (b) clear-sky OLR and (c) reflected short-wave (RSW) radiation at the top of the atmosphere measured by satellite (red and blue) and derived from Hadley Centre models. CERES: Clouds and Earth Radiant Energy System instrument; ERBS: Earth Radiation Budget Satellite; ScaRaB: Scanner for Radiation Budget satellites ; WFOV: Wide Field of View.

Tropospheric lapse rates

Despite the widespread surface warming, zonally-averaged annual radiosonde temperature anomalies (Fig. 59) indicate that most of the troposphere has cooled since 1979 in the tropics and the mid-latitude southern hemisphere. By contrast, the northern extratropical troposphere has warmed almost as much as the surface. The tropical cooling moves seasonally with the inter-tropical convergence zone, suggesting that the tropospheric cooling could be related to changes in cloudiness. This hypothesis is supported by an observed increase in outgoing long-wave radiation (OLR), despite relatively constant clear-sky OLR and a decrease in reflected short-wave (RSW) radiation (Fig. 60), which would tend to cool the free atmosphere and warm the surface, respectively, thereby increasing the lower tropospheric lapse rate as observed. However, the atmospheric model HadAM3, when forced with observed sea-surface temperatures (SSTs), with or without natural forcings, has not reproduced the tropical radiative trends (Fig. 60). In the figure, grey shading shows the intra-ensemble standard error for HadAM3, forced by observed global analysis of sea-ice and sea-surface temperature (GISST); the dotted line (denoted HadAM3 GISST+) shows similar experiments including natural and anthropogenic forcings. The eruption of Mount Pinatubo in 1991 reduced overall and clear-sky OLR and increased RSW in HadAM3, in accordance with observations. The error bars show the variability from the coupled ocean–atmosphere model (HadCM3), calculated as one standard deviation, for a 100-year control experiment and a greenhouse gas-forced experiment for the period of the satellite data. In the northern winter, a signal from the strengthening westerly phase of the Arctic Oscillation is present in the radiosonde observations in the form of cooling (warming) in the middle and upper troposphere north (south) of 60° N, and an increase in lower-tropospheric lapse rate in mid-latitudes. Microwave Sounding Unit (MSU) retrievals yield weaker cooling than radiosondes for the tropical troposphere, suggesting that either the radiosonde results have been affected by under-sampling, or that there are radiosonde instrumental biases that have not been compensated for — or both. The MSU retrievals

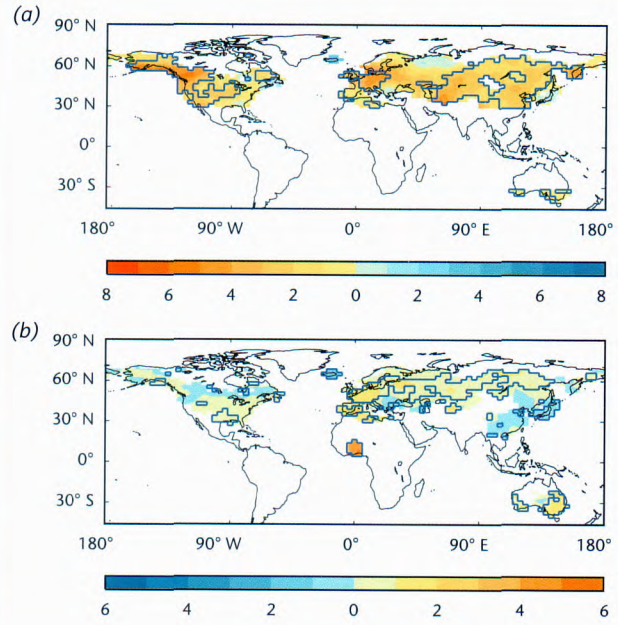

Figure 61. Trends per decade over 1950–95 in (a) number of frost days, and (b) frequency of warm nights (% of days with minimum temperature exceeding 90% threshold). Blue lines enclose regions where trends are significant at the 5% level.

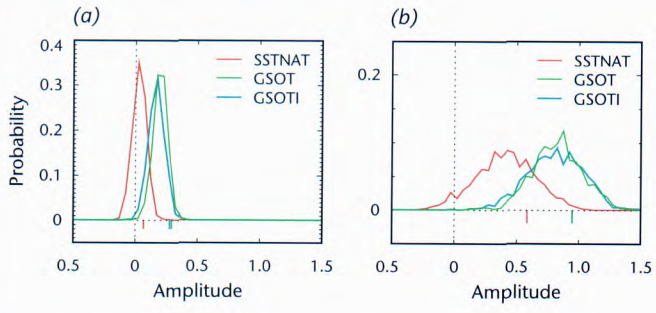

Figure 62. Probability density functions of HadAM3 ensemble mean trend patterns projected onto the observed trend pattern for (a) number of frost days, and (b) warm nights. The amplitude reflects the relative magnitude and pattern similarity between the modelled and observed changes.

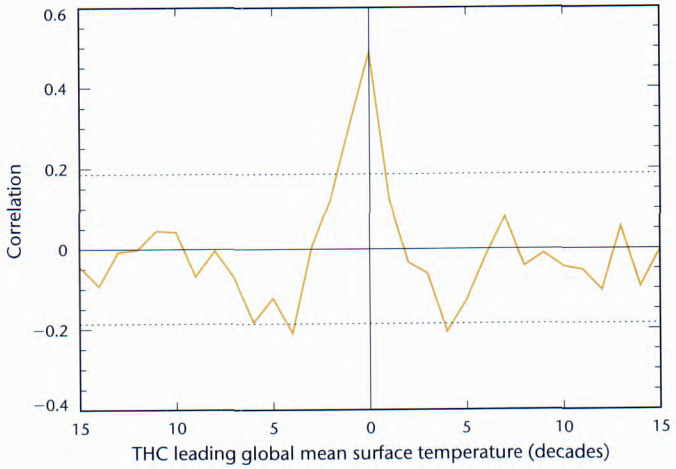

Figure 63. Correlation of the HadCM3 global surface temperature with its decadal THC index at leads and lags of up to 150 years. For positive (negative) times, the temperature is compared to the past (future) THC. Dotted lines show the 95% confidence limits for the null hypothesis that the correlation is zero.

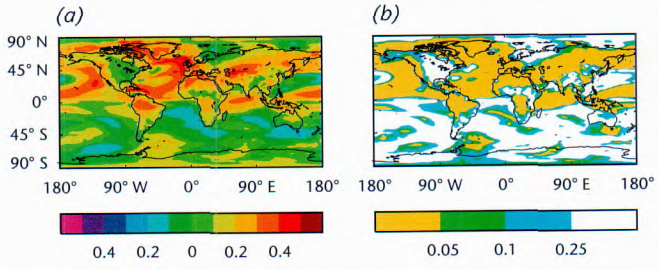

Figure 64. HadCM3 annual screen level temperature correlations with the simultaneous strength of the THC (a) and (b) significance (defined as the fractional probability that the correlation is zero).

qualitatively agree with the radiosonde-based profiles in the extratropical northern hemisphere. In high latitudes of the southern hemisphere, the MSU trends are consistent with an observed strengthening of the westerly phase of the Antarctic Oscillation.

Changes in extremes

In the Third Assessment Report of the Intergovernmental Panel on Climate Change (IPCC), changes in climate extreme indicators derived from daily data were used to assess changes in extreme daily temperature and precipitation over much of the globe. However, local climatic effects can yield diverse trends within small regions, so individual stations' data may be unrepresentative of changes on larger spatial scales. To alleviate this problem and allow data from all stations to be incorporated, we have used angular-distance weighting to place all the station-based trends in climate extreme indicators onto a regular grid. Estimates of trends, and their uncertainties, over the period 1950–95 show that there have been significant decreases in the number of frost days (nights with minima of less than 0 °C) over much of the northern hemisphere and increases in the number of warm nights over Europe, mid-Eurasia and Australia (Fig. 61). Regions of significant trends in rainfall extremes are smaller in extent but suggest an increase in wet extremes and a decrease in the length of dry periods over much of the northern hemisphere. These more objectively derived results confirm the key conclusions reported by the IPCC. The use of gridded observed trends has also allowed objective comparisons with trends simulated by the atmospheric model HadAM3 when forced by observed changes in SST, sea-ice extent and various combinations of human-induced forcings. This is the first time such a study has been undertaken. Inclusion of anthropogenic effects in the model significantly improves the simulation of changing extremes in temperatures (Fig. 62), although the model underestimates the observed decrease in frost days. Figure 62 shows the probability density functions of HadAM3 ensemble mean trend patterns for SST + solar + volcanic forcings (SSTNAT), SSTNAT plus well-mixed greenhouse gases, direct sulphate aerosol and changing ozone (GSOT), and GSOT plus indirect aerosol effects (GSOTI).

Decadal and multidecadal climatic variability

Analysis of a 1,400-year coupled-climate model calculation, without external forcings, using the HadCM3 model has revealed a quasi-periodic mode of internal climate variability with a characteristic timescale of about 100 years. This mode affects the modelled thermohaline circulation (THC) and has a coherent phase evolution for periods of up to 50 years (Fig. 63); it also influences surface temperature in broad regions of the northern hemisphere, particularly in the North Atlantic, Pacific and Asia. Thus, these areas are predominantly warm at times of maximum THC (Fig. 64), and cold at times of minimum THC, typically 60 years earlier or 40 years later (not shown). The model results imply that THC-related climate variability may have been significant during the instrumental period as broadly similar temperature fluctuations have been observed. In particular, it is likely that European (including UK) temperature has been influenced by these fluctuations over the last century.

Interannual to interdecadal predictability

Using statistical methods and dynamical forecasts of El Niño, we predicted in December 2001 that the global surface in 2002 would be slightly warmer than in 2001, at 0.47 °C above the 1961–90 average, with a 95% confidence range of 0.33 °C to 0.61 °C. We estimated a probability of about 75% that 2002 would be warmer than 2001, but only about a 10% likelihood that 2002 would be as warm or warmer than the warmest year, 1998. The accuracy of the forecast depends on the development of a weak to moderate El Niño warming in the tropical Pacific in 2002. The forecast of 0.47 °C for 2001, made in December 2000, successfully predicted appreciable global warming compared to 2000, i.e. from 0.27 °C to 0.42 °C.

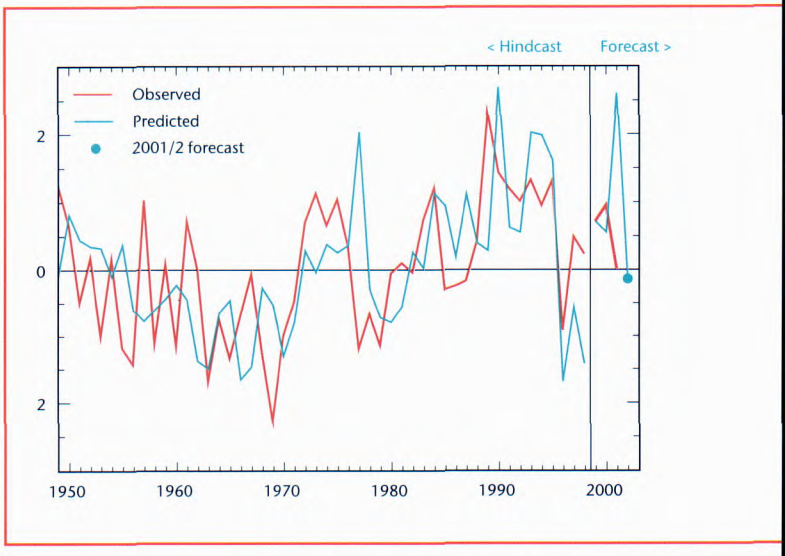

Figure 65. Observed and predicted index. Forecast made 1 June 2001: the NAO is forecast to be weakly negative for Winter 2001/2.

We have also developed a technique to predict the winter (i.e. December to February) strength of the North Atlantic Oscillation (NAO) using SST anomaly patterns from the previous May. The technique yields skilful hindcasts: correlation skill is 0.45, and 66% of hindcasts have the correct sign (Fig. 65). Forecasts are available on the Met Office web site.

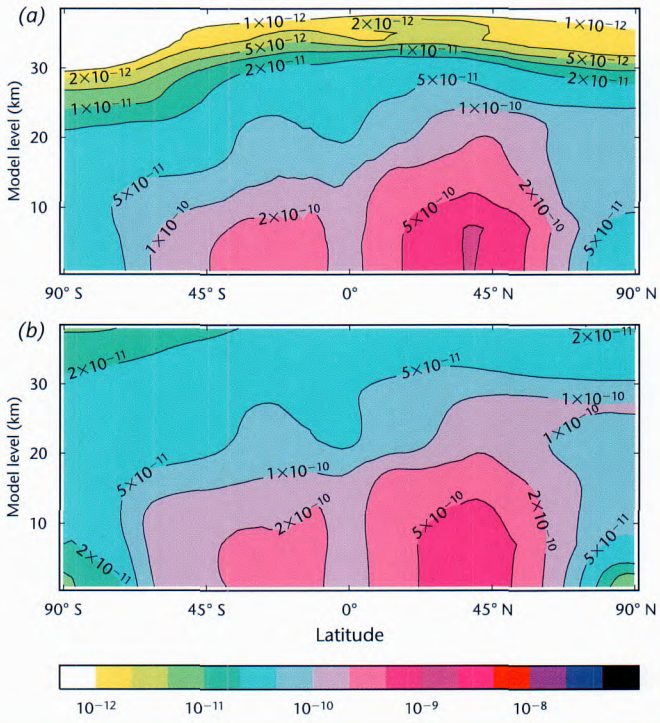

Figure 66. Zonal annual mean mass mixing ratio of sulphur in sulphate aerosol, from Unified Model experiments with (a) the new dynamical scheme and (b) current scheme using the same sulphur emissions.

Climate change predictions

Our existing climate model, HadCM3 is one of the leading climate models in the world. We are currently working to develop a new climate model, the Hadley Centre Global Environmental Model (HadGEM), which will incorporate improvements to the dynamical and physical processes in the present forecast model, along with the facility to include fully interactive chemical and biological cycles for climate change studies; the model will also offer much higher vertical and horizontal resolution. Overall, this will enable us to remain at the forefront of environmental research. An example of the impact of the new dynamical scheme can be seen in the simulation of atmospheric sulphate concentrations. In the current model, sulphate is erroneously diffused across the tropopause, whereas in the new scheme, concentrations fall sharply between the troposphere and the stratosphere, as expected (Fig. 66).

Although the new model will have a higher resolution, leading to improved simulation of the atmospheric circulation and, in particular, the storm tracks affecting the British Isles, there is a need for climate change information on even smaller spatial scales for use in climate impact studies. Providing Regional Climates for Impact Studies (PRECIS) has produced a nested regional model that runs on a PC and can be placed over any part of the globe (Fig. 67). The initial project is intended to enable developing countries to run simulations of both present and potential future climates for their own region, although there are many other purposes for which such a portable model can be used.

The output from the regional model over the British Isles has been used to drive a storm surge model (courtesy of Proudman Oceanographic Laboratory) to produce changes in maximum surge heights at the end of the 21st century under the A2 scenario. The combination of sea level rise, change in winds and isostatic rebound at the southern end of the North Sea leads to a maximum increase of well over one metre, as shown in Fig. 68 for scenario A2 of the Special Report on Emissions Scenarios (SRES)-IPCC.

Although the regional model provides greater detail in predictions of future climate, its accuracy is limited by the accuracy of the global model that drives it.

The validation of climate models remains one of the more difficult aspects of climate research. A new data set on changes in the heat content of the ocean over the last few decades has recently become available. This has been compared with the estimated change in heat content obtained from simulations considering only natural factors (solar variations, major volcanic eruptions), and simulations taking into account both natural and anthropogenic factors (increases in greenhouse gases and aerosols). Only when the anthropogenic factors are included does the model reproduce the trend seen in the observations (Fig. 69). The model does not produce the same level of interdecadal variability seen in the observed data set, but it is not yet clear whether this is due to sampling errors in the observations, or insufficient internal variability in the model.

Despite the constraints imposed by observations of surface and atmospheric temperatures and ocean heat content, there is still a large range of uncertainty in the sensitivity of climate to increases in greenhouse gases. We have set up a new project, in conjunction with the University of Oxford, to look at the distribution of predicted changes as the different parameters used in the model are varied, and to provide a better quantification of this uncertainty.

Much of the uncertainty arises from climate feedback through water vapour and cloud. It has been suggested that models produce an erroneously strong positive water vapour feedback (leading to exaggerated predictions of climate change) because of insufficient vertical resolution. This now seems unlikely since the strength of this particular feedback in the Hadley Centre model changes little if the vertical resolution is increased from 11 to 200 layers. Cloud feedback remains much more uncertain and we are developing new techniques to identify shortcomings in the model's simulation of cloud, guiding research for model improvement. For example, variations in observed high cloud amount depend primarily on variations in vertical velocity, with some dependence on local variations in sea-surface temperature (Fig. 70 (a)). A similar dependence on vertical velocity and sea temperatures is found when the model is run with observed sea-surface temperatures, suggesting that this aspect of the model's cloud response is correct (Fig. 70 (b)). As the processes governing year-to-year variations in cloud may not be the same as those accompanying global warming, this diagnostic has also been computed from a model experiment in which CO_2

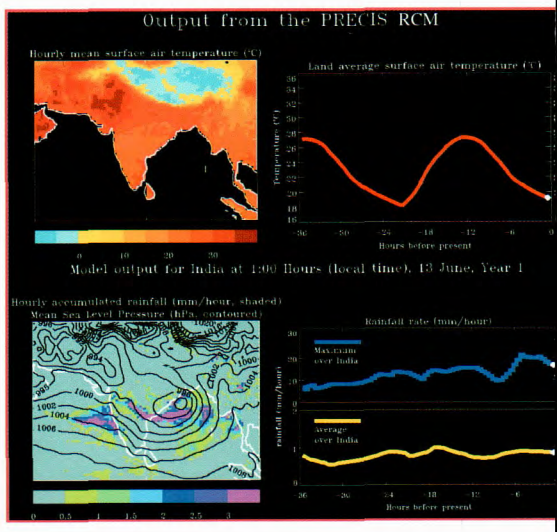

Figure 67. An example of output monitoring the PRECIS model running over the southern Asian region showing (from top left, clockwise): surface temperature over the model's land region for the model time displayed; a time series of average temperature over India for the previous 36 hours (note the diurnal cycle); maximum and average rainfall over India for the same 36-hour period and a map of rainfall and surface pressure isobars for the model time displayed.

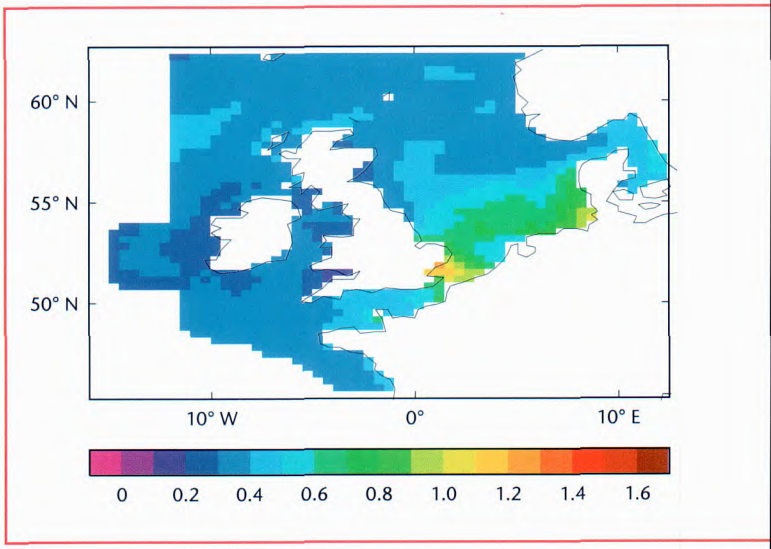

Figure 68. Changes in surge height (m) caused by changes in storminess, mean sea-level rise and isostatic rebound A2 emissions.

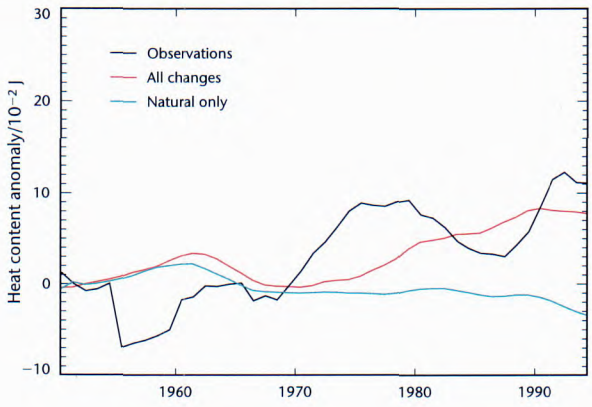

Figure 69. Comparison of observed and simulated changes in ocean heat content (1,022 J).

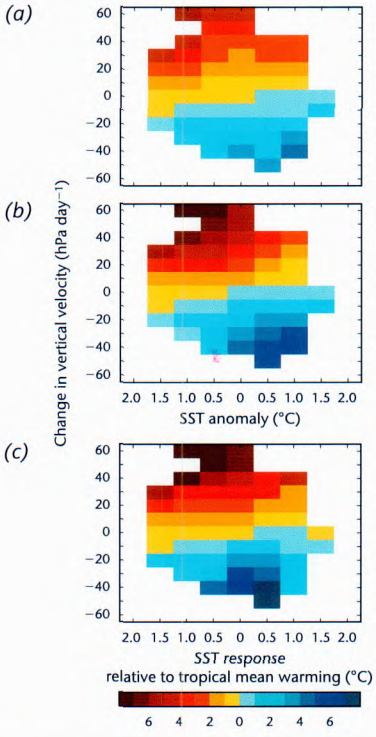

Figure 70. Changes in thick high cloud over the tropical oceans as a function of changes in vertical velocity and changes in local sea-surface temperature anomaly. (a) Derived from satellite observations; (b) from an atmospheric model simulation for the same period with sea-surface temperatures prescribed from observations; (c) due to the differences occurring on doubling atmospheric CO_2 in a model with a simple ocean.

was doubled. The variation of high cloud in this experiment (Fig. 70 (c)) was similar to the observations, suggesting that, in this case, similar processes may control the mean cloud response to climate change as control the present-day spatio-temporal variability of cloud. Therefore, in this case, validation against current climate is relevant for climate changes. However, other aspects of the cloud response are less realistic and there is clearly much more work to do in this area.

Stratospheric processes research

Our research programme continues to concentrate on the interaction between climate and atmospheric chemistry, with the main aim of predicting how ozone might evolve over the next few decades. To this end, multi-decadal length integrations have been performed with the Unified Model with Eulerian transport and chemistry (UMETRAC), which is a coupled chemistry-climate version of the Unified Model (UM), enabling changes in the concentrations of greenhouse gases and halogen loading to be taken into consideration. We carried out a simulation for the period 1975–2020 for mid-latitude ozone, in comparison with Total Ozone Mapping Spectrometer (TOMS) observations (Fig. 71). For the period 1980–2000, the model results are in agreement with observations by showing the springtime ozone depletion, which is particularly strong in the southern hemisphere because of the influence of the Antarctic ozone hole. There is, however, considerable interannual variability, which is larger in the model than is observed while the model is also biased high by about 30 Dobson Units. Nonetheless, the model results indicate at least a partial recovery of ozone in southern mid-latitudes from about the year 2005. In the north, further depletion may still occur as late as the end of the next decade, despite the anticipated reduction in chlorine and bromine concentrations. This is likely to be due to the cooling effect of the increased greenhouse gas concentrations in the lower stratosphere and is a topic of continuing research.

Meteorological variability in the equatorial stratosphere is dominated by the quasi-biennial oscillation (QBO), which appears as alternating bands of descending westward and eastward winds with a period of about 28 months. In the tropics and sub-tropics, the QBO has a substantial influence on stratospheric ozone and other important chemical constituents. Building on our success in simulating a realistic QBO in the UM (see *Scientific and Technical Review 1999/2000*, Fig. 42), a simulation of the QBO in ozone has

been obtained (Fig. 72) using UMETRAC. Results from the simulation are being analysed to determine how the meteorological variability influences the ozone chemistry.

Atmospheric chemistry modelling

As a result of human activities, atmospheric concentrations of a number of greenhouse gases are anticipated to build up further during this century. To predict the rises in the global concentrations of methane, ozone and sulphate aerosols from their pre-industrial baseline levels, we use a global three-dimensional Lagrangian chemistry-transport model, STOCHEM, which is fully integrated within the coupled atmosphere–ocean climate model, HadCM3. We have performed two 110-year fully coupled model integrations from 1990 through to 2100 with HadCM3/STOCHEM using 'control' and 'climate change' climatologies, both with increasing man-made trace gas emissions from the IPCC SRES A2 scenario.

There is an important feedback between the changing climate and the growth of the atmospheric burdens of the two most important non-CO_2 greenhouse gases: methane and tropospheric ozone. As the climate system warms up under the combined influence of the increasing burdens of all of the greenhouse gases, water vapour concentrations also increase globally. This increase in water vapour leads to an increase in the oxidising capacity of the troposphere and decreased rates of build-up of methane and ozone. Overall, the interaction between climate change and tropospheric chemistry exerts a strong negative feedback on the ocean–atmosphere chemistry system.

As a consequence of the growing man-made emissions of the greenhouse gases and the feedback with the climate system, we anticipate that surface ozone concentrations will rise throughout the 21st century. Figure 73 illustrates the extent of this increase by the decade 2060–9, for the month of July. The increase in surface ozone over the major populated and industrialised regions of the northern hemisphere is striking. Taken at face value, ozone levels appear to approach and exceed the internationally accepted air quality standards that were set to protect human health, crops and natural vegetation. There is the possibility that crop yields could be threatened by increasing ozone exposures. In addition, increasing ozone levels could decrease the growth rate of trees and, since trees are currently storing much of the CO_2 emitted by human activities, could also exert a positive feedback on climate change by decreasing CO_2 sinks. Our current main activity, using our STOCHEM model, is an investigation into the coupling between climate, atmospheric chemistry and ecosystem sources and sinks of greenhouse gases.

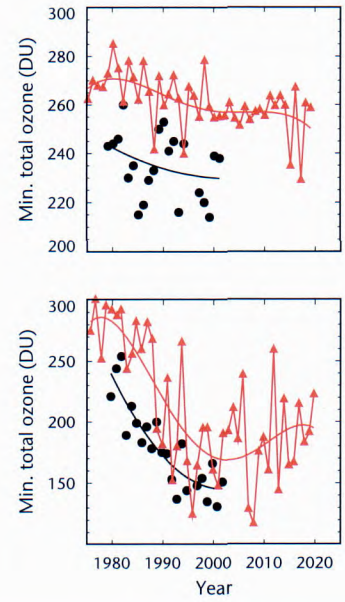

Figure 71. Model simulations of mid-latitude column ozone (red) in comparison with TOMS observations (black). The values plotted indicate the minimum values throughout spring within the latitude range 30–60 degrees. The smoothed lines are polynomial fits to the results.

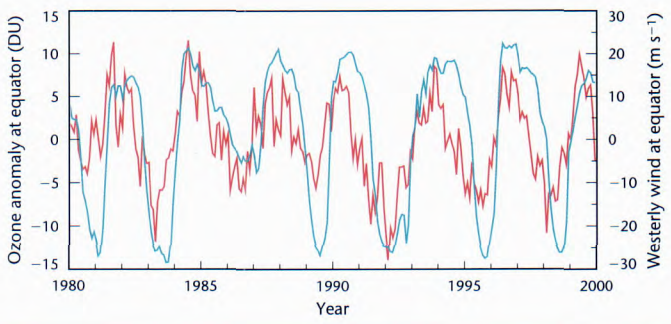

Figure 72. Monthly mean westerly wind at 20 hPa (blue curve) and column ozone deviations from the 20-year average (red curve) at the equator from the UMETRAC simulation. The QBO in the wind and ozone is clearly present.

Observation of sea-surface temperature

The Advanced Along-Track Scanning Radiometer (AATSR) is one of the instruments on the ESA satellite Envisat. This is the third in a series of accurately calibrated infrared radiometers, designed to establish a global record of sea-surface temperature (SST) at the levels of accuracy (~0.3 K) required for climate research.

SST observed by the satellite radiometer relates to the top few micrometres of the ocean (the skin), which can be significantly different from the bulk temperature sampled in situ by ships or buoys, typically at a depth of around 1 m. The Met Office will receive data from AATSR in near real time, at 10 arcminute spatial resolution. Skin SST will be retrieved from the radiance measurements, and bulk SST will be derived via physical models for the skin effect and diurnal thermocline. These temperatures can then be used to augment the Hadley Centre's existing SST climate data sets.

The first few months of Envisat's mission will be a commissioning phase and validation period. The Met Office is a key member of the AATSR validation team and will provide regular monitoring of the AATSR's performance, by comparing SSTs from the AATSR to those measured from buoys and to Hadley Centre SST analysis fields. Figure 74 shows the results of matching 1,240 ATSR-2 observations to measurements of SST from buoys; the observed skin-bulk temperature differences closely follow those expected from model calculations.

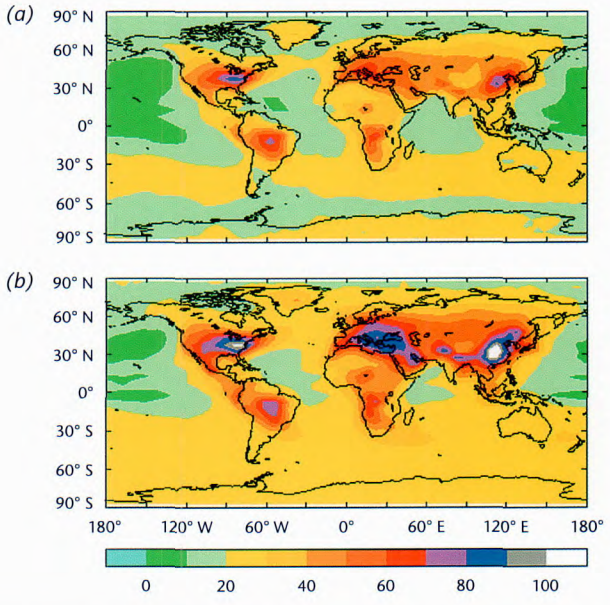

Figure 73. Surface ozone (ppb) during (a) July 2000–9 and (b) July 2060–9.

Model development and parametrizations

Climate modellers need to know whether their models have sufficient spatial resolution to represent the physical processes affecting the climate. We have investigated this using four horizontal resolutions of the climate model, ranging from N48 (2.5 × 3.75 degrees) to N144 (0.833 × 1.25 degrees). An inherent assumption in numerical modelling is that models will converge towards an ideal solution as resolution is increased, provided we

stay within the range for which the parametrizations are valid. However, we have shown that this assumption is not always justified. For example, Figure 75 shows that the warming in the troposphere when resolution is increased is largely converged at N96 (1.25 × 1.875 deg), whereas the cooling around the tropopause at the north pole is only apparent at N144. In principle, undesirable resolution dependencies in physical parametrizations can be removed. However, many processes, particularly intermittent processes such as convection, are inherently non-linear, making resolution dependency inevitable. In both the full model and in the dynamical core (in which the model is run with no parametrizations and a smooth uniform land surface), non-linear and non-local dynamics mean that certain aspects of the results do not converge when resolution is increased. These results show that it is important to explore the ability of models to simulate climate and the signals of climate change at a range of resolutions.

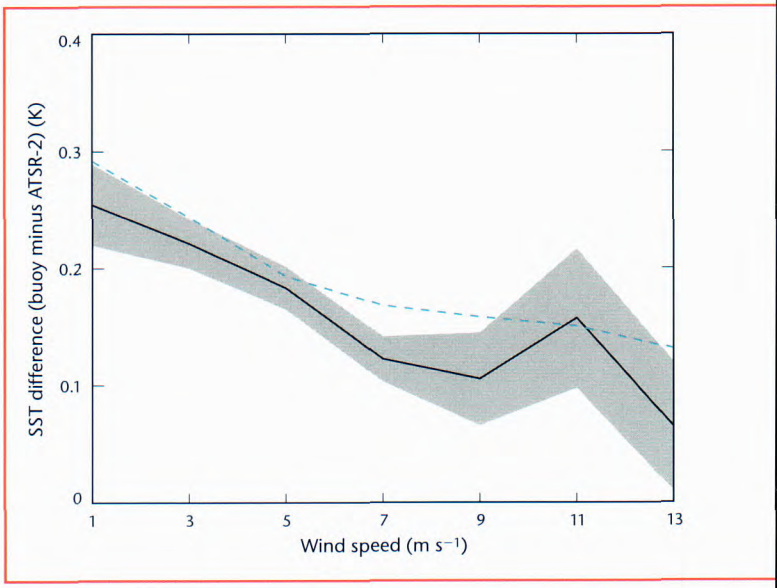

Figure 74. Night-time collocations of ATSR-2 with buoys during 1995–7. The temperature difference between buoy (i.e. bulk SST) and ATSR-2 (i.e. skin SST) is shown against wind speed, with the margin of error shaded. This trend of skin-bulk temperature difference, or skin effect, with wind is a commonly observed phenomenon; the dashed blue line shows the modelled skin effect.

We can now simulate smoke aerosol from biomass burning, and its radiative impact, in the climate model. The disastrous Indonesian forest fires of 1997 have been used as a case study. Regional reductions of over 50 W m^{-2} in monthly averaged surface solar radiation flux are simulated at the height of the event.

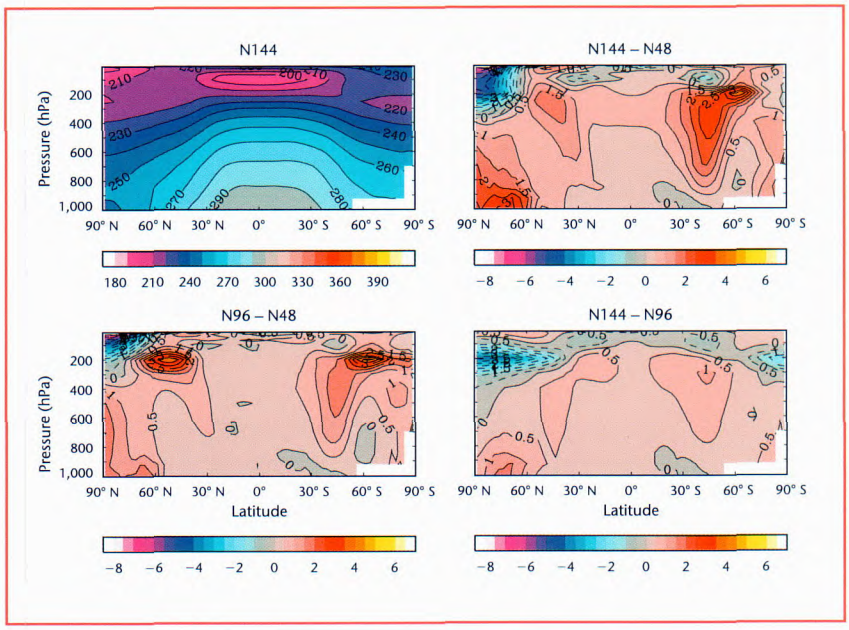

Figure 75. Zonal mean temperatures (K) from version HadAM3 of the climate model at a resolution of N144 (0.833×1.25 degrees) and differences between results at various resolutions.

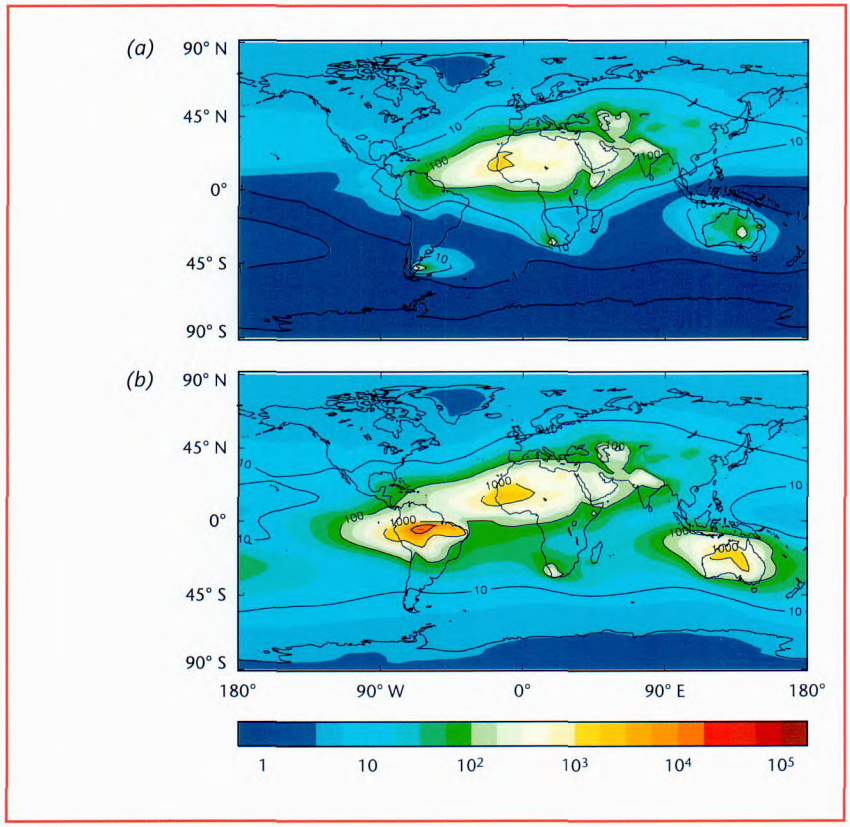

Figure 76. The annual mean column-integrated dust mass (mg m^{-2}), averaged over 10-year climate model experiments for (a) present day and (b) 2100.

Experiments have also begun to investigate the response of mineral dust aerosol to future climatic changes, using vegetation changes predicted by the coupled climate–carbon cycle model. Figure 76 compares the simulated dust distributions for the present day and 2100. The removal of the Amazonian rainforest by 2100 is shown to allow soil erosion, turning the region into a huge dust source comparable with the Sahara Desert. Australia and southern Africa also produce significantly more dust than at present.

Carbon cycle feedback will have a very important influence on climate change over the next century, with a potentially large positive feedback coming from the release of carbon from soils as global temperatures increase. However, the magnitude of this feedback is uncertain and depends particularly on the response of soil respiration to temperature. Observed CO_2 concentrations, and their response to naturally occurring climate anomalies, can be used to constrain the behaviour of soil respiration in our coupled climate–carbon cycle model. Our recent studies have shown that the model accurately simulates the carbon cycle's response to temperature changes caused by El Niño and volcanic eruptions. Suggestions that the soil is insensitive to temperature changes are not borne out by the observed carbon cycle variability. This enables us to put high and low sensitivity limits on the

soil's behaviour and quantify the uncertainty in our predictions of future CO_2 levels. Figure 77 shows the carbon cycle model's prediction of future CO_2 levels in the presence of climate–carbon cycle feedback and also the standard IS92a scenario for comparison. The shaded region between high and low sensitivity limits (red lines) shows the range of possible CO_2 values given the uncertainty in the release of soil carbon. It is clear that the feedback between the climate and the carbon cycle is large and positive, even for low values of the sensitivity.

Intergovernmental Panel on Climate Change (IPCC)

This year, the IPCC Working Group I (WGI) contributed towards the completion of the Synthesis Report of the Third Assessment Report. The Synthesis Report combined policy-relevant information drawn from each of the three Working Groups' volumes of the Third Assessment Report and also from all previously approved and accepted IPCC reports.

The IPCC was set up in 1988 by the World Meteorological Organization and the United Nations Environment Programme. The IPCC provides assessments of current scientific consensus concerning climate change, its potential impacts and the range of possible response strategies. A Met Office technical support unit co-ordinates the IPCC WGI and its focus is the scientific aspects of the climate system and of climate change. The IPCC WGI produced major assessments in 1990, 1995 and 2001, plus several reports and technical papers. These reports, written by international teams comprising the world's leading scientists, have played a major role in the negotiation and implementation of the UN Framework Convention on Climate Change.

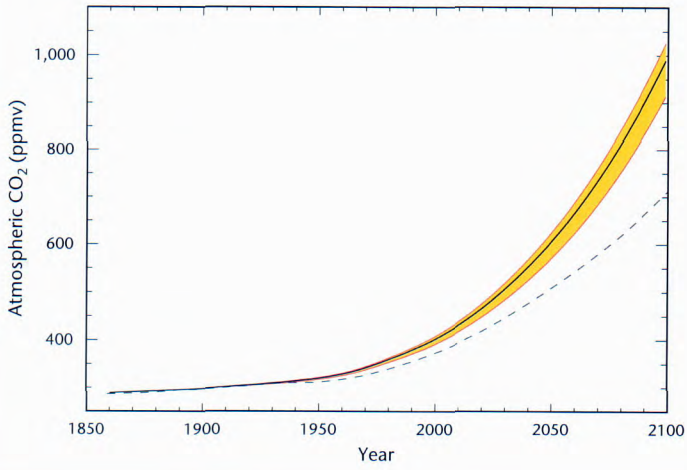

Figure 77. Atmospheric CO_2 concentrations simulated by the coupled climate–carbon cycle model to 2100. The central black line shows the model's 'best guess' simulation, based on the observed sensitivity of soil respiration to temperature changes. The dashed line shows the IS92a concentration scenario for reference.

Ocean Applications

Operational ocean modelling

Seasonal climate modelling and prediction

Ocean modelling for climate

Ocean observations — Argo

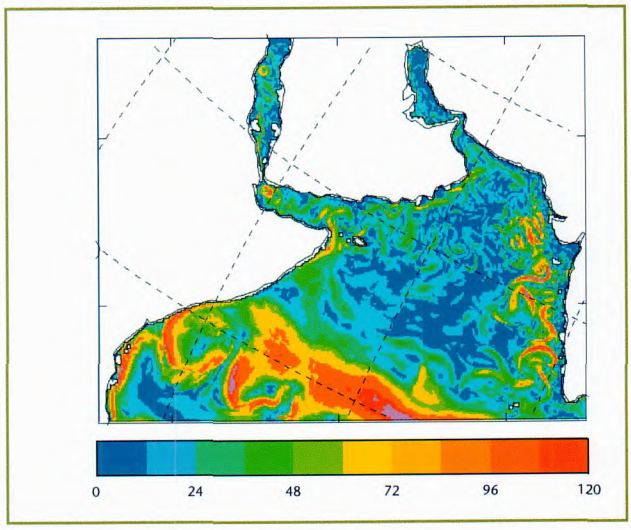

Figure 78. Mean current speeds (cm s^{-1}) from Arabian Sea FOAM.

Ocean Applications develops, and brings to implementation, the ocean modelling and seasonal forecasting systems required to meet Met Office customer needs. This includes ocean models for wave forecasting, our Forecasting Ocean Assimilation Model (FOAM), a global and basin-scale deep-ocean analysis and forecasting system, and regional shelf-seas models. We also carry out seasonal forecasting using a combination of atmospheric and coupled ocean–atmosphere models and statistical techniques. For climate research, we provide and validate the ocean component of the Hadley Centre's coupled ocean–atmosphere models. We also co-ordinate the UK's contribution to the international Argo programme for global ocean observing.

Real-time graphical products from FOAM and the shelf-seas model are now available on the Met Office web site (www.metoffice.com/research/ocean/operational) and the data are also freely available to research users via the NERC ESSC web server (www.nerc-essc.ac.uk/las). An enhanced range of seasonal forecasts is also publicly available on the Met Office web site (www.metoffice.com/research/seasonal).

Figure 79. View of extreme waves from a cargo ship.

Operational ocean modelling

Forecasting Ocean Assimilation Model

Each day, we run a global version of FOAM with 1° resolution, and a regional Atlantic and Arctic Ocean FOAM at 1/3°, to provide analyses and forecasts of ocean temperature, salinity, currents and sea ice. In recent years, we have been developing nested, high-resolution models to allow eddies to be represented. A 1/9° (~11 km) North Atlantic FOAM has been spun up and is being run for the Global Ocean Data Assimilation Experiment Atlantic prototype project during 2002.

We have made progress on the assimilation of observations into FOAM, establishing operational access to altimeter data that are now assimilated into regional configurations of FOAM. The accuracy of the model's surface temperature and height analyses depends significantly on the correlation scales and error estimates used in assimilating the data. Statistical estimates have been made of the model's errors at atmospheric 'synoptic' scales and oceanographic 'mesoscales'. The data assimilation scheme is being improved to use these statistics and enable observations to make a full impact on the day they arrive.

During September 2001, we ran nested high-resolution configurations of FOAM to provide daily forecasts in support of a joint forces exercise in Oman (Saif Sareea II). A model covering the Arabian Sea with a 13 km grid (Fig. 78) was nested inside a 30 km-resolution model of the Indian Ocean, which was in turn nested inside the 1° global model. The models were run daily using six-hourly surface fluxes from the numerical weather prediction (NWP) system, assimilating in situ temperature profiles and surface height data from satellite-borne altimeters.

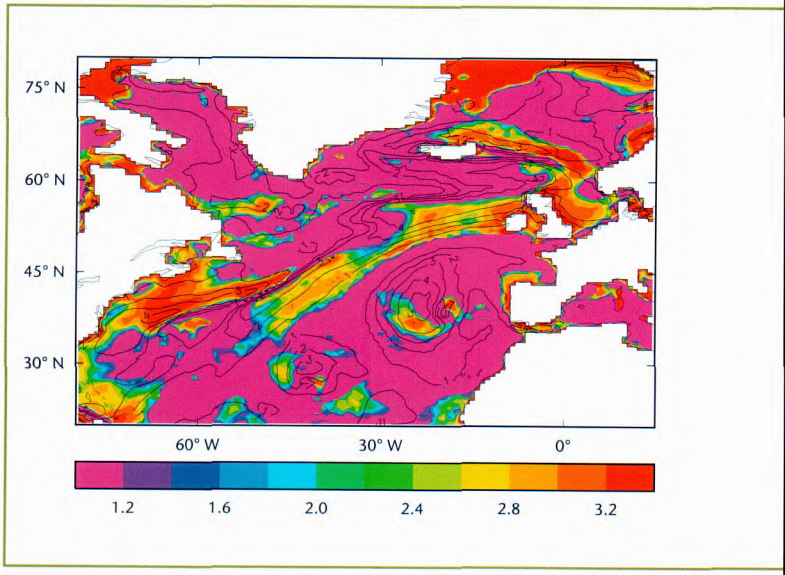

Figure 80. Predicted wave spectral peakedness overlaid on contours of wind-sea wave height (m) for 29 October 2001 in the North Atlantic.

Wave modelling

As part of the EC FP5 project 'MAXWAVE', we are developing a greater understanding of the occurrence of extreme waves (Fig. 79). We investigated two case studies: 25–26 October 1998 in the North Sea, when the vessel *Stenfjell* was damaged, and 10–11 November 1998, when the floating production storage and offloading (FPSO) system at Schiehallion, west of Shetland, was damaged. For both cases, we compared detailed spectral output from the wave model with in situ and remotely sensed observations of waves, to develop improved diagnostics. An example is the so-called 'peakedness parameter'. This varies between 1.0 for a fully developed sea state, to around 3.3 for young growing waves. Figure 80 shows a plot of this parameter from the global wave model, which can help identify those areas with waves that are both high and strongly growing, for example on the south-west flank of the storm to the west of Portugal.

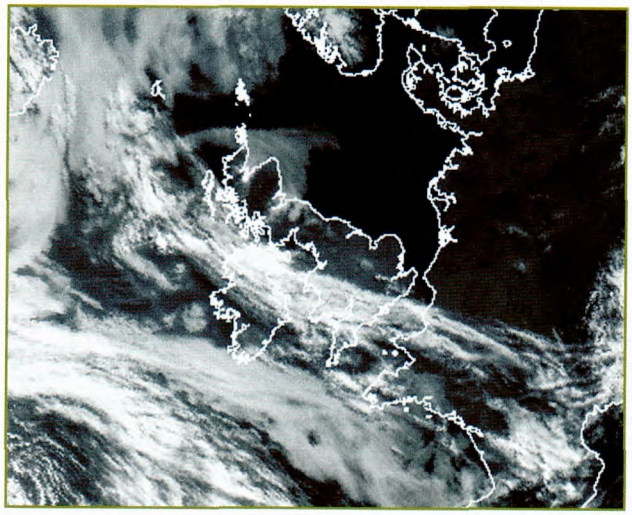

Figure 81. Visible satellite image at 07 UTC on 11 May 2001, showing coastal fog off north-east Scotland.

Shelf-seas modelling

We run daily a shelf-seas model with 12 km resolution to predict the temperature, salinity and currents over the north-west European shelf. In collaboration with the Joint Centre for Mesoscale Meteorology, we are investigating the impact of sea-surface temperature (SST) variability on the prediction of clearance of coastal fog through a case study for 10–11 May 2001 (Fig. 81). SST variability can arise from the influence of the daily cycle of heating, changes of weather and tidal forcing. SST in the operational mesoscale model is fixed in time throughout the model run and, in coastal waters, does not contain any spatial detail (Fig. 82 (a)). In contrast, the SST predicted by the shelf-seas

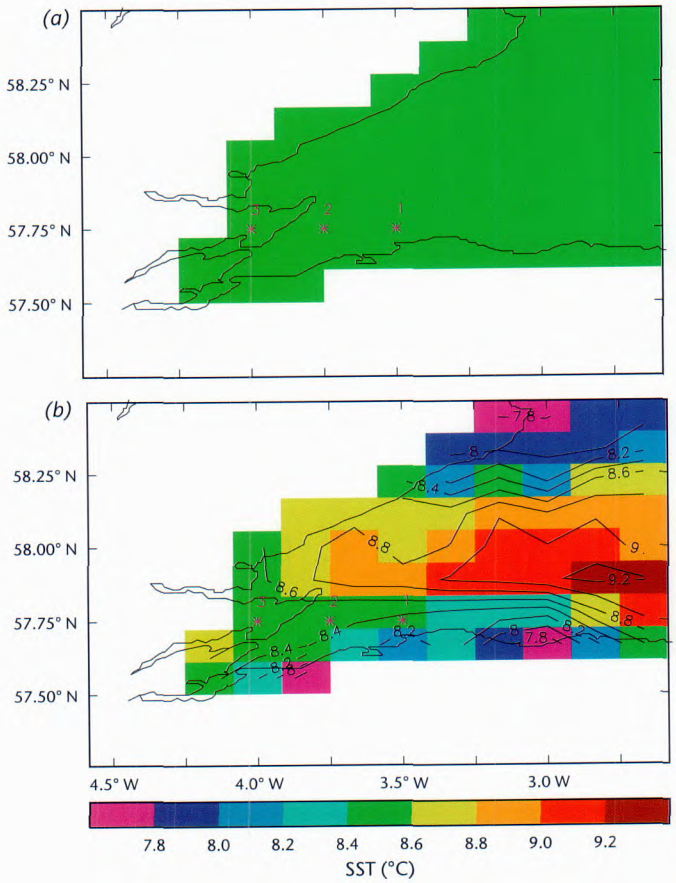

Figure 82. SST in the Moray Firth on 11 May 2001. (a) As used in the mesoscale model forecast and (b) from the shelf seas model with NWP mesoscale forcing at 01 UTC.

model varies in both time and space (Fig. 82 (b)). Hourly values of SST from the shelf-seas model are being input into the mesoscale model to assess the sensitivity of fog clearance to SST variability.

During 2001, we applied the shelf-seas model to the Persian Gulf, using climatological values of temperature and salinity at the open boundary in the Strait of Hormuz. Surface forcing is provided by hourly winds, pressures and six-hourly averaged heat and freshwater fluxes from the global NWP model. Circulation in the Persian Gulf is dominated by tidal flows and seasonal stratification; Fig. 83 shows the model surface-to-seabed temperature difference for early December 2001, indicating stratification in the deeper water off Iran.

Seasonal climate modelling and prediction

We carry out research and development on seasonal forecasting using dynamical models, together with statistical relationships based on historical data. The main source of predictive skill is SST, which changes relatively slowly and can be predicted on a seasonal timescale. We produce a variety of regional and global forecasts.

Seasonal forecasts with an atmospheric model

A quasi-operational seasonal prediction system is run to generate experimental seasonal predictions for all areas of the globe, providing long-term weather advice to UK Government departments and agencies. The forecasts are also made available to United Nations organisations, over 130 national meteorological services, the Drought Monitoring Centres of Africa, and commercial enterprises in the weather derivatives and energy trading sectors. To produce the predictions, we use a 'two-tier' representation of the atmosphere–ocean system. The atmosphere component is a version of the HadAM3 climate prediction model, integrated forward from current atmospheric conditions out to six months in a nine-member ensemble. The expected global SST evolution is supplied using an independent prediction of SST and sea ice based on the persistence of observed anomalies.

The El Niño and La Niña phenomena have a major influence on seasonal weather conditions in many parts of the globe. A case study for the 1987 El Niño and 1988 La Niña (Fig. 84) shows that, in many areas of the world, the

model is capable of predicting the precipitation responses associated with these events. The observed and predicted differences agree well over much of the tropics, particularly over the tropical Pacific, the Far East, and much of the Indian subcontinent. Correct responses are also indicated over parts of North America and Europe.

Ocean–atmosphere forecasts

We have also developed a more complex prediction system with a dynamical ocean coupled to the atmospheric component to represent air–sea interactions and feedbacks. The Global Seasonal (GloSea) system is based on the HadCM3 climate model, with enhanced ocean resolution in the tropics. Real-time, global ocean–atmosphere forecasts out to six months ahead are produced at monthly intervals using a 40-member ensemble. Figure 85 shows examples from an extensive set of retrospective forecasts aimed at predicting a period of substantial seasonal climate anomalies in the tropical Pacific.

Ocean modelling for climate

Ocean and sea-ice model development

Many important processes in the ocean occur at spatial scales not resolved by present climate models (e.g. boundary currents, eddies and sill overflows). To test the impact of better resolution of these processes, we have developed a new, coupled model, HadCEM. The model consists of the 'standard' atmosphere model HadAM3, coupled to a global ocean model with 1/3° resolution. The model has been run for 150 years with fixed, pre-industrial greenhouse gases, and a run with increasing greenhouse gases is in progress. This is the first extended run of a coupled global climate model with 'eddy-permitting' ocean resolution. The higher ocean resolution has resulted in many improvements in the simulation, e.g. better representation of the sill overflows between Greenland and Scotland (an important component of the ocean 'conveyor belt' circulation), resolution of important wave motions that

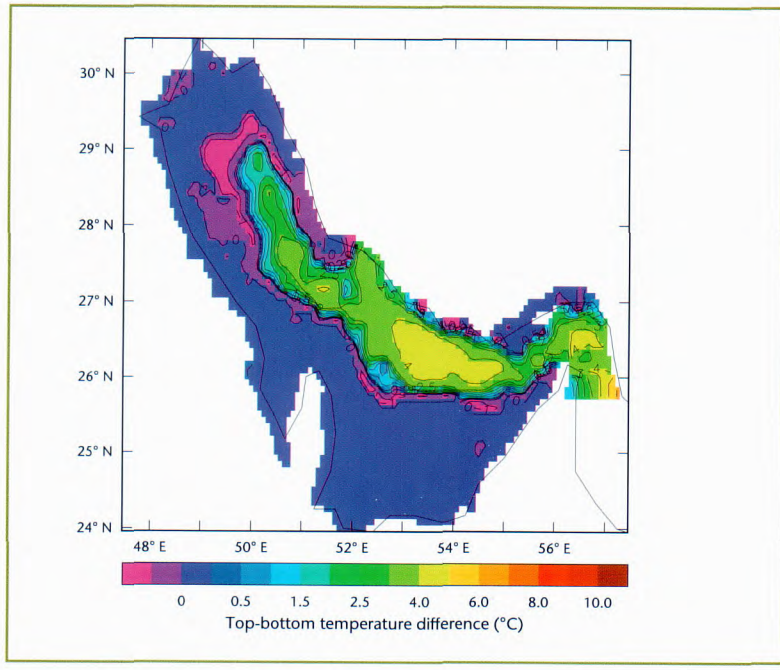

Figure 83. Predicted surface-to-seabed temperature difference for the Persian Gulf in early December 2001.

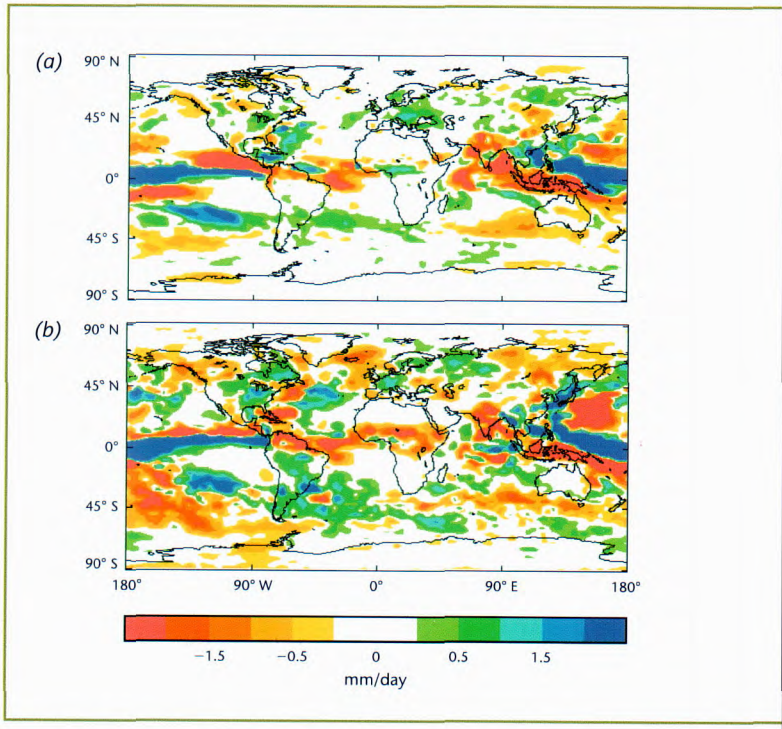

Figure 84. Differences in the precipitation anomalies (mm/day) for June/July/August 1987 (El Niño) and 1988 (La Niña). (a) Predicted by forecasts initialised at the beginning of May 1987 and 1988; (b) observed.

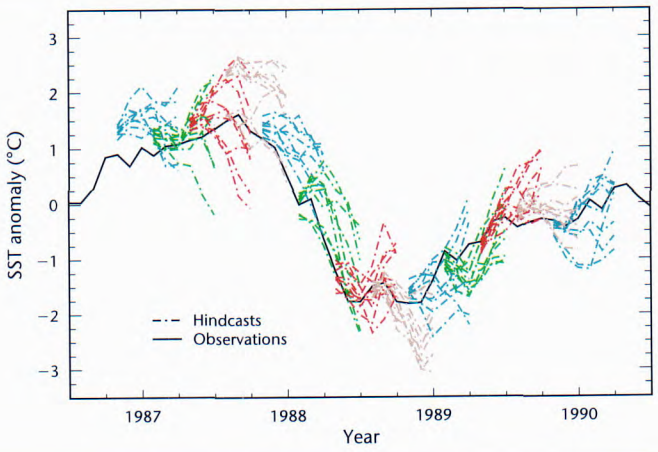

Figure 85. Retrospective nine-member ensemble forecasts of SST anomalies in the tropical Pacific when the El Niño/La Niña cycle was active.

have a significant effect on the transport of heat by the ocean (Fig. 86), and much-reduced drifts in many of the important water mass properties. There is a modest impact on global atmospheric climate, the main feature being an improvement in the temperature simulation in northern Europe; this may reflect a need for a matching increase in atmospheric resolution to respond to the finer scale ocean features.

A new version of the ocean climate model (HadGOM) is being developed in conjunction with the new coupled climate model HadGEM1. Compared with the current coupled model (HadCM3), this new ocean model has a higher horizontal resolution (particularly in the tropics), twice the number of vertical levels, a more realistic coastline, and a free ocean surface rather than a rigid lid. A more comprehensive sea-ice model is also being developed that greatly improves representation of sea-ice dynamics compared to that used in HadCM3. The model includes an elastic-viscous-plastic treatment of sea-ice flow, allowing the dynamics to predict movement of sea ice based on ocean currents, winds and material strength of the ice (Fig. 87).

The role of the ocean in climate

We have made considerable progress in understanding mechanisms of long-term climate variability in the North Atlantic. A mode of variability has been identified both in observations and in the HadCM3 model, in which the ocean appears to play an active role in driving decadal atmospheric variations in the North Atlantic sector. This suggests the possibility of predictability over decadal timescales. Over longer timescales (of the order of 50 years), variations in the Atlantic Thermohaline Circulation (THC) appear to modulate climate in the HadCM3 model; this is supported by the limited observational evidence available.

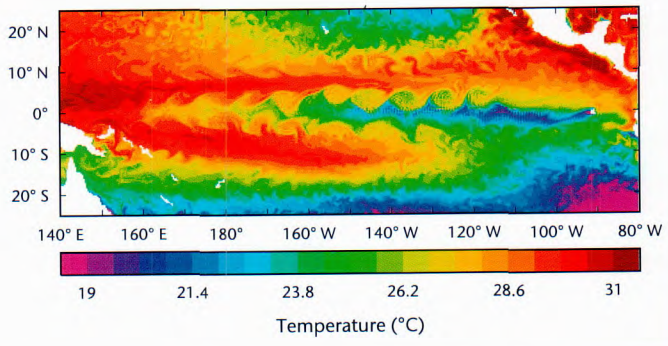

Figure 86. Instantaneous SST at 5 m in the tropical Pacific with the HadCEM model during September 1980. Note the large wave motions near the equator that are not resolved in lower-resolution climate models.

We have continued to work on the use of climate models to guide development of ocean monitoring systems. An important issue is to understand recent estimates of changes in ocean heat content over the past 50 years. Climate models have been unable to reproduce apparent decadal variations in heat content. However, the heat content estimates are based on historical data that have poor spatial coverage in many regions of the ocean.

By subsampling model temperatures at a similar resolution to the observations, we are gaining an insight into how to interpret the apparent differences between modelled and observed heat content. This insight can also be fed into future monitoring campaigns such as Argo (see below). Another application is in the design of observing systems for monitoring changes in the Atlantic THC. Using HadCM3, we are making estimates of quantities that are likely to provide a good signal-to-noise ratio in detection and attribution of THC changes, as an input to national and international monitoring programmes.

The ocean carbon cycle

It has been suggested that the release of dimethylsulphide (DMS) by plankton is part of an important feedback to climate. DMS released from the ocean produces sulphate aerosol in the atmosphere, which modifies cloud properties and so changes the amount of solar radiation reaching the ocean surface and affecting plankton growth. Experiments using an adapted version of the HadCM3 model have shown the potential for this feedback to be significant. Perturbing the ocean's DMS emissions has an impact on simulated climate, e.g. an increase in DMS emissions leads to cooling through an increase in cloud cover and albedo (Fig. 88).

Figure 87. Sea ice.

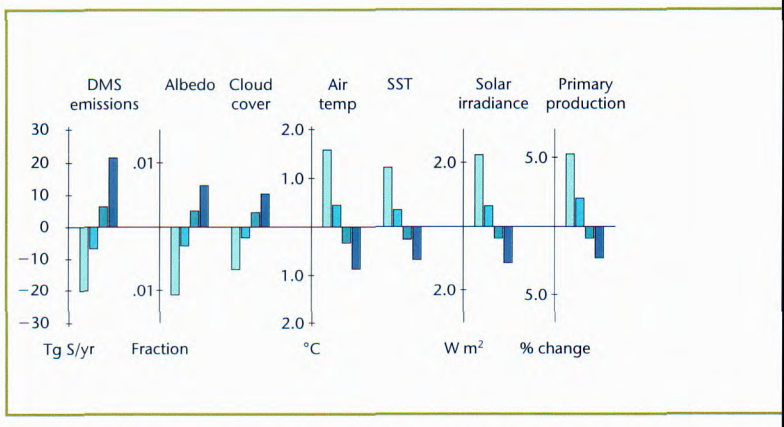

Figure 88. The global mean response in the HadCM3 model to altering DMS emissions from the ocean.

Ocean observations — Argo

Argo will be a global array of 3,000 free-drifting profiling floats that will measure the temperature and salinity of the upper 2,000 m of the ocean. During 2002, 29 UK floats were deployed in a number of different geographic areas: the Irminger Basin (north-west Atlantic), the north-east Atlantic, the Norwegian Sea, the south-west Indian Ocean and the Arabian Sea. Data from the UK floats are available in real time via the World Meteorological Organization's Global Telecommunication System and, together with all other available float data, are routinely assimilated into operational FOAM. The data are also available from the UK Argo Data Centre established at the British Oceanographic Data Centre.

In Spring 2002, 25 floats were deployed along the 32° S section in the southern Indian Ocean, and more floats will be deployed in the Arabian Sea. Hadley Centre climate simulations suggest that the freshening of intermediate waters in these two areas is a sign of man-made climate change. Floats have also been deployed in the Southern Ocean (Atlantic sector), with further floats in the Irminger Sea and Norwegian Sea.

Bibliography

AGNEW, P., LUNNON, R.W., HOAD, D.J., et al., 2001: Wake vortex alleviation strategies focus on influence of weather on vortex behaviour. *ICAO Journal*, **56 (no. 7)**, 8–10 and 28.

Albritton, D.L. et al. (including GRIGGS, D.J., FOLLAND, C.K., GREGORY, J.M., HAYWOOD, J.M., JOHNSON, C.A., MASKELL, K., MITCHELL, J.F.B., and NOGUER, M.), 2001: Summary for policymakers. *In* Climate Change 2001: The Scientific Basis. J.T. Houghton et al. (Eds). Cambridge University Press.

Albritton, D.L. et al. (including GRIGGS, D.J., MITCHELL, J.F.B. and NOGUER, M.), 2001: Technical summary. *In* Climate Change 2001: The Scientific Basis. J.T. Houghton et al. (Eds). Cambridge University Press.

ALEXANDER, L.V. and Jones, P.D., 2001: Updated precipitation series for the U.K. and discussion of recent extremes. *Atmos Sci Lett*, **1**, 142–150 (available only online at www.idealibrary.com/links/doi/10.1006/asle.2001.0025/pdf).

ALLEN, T. and BROWN, A.R., 2002: Large-eddy simulation of turbulent separated flow over rough hills. *Boundary-Layer Meteorol*, **102**, 177–198.

ALLOTT, T.P., HAND, W.H. and LEE, M.J., 2002: High-resolution observations of the Bracknell storm, 7 May 2000. *Weather,* **57**, 73–77.

Anderson, T.R., SPALL, S.A., Yool, A., Cipollini, P., Challenor, P.G. and Fasham, M.J.R., 2001: Global fields of sea surface dimethylsulfide predicted from chlorophyll, nutrients and light. *J Mar Syst,* **30**, 1–20.

ATHANASSIADOU, M. and Castro, I.P., 2001: Neutral flow over a series of rough hills: a laboratory experiment. *Boundary-Layer Meteorol*, **101**, 1–30.

ATKINSON, N.C., 2001: Calibration, monitoring and validation of AMSU-B. *Adv Space Res*, **28**, 117–126.

AUSTIN, J. et al., 2001: Stratospheric ozone and the link to climate change. *In* European research in the stratosphere, 1996–2000. European Commission.

AUSTIN, J., BUTCHART, N. and KNIGHT, J., 2001: Three-dimensional chemical model simulations of the ozone layer: 2015–2055. *QJR Meteorol Soc,* **127**, 959–974.

AUSTIN, J., 2002: A three-dimensional coupled chemistry-climate model simulation of past stratospheric trends. *J Atmos Sci,* **59**, 218–232.

Baker, H.C., Dodson, A.H., Penna, N.T., Higgins, M. and OFFILER, D., 2001: Ground-based GPS water vapour estimation: potential for meteorological forecasting. *J Atmos & Sol-Terr Phys*, **63**, 1,305–1,314.

BARAN, A.J., FRANCIS, P.N., HAVEMANN, S. and Yang, P., 2001: A study of the absorption and extinction properties of hexagonal ice columns and plates in random and preferred orientation, using exact *T*-matrix theory and aircraft observations of cirrus. *J Quant Spectrosc & Radiat Transfer*, **70**, 505–518.

BARAN, A.J., FRANCIS, P.N., Labonnote, L.-C. and Doutriaux-Boucher, M., 2001: A scattering phase function for ice cloud: tests of applicability using aircraft and satellite multi-angle multi-wavelength radiance measurements of cirrus. *QJR Meteorol Soc*, **127**, 2,395–2,416.

BARAN, A.J., Yang, P. and HAVEMANN, S., 2001: Calculation of the single-scattering properties of randomly oriented hexagonal ice columns: a comparison of the T-matrix and the finite- difference time-domain methods. *Appl Opt*, **40**, 4,376–4,386.

Bergstrom, R.W., Russell, P.B. and HIGNETT, P., 2002: Wavelength dependence of the absorption of black carbon particles: predictions and results from the TARFOX experiment and implications for the aerosol single scattering albedo. *J Atmos Sci*, **59**, 567–577.

BEST, M.J. and HOPWOOD, W.P., 2001: Modelling the local surface exchange over a grass-field site under stable conditions. *QJR Meteorol Soc*, **127**, 2,033–2,052.

BETTS, R.A., 2001: Biogeophysical impacts of land use on present-day climate near-surface temperature change and radiative forcing. *Atmos Sci Lett*, **2**, 39–51 (available only online at www.idealibrary.com/links/doi/10.1006/asle.2001.0023/pdf).

Boucher, O. and HAYWOOD, J., 2001. On summing the components of radiative forcing of climate change. *Clim Dyn*, **18**, 297–302.

BROWN, A.R. and WOOD, N., 2001: Turbulent form drag on anisotropic three-dimensional orography. *Boundary-Layer Meteorol*, **101**, 229–241.

BROWN, P.R.A. and Heymsfield, A.J., 2001: The microphysical properties of tropical convective anvil cirrus: A comparison of models and observations. *QJR Meteorol Soc*, **127**, 1,535–1,550.

BUTCHART, N. and SCAIFE, A.A., 2001: Removal of chlorofluorocarbons by increased mass exchange between the stratosphere and troposphere in a changing climate. *Nature*, **410**, 799–802.

Cardwell, J.R., Choularton, T.W., WILSON, D. and KERSHAW, R., 2002: Use of an explicit model of the microphysics of precipitating stratiform cloud to test a bulk microphysics scheme. *QJR Meteorol Soc*, **128**, 573–592.

CARNELL, R.E. and SENIOR, C.A., 2002: An investigation into the mechanisms of changes in mid-latitude mean sea level pressure as greenhouse gases are increased. *Clim Dyn*, **18**, 533–543.

Church, J.A. and GREGORY, J.M., 2001: Sea level change. *In* Encyclopedia of ocean sciences. J.H. Steele, S.A. Thorpe and K.K. Turekian (Eds). London, Academic Press.

Church, J.A. et al. (including GREGORY, J.M.), 2001: Changes in sea level. *In* Climate Change 2001: The Scientific Basis. J.T. Houghton et al. (Eds). Cambridge University Press.

CLARK, P.A. and HOPWOOD, W.P., 2001: One-dimensional site-specific forecasting of radiation fog. Part I: Model formulation and idealised sensitivity studies. *Meteorol Appl*, **8**, 279–286.

CLARK, P.A. and HOPWOOD, W.P., 2001: One-dimensional site-specific forecasting of radiation fog. Part II: Impact of site observations. *Meteorol Appl*, **8**, 287–296.

COLLINS, M., TETT, S.F.B. and COOPER, C., 2001: The internal climate variability of HadCM3, a version of the Hadley Centre coupled model without flux adjustments. *Clim Dyn*, **17**, 61–81.

COLLINS, W.J., DERWENT, R.G., JOHNSON, C.E. and STEVENSON, D.S., 2001: The oxidation of organic compounds in the troposphere and their global warming potentials. *Clim Change*, **52**, 453–479.

COLLINS, W.J., DERWENT, R.G., JOHNSON, C.E. and STEVENSON, D.S., 2001: The origins of an early spring maximum in the global tropospheric ozone burden in a 3-D chemistry-transport model. *In* TOR-2 Annual Report. Munich, EUROTRAC-2 ISS, GSF National Research Center for Environment and Health.

COLMAN, A. and DAVEY, M., 2001: Experimental forecast of 2001 seasonal rainfall in the Sahel and other regions of tropical North Africa. *Exp Long-Lead Forecast Bull*, **10**, No. 2 (available only online at http://grads.iges.org/ellfb/Jun01/colman.jun01.htm).

COLMAN, A., 2001: Experimental forecast of east African rainfall for October–December 2001. *Exp Long-Lead Forecast Bull*, **10**, No. 3 (available only online at http://grads.iges.org/ellfb/Sep01/coleman/coleman.htm).

COLMAN, A.W., DAVEY, M.K., MCLEAN, P. and GRAHAM, R.J., 2001: Forecast of north Brazil seasonal rainfall for February to May 2002 using empirical and dynamical methods based on atmosphere and sea temperatures up to mid-December 2001. *Exp Long-Lead Forecast Bull*, **10**, No. 4 (available only online at http://grads.iges.org/ellfb/Dec01/coleman/colman.htm).

COOPER, C. and GORDON, C., 2002: North Atlantic oceanic decadal variability in the Hadley Centre coupled model. *J Clim*, **15**, 45–72.

COX, P.M., BETTS, R.A., JONES, C.D., SPALL, S.A. and Totterdell, I.J., 2001: Modelling vegetation and the carbon cycle as interactive elements of the climate system. *In* Meteorology at the millennium. R.P. Pearce (Ed.). Academic Press.

Cramer, W. et al. (including BETTS, R.A. and COX, P.M.), 2001: Global response of terrestrial ecosystem structure and function to CO_2 and climate change: results from six dynamic global vegetation models. *Glob Change Biol*, **7**, 357–373.

DAVEY, M.K., HUDDLESTON, M.R., et al., 2002: STOIC: a study of coupled model climatology and variability in tropical ocean regions. *Clim Dyn*, **18**, 403–420.

DAVIES, L.A. and BROWN, A.R., 2001: Assessment of which scales of orography can be credibly resolved in a numerical model. *QJR Meteorol Soc*, **127**, 1,225–1,237.

DERWENT, R.G., RYALL, D.B., Jennings, S.G., Spain, T.G. and Simmonds, P.G., 2001: Black carbon aerosol and carbon monoxide in European regionally polluted air masses at Mace Head, Ireland during 1995–1998. *Atmos Environ*, **35**, 6,371–6,378.

DERWENT, R.G., COLLINS, W.J., JOHNSON, C.E. and STEVENSON, D.S., 2001: Transient behaviour of tropospheric ozone precursors in a global 3-D CTM and their indirect greenhouse effects. *Clim Change*, **49**, 463–487.

DERWENT, R.G., Jenkin, M.E., Saunders, S.M. and Pilling, M.J., 2001: Characterisation of the reactivities of volatile organic compounds using a Master Chemical Mechanism. *J Air and Waste Manage Assoc*, **51**, 699–707.

Dixon, J., MIDDLETON, D.R. and DERWENT, R.G., 2001: Sensitivity of nitrogen dioxide concentrations to oxides of nitrogen controls in the United Kingdom. *Atmos Environ*, **35**, 3,715–3,728.

Dixon, J., MIDDLETON, D.R. and DERWENT, R.G., 2000: Using measurements of nitrogen oxides to estimate the emission controls required to meet the UK nitrogen dioxide standard. *Environ Monit and Assess*, **65**, 3–11.

Donnell, E.A., Fish, D.J., Dicks, E.M. and THORPE, A.J., 2001: Mechanisms for pollutant transport between the boundary layer and the free troposphere. *J Geophys Res*, **106**, 7,847–7,856.

DURMAN, C.F., GREGORY, J.M., HASSELL, D.C., JONES, R.G. and MURPHY, J.M., 2001: A comparison of extreme European daily precipitation simulated by a global and a regional climate model for present and future climates. *QJR Meteorol Soc*, **127**, 1,005–1,015.

ESSERY, R., 2001: Spatial statistics of windflow and blowing-snow fluxes over complex topography. *Boundary-Layer Meteorol*, **100**, 131–147.

EYRE, J.R., 2001: Planet Earth seen from space: basic concepts. *In* Proceedings of ECMWF seminar on exploitation of the new generation of satellite instruments for numerical weather forecasts; 4–8 September 2000. Reading, ECMWF.

FIELD, P.R., COTTON, R.J., JOHNSON, D., et al., 2001: Ice nucleation in orographic wave clouds: measurements made during INTACC. *QJR Meteorol Soc*, **127**, 1,493–1,512.

FOLLAND, C. and COLMAN, A., 2001: Empirical prediction of the global temperature anomaly for 2002. *Exp Long-Lead Forecast Bull*, **10**, No. 4 (available only online at http://grads.iges.org/ellfb/Dec01/folland/folland2.htm).

FOLLAND, C.K. and Karl, T.R., 2001: Recent rates of warming in the marine environment: examining the controversy. *EOS Trans*, **82**, 453 and 458–459.

FOLLAND, C.K., COLMAN, A.W., ROWELL, D.P. and DAVEY, M.K., 2001: Predictability of northeast Brazil rainfall and real-time forecast skill, 1987–98. *J Clim*, **14**, 1,937–1,958.

FOLLAND, C.K., FRICH, P., PARKER, D., ALEXANDER, L., MACADAM, I., RAYNER, N.A., et al., 2001: Observed climate variability and change. *In* Climate Change 2001: The Scientific Basis. J.T. Houghton et al. (Eds). Cambridge University Press.

FOLLAND, C.K., RAYNER, N.A., BROWN, S.J., PARKER, D.E., MACADAM, I., SEXTON, D.M.H., et al., 2001: Global temperature change and its uncertainties since 1861. *Geophys Res Lett*, **28**, 2,621–2,624.

Fowler, D. et al. (including DERWENT, R.G.), 2001: Transboundary air pollution. Acidification, eutrophication and ground-level ozone in the UK. *In* National Expert Group on Transboundary Air Pollution. London, Department for the Environment, Food and Rural Affairs.

FRICH, P., ALEXANDER, L.V., et al., 2002: Observed coherent changes in climatic extremes during the second half of the 20th century. *Clim Res*, **19**, 193–212.

Garand, L. et al. (including RAYER, P.J. and SAUNDERS, R.), 2001: Radiance and Jacobian intercomparison of radiative transfer models applied to HIRS and AMSU channels. *J Geophys Res*, **106**, 24,017–24,031.

Gillett, N.P., Allen, M.R., MCDONALD, R.E., SENIOR, C.A., Shindell, D.T. and Schmidt, G.A., 2002: How linear is the Arctic Oscillation response to greenhouse gases? *J Geophys Res*, **107 (D3)**, ACL 1-1 to ACL 1-7.

Gillett, N.P., Hegerl, G.C., Allen, M.R., STOTT, P.A. and Schnur, R., 2002: Reconciling two approaches to the detection of anthropogenic influence on climate. *J Clim*, **15**, 326–329.

Giorgi, F. et al. (including JONES, R.G.), 2001: Emerging patterns of simulated regional climatic changes for the 21st century due to anthropogenic forcings. *Geophys Res Lett*, **28**, 3,317–3,320.

GLOSTER, J., HEWSON, H.J., et al., 2001: Spread of foot-and-mouth disease from the burning of animal carcases on open pyres. *Vet Rec*, **148**, 585–589.

Gray, S.L. and THORPE, A.J., 2001: Parcel theory in three dimensions and the calculation of SCAPE. *Mon Weather Rev*, **129**, 1,656–1,672.

GREGORY, D., 2001: Estimation of entrainment rate in simple models of convective clouds. *QJR Meteorol Soc*, **127**, 53–72.

GREGORY, J.M., LOWE, J.A., et al., 2001: Comparison of results from several AOGCMs for global and regional sea-level change 1900–2100. *Clim Dyn*, **18**, 225–240.

HAND, W.H., 2002: The Met Office convection diagnosis scheme. *Meteorol Appl*, **9**, 69–83.

HAVEMANN, S. and BARAN, A.J., 2001: Extension of *T*-matrix to scattering of electromagnetic plane waves by non-axisymmetric dielectric particles: application to hexagonal ice cylinders. *J Quant Spectrosc & Radiat Transfer*, **70**, 139–158.

HAYWOOD, J.M., FRANCIS, P.N., GLEW, M.D. and TAYLOR, J.P., 2001: Optical properties and direct radiative effect of Saharan dust: A case study of two Saharan dust outbreaks using aircraft data. *J Geophys Res*, **106**, 18,417–18,428.

HAYWOOD, J.M., FRANCIS, P.N., Geogdzhayev, I., Mishchenko, M. and Frey, R., 2001: Comparison of Saharan dust aerosol optical depth derived using aircraft mounted pyranometers and 2-channel AVHRR retrieval algorithms. *Geophys Res Lett*, **28**, 2,393–2,396.

HEALY, S.B., 2001: Smoothing radio occultation bending angles above 40 km. *Ann Geophys*, **19**, 459–468.

HEALY, S.B., 2001: Radio occultation bending angle and impact parameter errors caused by horizontal refractive index gradients: A simulation study *J Geophys Res*, **106**, 11,875–11,889.

HEWITT, C.D., SENIOR, C.A. and MITCHELL, J.F.B., 2001: The impact of dynamic sea-ice on the climatology and climate sensitivity of a GCM: a study of past, present, and future climates. *Clim Dyn*, **17**, 655–668.

Hill, D.C., Allen, M.R. and STOTT, P.A., 2001: Allowing for solar forcing in the detection of human influence on tropospheric temperatures. *Geophys Res Lett*, **28**, 1,555–1,558.

Hogan, R.J., FIELD, P.R., Illingworth, A.J., COTTON, R.J. and Choularton, T.W., 2002: Properties of embedded convection in warm-frontal mixed-phase cloud from aircraft and polarimetric radar. *QJR Meteorol Soc*, **128**, 451–476.

Holt, M.A., HARDAKER, P.J. and McLelland, G.P., 2001: A lightning climatology for Europe and the UK, 1990–99. *Weather*, **56**, 290–296.

HORTON, E.B., FOLLAND, C.K. and PARKER, D.E., 2001: The changing incidence of extremes in worldwide and central England temperatures to the end of the twentieth century. *Clim Change*, **50**, 267–295.

HORTON, E.B., PARKER, D.E., FOLLAND, C.K., Jones, P.D. and Hulme, M., 2001: The effect of increasing the mean on the percentage of extreme values in Gaussian and skew distributions. Response to X. Zhang et al. *Clim Change*, **50**, 509–510.

Hurrell, J.W., Hoerling, M.P. and FOLLAND, C.K., 2001: Climate variability over the North Atlantic. *In* Meteorology at the millennium. R.P. Pearce (Ed.). Academic Press.

INGLEBY, N.B., 2001: Comment on 'A statistical determination of the random observational errors present in Voluntary Observing Ships meteorological reports'. *J Atmos and Oceanic Technol*, **18**, 1,102–1,107.

Inness, P.M., Slingo, J.M., Woolnough, S.J., Neale, R.B. and POPE, V.D., 2001: Organization of tropical convection in a GCM with varying vertical resolution; implications of the Madden–Julian Oscillation. *Clim Dyn*, **17**, 777–793.

JACKSON, D.R., 2001: Ozone data assimilation at the Met Office. *In* Proceedings of EUMETSAT SAF Training Workshop: ozone monitoring, Halkidiki, Greece, 21–23 May 2001.

JACKSON, D.R., AUSTIN, J. and BUTCHART, N., 2001: An updated climatology of the troposphere–stratosphere configuration of the Met Office's Unified Model. *J Atmos Sci*, **58**, 2,000–2,008.

Jenkin, M.E. et al. (including DERWENT, R.G. and COLLINS, W.J.), 2001: Modelling of tropospheric ozone formation. AEA Technology Report AEAT/R/ENV/0485 Issue 1. AEA Technology, Culham Laboratory, Oxfordshire.

JOHNSON, C.E., STEVENSON, D.S., COLLINS, W.J. and DERWENT, R.G., 2001: Role of climate feedback on methane and ozone studied with a coupled ocean–atmosphere-chemistry model. *Geophys Res Lett*, **28**, 1,723–1,726.

JONES, A., ROBERTS, D.L., WOODAGE, M.J. and JOHNSON, C.E., 2001: Indirect sulphate aerosol forcing in a climate model with an interactive sulphur cycle. *J Geophys Res*, **106**, 20,293–20,310.

JONES, C.D. and COX, P.M., 2001: Constraints on the temperature sensitivity of global soil respiration from the observed interannual variability in atmospheric CO_2. *Atmos Sci Lett*, **2**, 166–172 (available only online at www.idealibrary.com/links/doi/10.1006/asle.2001.0041/pdf).

JONES, C.D., COLLINS, M., COX, P.M. and SPALL, S.A., 2001: The carbon cycle response to ENSO: A coupled climate–carbon cycle model study. *J Clim*, **14**, 4,113–4,129.

JONES, C.D. and COX, P.M., 2001: Modeling the volcanic signal in the atmospheric CO_2 record. *Global Biogeochem Cycle*, **15,** 453–465.

KEIL, M., Heun, M., AUSTIN, J., Lahoz, W., Lou, G.P. and O'Neill, A., 2001: The use of long-duration balloon data to determine the accuracy of stratospheric analyses and forecasts. *J Geophys Res*, **106**, 10,299–10,312.

Labitzke, K. et al. (including AUSTIN, J., BUTCHART, N. and KNIGHT, J.), 2002: The global signal of the 11-year solar cycle in the stratosphere: observations and models. *J Atmos Sol-Terr Phys,* **64**, 203–210.

Larson, V.E., WOOD, R., FIELD, P.R., Golaz, J.-C., Vonder Haar, T.H. and Cotton, W.R., 2001 Systematic biases in the microphysics and thermodynamics of numerical models that ignore subgrid-scale variability. *J Atmos Sci*, **58**, 1,117–1,128.

Larson, V.E., WOOD, R., FIELD, P.R., Golaz, J.-C., Vonder Haar, T.H. and Cotton, W.R., 2001: Small-scale and mesoscale variability of scalars in cloudy boundary layers: One-dimensional probability density functions. *J Atmos Sci*, **58**, 1,978–1,994.

Lawrimore, J.H. et al. (including ALEXANDER, L.), 2001: Climate assessment for 2000. *Bull Am Meteorol Soc*, **82**, S1–S55.

Le Traon, P.Y. et al. (including BELL, M.), 2001: Operational oceanography and prediction: A GODAE perspective. *In* Observing the oceans in the 21st century. C.J. Koblinsky and N.R. Smith (Eds). Melbourne, GODAE Project Office and Bureau of Meteorology.

LOCK, A.P., 2001: The numerical representation of entrainment in parametrizations of boundary layer turbulent mixing. *Mon Weather Rev*, **129**, 1,148–1,163.

LOWE, J.A., GREGORY, J.M. and Flather, R.A., 2001: Changes in the occurrence of storm surges around the United Kingdom under a future climate scenario using a dynamic storm surge model driven by the Hadley Centre climate models. *Clim Dyn*, **18**, 179–188.

McAvaney, B.J. et al. (including WOOD, R.A.), 2001: Model evaluation. *In* Climate Change 2001: The Scientific Basis. J.T. Houghton et al. (Eds). Cambridge University Press.

MCGRATH, A.J. and HEWISON, T.J., 2001: Measuring the accuracy of MARSS — an airborne microwave radiometer. *J Atmos and Oceanic Technol*, **18**, 2,003–2,012.

MACPHERSON, B., 2001: Operational experience with assimilation of rainfall data in the Met Office mesoscale model. *Meteorol Atmos Phys*, **76**, 3–8.

Manney, G.L., Sabutis, J.L. and SWINBANK, R., 2001: A unique stratospheric warming event in November 2000. *Geophys Res Lett*, **28**, 2,629–2,632.

Mecklenburg, S., Bell, V.A., Carrington, D.S., COOPER, A.M., Moore, R.J. and PIERCE, C.E., 2001: Applying COTREC-derived rainfall forecasts to the rainfall-runoff model PDM — estimating error sources. Abstract. 30th International conference on radar meteorology, Munich, Germany, 19–24 July 2001. American Meteorological Society, Paper 1.7, 14–16.

Mecklenburg, S., Bell, V.A., Carrington, D.S., COOPER, A.M., Moore, R.J. and PIERCE, C.E., 2001: Interfacing COTREC-derived rainfall forecasts with the rainfall-runoff model PDM. *In* Fifth International Symposium on hydrological applications of weather radar — radar hydrology. Kyoto, Japan 19–22 November 2001.

Metcalfe, S.E. et al. (including DERWENT, R.G.), 2001: Developing the Hull Acid Rain Model: its validation and implications for policy makers. *Environ Sci and Policy*, **4**, 25–37.

Mitchell, D.L., Arnott, W.P., Schmitt, C., BARAN, A.J., HAVEMANN, S. and Fu, Q., 2001: Photon tunneling contributions to extinction for laboratory grown hexagonal columns. *J Quant Spectroscop and Radiat Transfer*, **70**, 761–776.

MITCHELL, J.F.B. et al., 2001: Detection of climate change and attribution of causes. *In* Climate Change 2001: The Scientific Basis. J.T. Houghton et al. (Eds). Cambridge University Press.

Morland, J.C., Grimes, D.I.F. and HEWISON, T.J., 2001: Satellite observations of the microwave emissivity of a semi-arid land surface. *Remote Sensing Environ*, **77**, 149–164.

Moron, V. et al. (including FOLLAND, C.K.), 2001: Analysing and combining atmospheric general circulation model simulations forced by prescribed SST: tropical response. *Ann Geofis*, **44**, 755–780.

Moron, V. et al. (including FOLLAND, C.K.), 2001: Analysing and combining atmospheric general circulation model simulations forced by prescribed SST: northern extratropical response. *Ann Geofis*, **44**, 781–794.

MYLNE, K.R., EVANS, R.E. and Clark, R.T., 2002: Multi-model multi-analysis ensembles in quasi-operational medium-range forecasting. *QJR Meteorol Soc*, **128**, 361–384.

Nagata, M. et al. (including WILSON, C.), 2001: A mesoscale model inter-comparison: a case of explosive development of a tropical cyclone (COMPARE III). *J Meteorol Soc Jpn*, **79**, 999–1,033.

O'Doherty, S. et al. (including RYALL, D. and DERWENT, R.G.), 2001: In situ chloroform measurements at Advanced Global Atmospheric Gases Experiment atmospheric research stations from 1994 to 1998. *J Geophys Res*, **106**, 20,429–20,444.

Orr, J.C. et al. (including TAYLOR, N.K. and PALMER, J.), 2001: Estimates of anthropogenic carbon uptake from four three-dimensional global ocean models. *Global Biogeochem Cycle*, **15**, 43–60.

OSBORNE, S.R., JOHNSON, D.W., Bower, K.N. and WOOD, R., 2001: Modification of the aerosol size distribution within exhaust plumes produced by diesel-powered ships. *J Geophys Res*, **106**, 9,827–9,842.

PALMER, J.R. and Totterdell, I.J., 2001: Production and export in a global ocean ecosystem model. *Deep-Sea Res Part I — Oceanogr Res Pap*, **48**, 1,169–1,198.

PARKER, D.E. and ALEXANDER, L.V., 2001: Global and regional climate in 2000. *Weather*, **56**, 255–267.

PETCH, J.C., 2001: Using a cloud-resolving model to study the effects of subgrid-scale variations in relative humidity on direct sulphate-aerosol forcing. *QJR Meteorol Soc*, **127**, 2,385–2,394.

PETCH, J.C. and GRAY, M.E.B., 2001: Sensitivity studies using a cloud-resolving model simulation of the tropical west Pacific. *QJR Meteorol Soc*, **127**, 2,287–2,306.

Phillips, V.T.J., Blyth, A.M., BROWN, P.R.A., Choularton, T.W. and Latham, J., 2001: The glaciation of a cumulus cloud over New Mexico. *QJR Meteorol Soc*, **127**, 1,513–1,534.

POPE, V.D., PAMMENT, J.A., JACKSON, D.R. and SLINGO, A., 2001: The representation of water vapor and its dependence on vertical resolution in the Hadley Centre Climate Model. *J Clim*, **14**, 3,065–3,085.

Prather, M. et al. (including DERWENT, R.), 2001: Atmospheric chemistry and greenhouse gases. *In* Climate Change 2001: The Scientific Basis. J.T. Houghton et al. (Eds). Cambridge University Press.

PRICE, J.D., 2001: A study of probability distributions of boundary-layer humidity and associated errors in parametrized cloud-fraction. *QJR Meteorol Soc*, **127**, 739–758.

PRICE J.D., 2002: A semi-emperical parametrization for total *in situ* specific humidity standard deviation derived from tethered balloon observations. *QJR Meteorol Soc*, **128**, 733–739.

PRICE, J.D., 2002. A study on observed evolution of boundary layer humidity distributions. *Atmos Sci Lett*, **2**, 125–131 (available only online at www.idealibrary.com/links/doi/10.1006/asle.2001.0045/pdf).

Ramaswamy, V. et al. (including NASH, J. and SWINBANK, R.), 2001: Stratospheric temperature trends: observations and model simulations. *Rev Geophys*, **39**, 71–122.

Raper, S.C.B., GREGORY, J.M. and Osborn, T.J., 2001: Use of an upwelling-diffusion energy balance climate model to simulate and diagnose A/OGCM results. *Clim Dyn*, **17**, 601–613.

Raper, S.C.B., GREGORY, J.M. and Stouffer, R.J., 2002: The role of climate sensitivity and ocean heat uptake on AOGCM transient temperature response. *J Clim*, **15**, 124–130.

RICKARD, G.J., LUNNON, R.W. and Tenenbaum, J., 2001: The Met Office upper air winds: Prediction and verification in the context of commercial aviation data. *Meteorol Appl*, **8**, 351–360.

Rizzi, R., di Pietro, P., Loffredo, G. and SMITH, J.A., 2001: Comparison of measured and modeled stratus cloud infrared spectral signatures. *J Geophys Res*, **106**, 34,109–34,119.

Roach, W.T. and BYSOUTH, C.E., 2002: How often does severe clear air turbulence occur over tropical oceans? *Weather*, **57**, 8–19.

ROBERTS, M.J. and Marshall, D.P., 2000: On the validity of downgradient eddy closures in ocean models. *J Geophys Res*, **105**, 28,613–28,627.

Rodwell, M.J., 2001: Atlantic air-sea interaction revisited. *In* Meteorology at the millennium. R.P. Pearce (Ed.). Academic Press.

RODWELL, M.J. and Hoskins, B.J., 2001: Subtropical anticyclones and summer monsoons. *J Clim*, **14**, 3,192–3,211.

Rother, T., Schmidt, K. and HAVEMANN, S., 2001: Light scattering on hexagonal ice columns. *J Op Soc Am A: Optics Image Science and Vision*, **18**, 2,512–2,517.

Roubtsov, V.N. and ROULSTONE, I., 2001: Holomorphic structures in hydrodynamical models of nearly geostrophic flow. *Proc R Soc London*, **A457**, 1,519–1,531.

ROWELL, D.P., 2001: Teleconnections between the tropical Pacific and the Sahel. *QJR Meteorol Soc*, **127**, 1,683–1,706.

RYALL, D.B., DERWENT, R.G., MANNING, A.J., REDINGTON, A.L., et al., 2002: The origin of high particulate concentrations over the United Kingdom, March 2000. *Atmos Environ*, **36**, 1,363–1,378.

SAUNDERS, F., GÖBER, M. and CHALCRAFT, B., 2001: The exceptional rainfall event of 11 and 12 October 2000 in Kent and Sussex, as observed and as forecast by the Met Office Mesoscale Model. *Weather*, **56**, 360–367.

SCAIFE, A.A., BUTCHART, N., Warner, C.D., Stainforth, D., Norton, W.A. and AUSTIN, J., 2000: Realistic quasi-biennial oscillations in a simulation of the global climate. *Geophys Res Lett*, **27**, 3,481–3,484.

SCAIFE, A.A., BUTCHART, N., Warner, C.D. and SWINBANK, R., 2002: Impact of a spectral gravity wave parametrization on the stratosphere in the Met Office Unified Model. *J Atmos Sci*, **59**, 1,473–1,489.

Seaton, A. et al. (including DERWENT, R.G.), 2001: Airborne particles. Expert Panel on Air Quality Standards. London, The Stationery Office.

SEXTON, D.M.H., 2001: The effect of stratospheric ozone depletion on the phase of the Antarctic Oscillation. *Geophys Res Lett*, **28**, 3,697–3,700.

SEXTON, D.M.H., ROWELL, D.P., FOLLAND, C.K. and Karoly, D.J., 2001: Detection of anthropogenic climate change using an atmospheric GCM. *Clim Dyn*, **17**, 669–685.

SHUTTS, G.J., 2001: A linear model of back-sheared flow over an isolated hill in the presence of rotation. *J Atmos Sci*, **58**, 3,293–3,311.

Slater, A.G. et al. (including COX, P.M. and GEDNEY, N.), 2001: The representation of snow in land surface schemes: Results from PILPS 2(d). *J Hydrometeorol*, **2**, 7–25.

STANIFORTH, A., 2001: Developing efficient unified nonhydrostatic models. *In* Proceedings of 50th anniversary of NWP commemorative symposium, Berlin 9–10 March 2000. Berlin, Deutsche Meteorologische Gesellschaft.

Stevens, B. et al. (including MACVEAN, M.K.), 2001: Simulations of trade wind cumuli under a strong inversion. *J Atmos Sci*, **58**, 1,870–1,891.

STEVENSON, D.S., DERWENT, R.G., COLLINS, W.J. and JOHNSON, C.E., 2001: Comparison of the observed and 3-D CTM model calculated seasonal cycles in surface ozone concentrations. *In* TOR-2 Annual Report. Munich, EUROTRAC-2 ISS, GSF National Research Center for Environment and Health.

STILLER, O. and Craig, G.C., 2001: A scaling hypothesis for moist convective updraughts. *QJR Meteorol Soc*, **127**, 1,551–1,570.

SWANN, H., 2001: Evaluation of the mass-flux approach to parametrizing deep convection. *QJR Meteorol Soc*, **127**, 1,239–1,260.

SWARBRICK, S.J., 2001: Applying the relationship between potential vorticity fields and water vapour imagery to adjust initial conditions in NWP. *Meteorol Appl*, **8**, 221–228.

Thorne, P.W., Jones, P.D., TETT, S.F.B., PARKER, D.E., Osborn, T.J. and Davies, T.D., 2001: Ascribing potential causes of recent trends in free atmosphere temperatures. *Atmos Sci Lett,* **2**, 132–142 (available only online at www.idealibrary.com/links/doi/10.1006/asle.2001.0046/pdf).

THORPE, R.B., GREGORY, J.M., JOHNS, T.C., WOOD, R.A. and MITCHELL, J.F.B., 2001: Mechanisms determining the Atlantic thermohaline circulation response to greenhouse gas forcing in a non-flux-adjusted coupled climate model. *J Clim*, **14**, 3,102–3,116.

Turner, J., Connolley, W., CRESSWELL, D. and Harangozo, S., 2001: The simulation of Antarctic sea ice in the Hadley Centre climate model (HadCM3). *Ann Glaciol*, **33**, 585–591.

TURTON, J.D. and Ryder, P. (Eds), 2001: United Kingdom report on systematic observations for climate for the Global Climate Observation System (GCOS). Report provided by the Department for Environment, Food & Rural Affairs (DEFRA) for the Third National Communication to the Conference of the Parties to the United Nations Framework Convention on Climate Change (UNFCCC), October 2001.

VELLINGA, M., WOOD, R.A and GREGORY, J.M., 2002: Processes governing the recovery of a perturbed thermohaline circulation in HadCM3. *J Clim*, **15**, 764–780.

WATSON R.T., et al. (including GRIGGS, D.J., MITCHELL, J.F.B. and GREGORY, J.), 2001: Climate Change 2001: Synthesis Report. R.T. Watson et al. (Eds). Cambridge University Press.

WEBB, M., SENIOR, C., Bony, S. and Morcrette, J.J., 2001: Combining ERBE and ISCCP data to assess clouds in the Hadley Centre, ECMWF and LMD atmospheric climate models. *Clim Dyn*, **17**, 905–922.

White, W.B. and ALLAN, R.J., 2001: A global quasi-biennial wave in surface temperature and pressure and its decadal modulation from 1900 to 1994. *J Geophys Res*, **106**, 26,789–26,803.

WHYTE, K.W., Klaes, K.D. and Schraidt, R., 2001: Further development of the European ATOVS and AVHRR processing package Tech. *In* Proceedings of the 11th international TOVS study conference. J. Le Marshall and J.D. Jasper (Eds). Bureau of Meteorology Research Centre.

Wielicki, B.A. et al. (including ALLAN, R.P. and SLINGO, A.), 2002: Evidence for large decadal variability in the tropical mean radiative energy budget. *Science*, **295**, 841–844.

Wild, M., Ohmura, A., Gilgen, H., Morcrette, J.-J. and SLINGO, A., 2001: Evaluation of downward longwave radiation in general circulation models. *J Clim*, **14**, 3,227–3,239.

WILLIAMS, K.D., JONES, A., ROBERTS, D.L., SENIOR, C.A. and WOODAGE, M.J., 2001: The response of the climate system to the indirect effects of anthropogenic sulfate aerosol. *Clim Dyn*, **17**, 845–856.

WILLIAMS, K.D., SENIOR, C.A. and MITCHELL, J.F.B., 2001: Transient climate change in the Hadley Centre models: the role of physical processes. *J Clim*, **14**, 2,659–2,674.

Williams, V., AUSTIN, J. and Haigh, J., 2001: Model simulations of the impact of the 27-day solar rotation period on stratospheric ozone and temperature. *Adv Space Res*, **27**, 1,933–1,942.

WOOD, N., BROWN, A.R. and HEWER, F.E., 2001: Parametrizing the effects of orography on the boundary layer: an alternative to effective roughness lengths. *QJR Meteorol Soc*, **127**, 759–777.

WOOD, R. and TAYLOR, J.P., 2001: Liquid water path variability in unbroken marine stratocumulus cloud. *QJR Meteorol Soc*, **127**, 2,635–2,662.

WOODWARD, S., 2001: Modeling the atmospheric life cycle and radiative impact of mineral dust in the Hadley Centre climate model. *J Geophys Res*, **106**, 18,155–18,166.

Yeh, K.-S., Côte, J., Gravel, S., Méthot, A., Patoine, A., Roch, M. and STANIFORTH, A., 2002: The CMC-MRB Global Environmental Multiscale (GEM) Model. Part III: Nonhydrostatic formulation. *Mon Weather Rev*, **130**, 339–356.

Zhu, Y., Toth, Z., Wobus, R., Richardson, D. and MYLNE, K., 2002: The economic value of ensemble-based weather forecasts. *Bull Am Meteorol Soc*, **83**, 73–83.

Acronyms

AATSR	Advanced Along-Track Scanning Radiometer
AIRS	Advanced Infrared Sounder
AMDAR	Aircraft Meteorological Data and Reporting
AMSU	Advanced Microwave Sounding Unit (a component of ATOVS)
ATOVS	Advanced TIROS Operational Vertical Sounder
AVHRR	Advanced Very High Resolution Radiometer
AWS	Automatic weather station
BODC	British Oceanographic Data Centre
BoM	Bureau of Meteorology (Australia)
CAT	Clear air turbulence
CEH	Centre for Ecology and Hydrology
CET	Central England Temperature
COST	(European) Co-operation in Science and Technology
DEFRA	Department for Environment, Food and Rural Affairs
DPDS	Data and Products Distribution System
EC FP5	European Commission Framework Programme 5
ECMWF	European Centre for Medium-range Weather Forecasts
EPS	Ensemble Prediction System
ESA	European Space Agency
ESSC	Environmental Systems Science Centre
ETS	Equitable Threat Score
FOAM	Forecasting Ocean Assimilation Model
FPSO	Floating Production, Storage and Offloading system
FROST	Future options for Tropics
FSSSI	Forecasting for specific sites: system implementation
GANDOLF	Generating Advanced Nowcasts for Deployment in Operational Land-based flood Forecasts
GIS	Geographical Information System
GISST	Global analysis of sea-ice and sea-surface temperature
GLOBE	Global Land One-km Based Elevation
GODAE	Global Ocean Data Assimilation Experiment
GPCS	General Purpose Computing Service
GPS	Global Positioning System
GTS	Global Telecommunication System
IN	Ice-forming nuclei
IP	Internet protocol
IPCC	Intergovernmental Panel on Climate Change
ITCZ	Inter-tropical convergence zone
IWC	Ice water content
JCMM	Joint Centre for Mesoscale Meteorology
KED	Kriging with external drift
LCBR	Laser cloud-base recorder

MAP	Mesoscale Alpine Programme
MASS	Managed archive storage system
MoD	Ministry of Defence
MORECS	Met Office Rainfall and Evaporation Calculation System
MORSN	Met Office Remote Sites Network
MORST	Met Office Road Surface Temperature
MOS	Model output statistics
MOSES	Met Office Surface Exchange Scheme
MPS	Marine Production System
MSG	Meteosat Second Generation
MSU	Microwave Sounding Unit
NASA	National Aeronautics and Space Administration (USA)
NATO	North Atlantic Treaty Organization
NERC	Natural Environment Research Council
NESDIS	National Environmental Satellite, Data and Information Service (part of NOAA)
NHS	National Health Service
NMS	National meteorological service
NOAA	National Oceanic and Atmospheric Administration (USA)
NWP	Numerical weather prediction
OLR	Outgoing long-wave radiation
PDF	Probability Density Function
PDM	Probability Distributed Moisture
PRECIS	Providing Regional Climates for Impact Studies
QBO	Quasi-biennial oscillation
RAID	Redundant array of inexpensive disks
RSW	Reflected short-wave
SAMOS	Semi-automatic Meteorological Observing System
SRES	Special Report on Emissions Scenarios
SSFM	Site-specific Forecast Model
SSMI	Special Sensor Microwave Imager
SST	Sea-surface temperature
TDA	Tactical decision aid
THC	Thermohaline circulation
TIROS	Television Infrared Observation Satellite
TOMS	Total Ozone Mapping Spectrometer
TWV	Total water vapour
UM	Unified Model
UMETRAC	Unified Model with Eulerian transport and chemistry
WIN	Weather Information Network
WMO	World Meteorological Organization
WVBC	Wake Vortex Behaviour Classes

Copies of the *Annual Report and Accounts 2001/2* can be obtained from the Met Office on 01344 854623.

The Annual Report and Accounts 2001/2 and *Scientific and Technical Review 2001/2* can also be accessed from our web site at

www.metoffice.com

All other enquiries, including those relating to products and services, should be directed to our Customer Centre on 0845 300 0300.

Designed and produced by the Met Office. The Met Office and Met Office logo are registered trademarks.

01/0869

Printed on totally chlorine-free paper (using wood from sustainable forests). Paper waste from the mill is also included and can be up to 25% of the final paper content.

ISBN 0 86180 363 9

Met Office London Road Bracknell Berkshire RG12 2SZ United Kingdom
Tel: +44 (0)1344 855680 Fax: +44 (0)1344 855681
E-mail: enquiries@metoffice.com www.metoffice.com